The Effects of Ocean Acidification on Multiple Life History Stages of the Pacific Oyster, *Crassostrea gigas*: Implications for Physiological Trade-offs

Emma B. Timmins-Schiffman

A dissertation
Submitted in partial fulfillment of the
Requirements for the degree of

Doctor of Philosophy

University of Washington
2014

Reading Committee:
Steven B. Roberts, Chair
Carolyn S. Friedman
Jonathan P. Davis

Program Authorized to Offer Degree:
Aquatic and Fishery Sciences

University of Washington

Abstract

The Effects of Ocean Acidification on Multiple Life History Stages of the Pacific Oyster, *Crassostrea gigas*: Implications for Physiological Trade-offs

Emma Timmins-Schiffman

Chair of the Supervisory Committee:
Associate Professor Steven B. Roberts
School of Aquatic and Fishery Sciences

As global climate change accelerates, due in large part to increasing emissions of carbon dioxide and other greenhouse gases from fossil fuel use, agriculture, and large-scale changes in land use, natural ecosystems bear the consequences. For marine systems these include increased mean seawater temperature, changes in carbonate chemistry equilibria, and increased pollutant loading due to non-point run-off, among other effects. Human-induced environmental changes will not have the same magnitude of effect in all regions, but on average the changes occurring are rapid and significant. Natural populations will either need to acclimatize and/or adapt, or shift their ranges to enable continued existence. This dissertation explores the effects of ocean acidification on the Pacific oyster, *Crassostrea gigas*. Oysters are sedentary and inhabit a naturally variable environment (the intertidal zone) and thus may be pre-adapted to withstand rapid environmental change. Oysters and similarly sedentary organisms are ideal for investigating the effects of environmental change on biology because they are not able to escape these changes, but must respond physiologically (acclimatize) if they are to survive. Due to this ecological history, oysters provide a model that allows us to explore potential physiological mechanisms that are needed in a response to specific environmental changes as well as the limits of these mechanisms.

In the first chapter, the effects of elevated partial pressure of CO_2 (pCO_2, a major driver of ocean acidification) on oyster larvae are explored. Larvae were exposed to low pH during early development, a period that included the transition from energetic

dependence on maternally derived lipids to dependence on exogenous resources. Larvae were found to experience a developmental delay at elevated pCO_2, manifested as smaller size and slower rate of shell deposition. These significant effects of ocean acidification on early larval development may indicate a bottleneck in the oyster life cycle as the pH of marine waters decreases. Subsequent research has shown that these effects at early larval stages can carry over into later stages after settlement in another oyster species (Hettinger et al. 2012).

In order to better understand the effects of environmental change on oyster physiology, we developed proteomic tools to explore changes in protein pathways in oyster gill (ctenidia) tissue. The second chapter explores the gill proteome (suite of expressed proteins) of adult oysters. Characterization of the proteome provides insight into the physiological mechanisms that may be available to the oyster during response to an environmental stress. The results revealed that the ctenidia proteome includes a diverse array of proteins that accomplish many functions and that it is a metabolically active tissue. The proteome sequencing lays the groundwork for exploring how ocean acidification affects various proteomic pathways in the tissue that acts as the interface between the oyster and its environment.

Lastly, the adult oyster response to ocean acidification and a second stress are explored via proteomics, fatty acid profiles, glycogen content, shell microstructure, and mortality in response to heat shock. There was a significant impact of ocean acidification on oyster shell integrity, but no effects after one month of exposure on relative amounts of fatty acid, glycogen or response to acute heat shock. Through the proteomic analysis, we revealed an active and significant proteomic response to ocean acidification exposure, uncovering some of the mechanisms behind the observed macro-phenotypic changes. Additionally, the proteomic response to mechanical stimulation was largely altered between low and high pCO_2, suggesting that ocean acidification can fundamentally change how oysters respond to a second stress.

Works Cited

Hettinger, A., Sanford, E., Hill, T.M., Russell, A.D., Sato, K.N., Hoey, J., Forsch, M., Page, H.N. and Gaylord, B. (2012). Persistent carry-over effects of planktonic exposure to ocean acidification in the Olympia oyster. *Ecology* , *93*(12): 2758-2768.

Table of Contents

List of Figures

List of Tables

Introduction

Background

Global climate change and human activities are already impacting natural aquatic environments and are expected to increase in intensity in the coming decades. These diverse changes include input of pollutants into waterways, altered river flow that can affect water chemistry and hydrography, sea level rise, increasing intensity of temperature fluctuations and overall temperature rise, and decreasing ocean pH. The nearshore marine environment is already hypervariable and home to inherent stressors for marine organisms. There are frequent fluctuations in temperature (Pennington and Chavez 2000; Kaplan et al. 2003), pH (Feely et al. 2008), salinity (Pennington and Chavez 2000), nutrients (Pennington and Chavez 2000), and exposure to contaminants (Barkovskii et al. 2010). As the environment continues to change, local populations will either have to adapt to new sources of environmental variability and weather new stressors, or they will be forced to shift their ranges to more suitable habitats. In this way, both the ecology and biology of aquatic animals can give us insight into the kinds of changes that are occurring in the marine environment, as well as how those changes are affecting organism physiology and fitness. Sessile marine organisms are especially useful in this regard since they can serve as environmental sentinels.

In situ observations, such as biomonitoring, give insight into how a specific location's environment impacts local populations; however, controlled laboratory exposures can provide greater information on specific responses to targeted stressors. In a laboratory setting, dose-dependent responses can also be more easily established (e.g. Lüchmann et al., 2011). This precise information can then be applied in a field context to better understand how organisms react to environmental change.

Pacific oysters, *Crassostrea gigas*, have a long history as subjects of ecological and physiological research as well as extensive molecular resources (e.g. Zhang et al. 2012), making them a strong model for further explorations of response to environmental change. Scientific investigations in *C. gigas* began with interest in its aquaculture. For example, a publication on the culture of the Pacific oyster in Japan dates to 1902 (Dean 1902) and in 1930 Galstoff published an investigation into stimulating spawning in what

was then known as *Ostrea gigas* (Galtsoff 1930). *C. gigas* and other oysters within the genus are dioecious, broadcast spawners that inhabit intertidal and subtidal environments, many of which are subject to daily, seasonal, and annual environmental fluctuations. *C. gigas* has a long history of exotic introduction to habitats worldwide (Mann 1983), mainly for aquaculture production (molluscs constitute 75.5% of worldwide aquaculture, FAO 2012) and has often been implicated in well documented disruptions to native species assemblages (Trimble et al. 2009; reviewed in Padilla 2010). The same characteristics that make *C. gigas* a successful invader (i.e. ability to withstand environmental fluctuations found in the nearshore environment, high fecundity, tolerance to a variety of diseases) suggest that this species is well adapted to environmental change, at least the natural sources of change that it has encountered to this point. As such, it is a robust physiological model in which to study the effects of environmental extremes.

Ocean acidification

Ocean acidification is the reduction of ocean water pH due directly to rising levels of atmospheric CO_2. Since the industrial revolution (beginning in the 1750s), CO_2 deposition into the atmospheric has increased at an accelerating rate. The increasing partial pressure of CO_2 (pCO_2), and other greenhouse gases, have contributed an overall global warming. Ocean acidification is also due to increased pCO_2 in seawater. Current average atmospheric pCO_2 is approximately 400 ppm, higher than the highest pCO_2 over the past 2.1 million years (approximately 300 ppm; Hönisch et al. 2009). According to the Intergovernmental Panel on Climate Change's (IPCC) B1 scenario (stabilized population growth by 2050 and a more service- and information–driven economy), average global CO_2 emissions will attain 650 ppm by 2100 (Caldeira and Wickett 2005). If population growth occurs at a higher rate accompanied by slow economic development and limited technological changes (IPCC's A2 scenario), emissions will likely reach 970 ppm by 2100 (Caldeira and Wickett 2005). The atmospheric pCO_2 increases that have already occurred have caused a global trend of an increasingly more shallow undersaturation horizon of $CaCO_3$ (Feely et al., 2004, 2012), which is projected to become more persistent and widespread by 2050 and beyond (Gruber et al., 2012).

Chemistry

The reduction in pH from atmospheric CO_2 equilibration with ocean water occurs according to the following reaction:

$$CO_2 + H_2O \rightarrow H_2CO_3 \rightarrow H^+ + HCO_3^- \rightarrow H^+ + CO_3^{2-}$$

The thermodynamic equilibrium of the reaction favors the production of bicarbonate (HCO_3^-) and hydrogen ions (H^+), and results in a lower saturation state (Ω) for carbonate ion (CO_3^{2-}). Since pH is a direct measure of the $[H^+]$ in solution, this reaction is directly responsible for lower oceanic pH. Additionally, the lower Ω creates a less favorable environment for maintaining and creating calcified structures (i.e. Gazeau et al. 2007).

Certain ions in ocean water contribute to total alkalinity (A_T) and buffer changes in pH. Total alkalinity represents a balance between H^+ donors and acceptors in water. The greater A_T in a body of water, the greater its ability to mitigate changes in pH. Thus, different geographic areas with different A_T – which can change according to riverine inputs, biological activity, weathering of rocks, etc. – will experience different degrees of ocean acidification. On a global scale, however, the trend is towards lower pH (Caldeira and Wickett 2005). The equilibration of anthropogenic CO_2 is increasing the total inorganic carbon (DIC), shifting the relative amounts DIC and A_T and contributing to $CaCO_3$ undersaturated waters at shallower depths (Feely et al., 2004, 2012). Changes in A_T based on the natural global carbon cycle (i.e. input from weathering on continents and removal through burial in ocean sediment) occur on the scale of thousands of years (Zeebe, 2012), much longer than the current changes in carbonate chemistry. Additionally, elevated pCO_2 can alter the buffering capacities of estuarine areas (Hu and Cai, 2013). Due to the current accelerated timescale of CO_2 input into the oceans (IPCC 2007), pH changes will continue largely unchecked by natural processes that have moderated fluctuations in the past (Zeebe 2012).

Nearshore environmental processes

Oceanic pH is affected by many other processes in addition to atmospheric pCO_2. Especially in the relatively shallow and productive nearshore environment, many

physical and biological processes contribute to fluctuations in pH on a variety of timescales (i.e. Booth et al., 2012). In upwelling zones along the coast, cold, CO_2-rich water can be pulled into productive areas as surface water is displaced. Upwelling represents a relatively transient yet strong signal in terms of pH fluctuations. In the California Current System, upwelling events bring water with aragonite saturation state of less than 2 into the nearshore environment for most of the spring, summer, and fall (Hauri et al. 2009). Greenhouse gases cause land masses to warm more quickly than the ocean, creating a low pressure cell over coastal areas. These low pressure cells increase wind strength and upwelling intensity, thereby augmenting a global trend towards winds favoring upwelling conditions (Bakun et al., 2010). Shellfish hatcheries on the Pacific coast of the United States have linked larval mortalities and decreased production with upwelling events (Barton et al., 2012) and have consequently changed their hatchery practices to avoid upwelled water.

The relatively high productivity of nearshore environments can lead to a strong CO_2 signal from respiration and photosynthesis occurring on a more short-term cycle (daily to seasonal). Photosynthesis and calcification decrease the amounts of CO_2 in seawater while respiration and dissolution of calcified structures increase CO_2 (Smith and Key, 1975). Since upwelled waters typically contain high amounts of nutrients they tend to stimulate primary production in the nearshore environment. During upwelling, changes in nearshore DIC occur mostly from organic matter production and respiration and $CaCO_3$ dissolution (Fassbender et al., 2011). As anthropogenic carbon inputs change the baseline of pCO_2 in seawater, these natural processes could contribute to making the overall pCO_2 even lower than predicted values for the open ocean (Feely et al. 2010).

Ocean acidification in Puget Sound

Puget Sound, WA and other similar bodies of water have hydrographies that contribute to variability in pH. Puget Sound is a semi-enclosed, urban estuary bordered by approximately 4.1 million people (U.S. Census Bureau, 2012 estimates). Puget Sound is subject to low transport/high water residence times in some basins (Babson et al., 2006), which can exacerbate low pH and low oxygen events. This pattern of hydrography results in relatively shallow low pH events in the summer months,

especially in southern Hood Canal where the longest residence times are found (Feely et al., 2010). Even though these pH fluctuations are caused by natural physical and biological processes, elevated atmospheric pCO_2 has also contributed to an overall decrease in pH in Puget Sound (Feely et al., 2010).

Implications for bivalves

Bivalves and many other aquatic invertebrates have proven to be sensitive to acute exposures to elevated pCO_2 across life stages. It is difficult to make direct comparisons across studies due to differences in exposure time, pCO_2 level, and, most importantly, ecological and evolutionary history of exposure to low pH events for the source population of study (i.e. Kelly et al., 2013; Parker et al., 2012). However, generalities of the effects of ocean acidification on bivalves do emerge from these and many other studies.

Bivalve larvae are generally more sensitive to changes in water chemistry than juveniles and adults, perhaps due to the energetic demands of early growth, requirements for rapid calcification, dependence on aragonite as a $CaCO_3$ source, and energetic requirements during metamorphosis. At the phenotypic level, growth and calcification of bivalve larvae are negatively impacted by elevated pCO_2 (Barros et al., 2013; Barton et al., 2012; Gaylord et al., 2011; Hettinger et al., 2012; Kurihara et al., 2007; Miller et al., 2009; Parker et al., 2010; Talmage and Gobler, 2011; Waldbusser et al., 2010). These phenotypic changes likely result from changes in energetic resource allocation in the larvae since they are manifested around the time when larvae make the transition from endogenous, maternally provided energetic resources to exogenous food (Barros et al., 2013; Barton et al., 2012; Timmins-Schiffman et al., 2012). The extra energetic demand of dependence upon external food resources means that fewer resources are available for other processes, such as growth and calcification, resulting in an overall developmental delay in ocean acidification-exposed larvae.

Around the same time as this metabolic shift, the first larval stages are initiating the process of calcification, which is more energetically demanding at the D-hinge stage than at later stages (Waldbusser et al., 2013). D-hinge larvae have higher amounts of seawater-derived carbon in their precipitated shell, suggesting that either they are unable

to fully isolate their calcifying space or they require relatively more DIC than later stage larvae (Waldbusser et al., 2013). Either hypothesis leads to the same result - that early stage calcification is highly sensitive to changes in carbon availability (i.e. $CaCO_3$ saturation state). The precise mechanisms behind developmental delay and other changes observed in bivalve larvae have yet to be fully characterized, but a proteomic investigation of *Crassostrea hongkongensis* larvae exposed to elevated pCO_2 revealed that ocean acidification causes a down-regulation of proteins involved in metabolic pathways (Dineshram et al., 2013).

Adult bivalves are generally less sensitive to changes in oceanic pCO_2, but still exhibit changes in growth, calcification, and many important physiological processes in response to ocean acidification. Bivalve shell deposition is negatively impacted by elevated pCO_2 (Gazeau et al., 2007) and some studies have illustrated decreased shell growth in low pH-exposed juveniles and adults (Beniash et al., 2010; Michaelidis et al., 2005; Thomsen and Melzner, 2010). The negative effects of decreased pH (and thereby decreased Ω of aragonite) are most often manifested in weaker shells that are structurally compromised (Dickinson et al., 2012; Dickinson et al., 2013; Welladsen et al., 2010).

Various other physiological processes have also been explored in the adult bivalve response to ocean acidification, illustrating the wide-ranging effects of this environmental stress. Changes in metabolic processes may change the energetic resources available for other physiological processes. In *C. virginica*, glycogen and lipid in whole body tissue decreased after an eleven week exposure to low pH (Dickinson et al., 2012). Similarly, metabolic shifts were evidenced in *C. gigas* after a 55-day exposure to low pH by changes in metabolites in the mantle and gill tissue (Lannig et al., 2010). During concurrent exposure to elevated temperature and ocean acidification, *C. gigas* increased metabolic usage of carbohydrates and lipids compared to proteins (Clark et al., 2013). The important impacts of ocean acidification on metabolic processes is further evidenced by studies that have revealed that the negative effects of elevated pCO_2 are largely mitigated when mussels have greater access to food resources (Melzner et al., 2011; Thomsen et al., 2013).

Bivalve hemolymph pH closely tracks environmental pH (Lannig et al., 2010; Thomsen et al., 2013). The change in hemolymph pH may be the main contributing

factor to changes in bivalve immune parameters during exposure to elevated pCO_2. Short-term ocean acidification exposure coupled with elevated temperature altered hemocyte parameters in the clam *Chamela gallina* and the mussel *Mytilus galloprovincialis* (Matozzo et al., 2012). There is also evidence of increased oxidative stress in bivalves at the cellular (Matoo et al., 2013), gene expression (Clark et al., 2013), and protein expression levels (Tomanek et al., 2011).

Applying Molecular Tools to Study Environmental Change

Molecular ecology is the use of molecular data (i.e. DNA, RNA, or protein) to explore interactions between organisms and their environment. These tools can be applied at the individual gene or protein level (targeted gene sequencing, qPCR, or Western blots) or on a global scale (genomics, transcriptomics, or proteomics). The latter is a non-biased approach in which the organism is assayed for its response to the environment and can be the basis for discovery of complex organism-environment interactions and biomarker development.

Genome sequencing can provide information on the genomic resources possessed by a species as well as insight into adaptation and evolution. The recent sequencing of the *C. gigas* genome revealed that oysters have an expanded repertoire of stress response genes compared to the genomes of seven other species (Zhang et al., 2012). Similarly, the *Daphnia pulex* genome contains expanded gene families for photoreactive/photoresponsive genes as well as high rates of gene duplication that could provide the basis for quick evolutionary responses to environmental changes (Colbourne et al., 2011).

Transcriptomics, or high throughput sequencing of mRNA, can also illustrate evolutionary-scale changes since single nucleotide polymorphisms (SNPs) are found at the DNA and mRNA levels. SNP frequency data at the transcriptomic level were used to detect an adaptive response to elevated pCO_2 in sea urchin larvae, specifically in genes involved in lipid metabolism, ion homeostasis, cell signaling, and protein modifications (Pespeni et al., 2013). Gene expression data can also elucidate functional molecular responses to an environmental change. In *C. gigas*, mRNA sequencing revealed that the

oyster transcriptomic response to elevated pCO_2 differed between different temperatures (Clark et al., 2013). A tag sequencing approach in *C. gigas* was used to identify genes responsible for different growth patterns between inbred and hybrid oysters, leading towards a better characterization of the physiology behind growth rate (Hedgecock et al. 2006; Meyer and Manahan 2010). Targeted amplification of cDNA of amino acid transporters in larval and adult Antarctic echinoderms revealed the importance of amino acid transport across all life stages (Applebaum et al. 2013), providing insight into energy acquisition from the environment.

Lastly, proteomics provide insight into the truly functional changes that occur at the molecular level in response to different habitats or environmental change. Proteins are functional molecules that effect changes at the phenotypic level (whereas changes in gene expression may not always translate into changes in protein expression). Proteomics have been used to reveal physiological changes that underlie adaptation to different environmental salinities in European whitefish (Papakostas et al., 2012), proteins that are associated with specific behavioral traits in the honey bee (R. Parker et al., 2012), as well as general changes in overall protein expression in response to a specific environmental stress (Dineshram et al., 2013; Jones et al., 2013; Letendre et al., 2011; Malécot et al., 2013; Parker et al., 2011; Tomanek et al., 2011; Wong et al., 2011). Changes in post-translational modifications (specifically phosphorylation status), which also play a role in whether or not a protein is expressed, can be investigated using phosphoproteomics (e.g. Dineshram et al., 2013; Li et al., 2013).

This dissertation explores the effects of ocean acidification on the Pacific oyster, *Crassostrea gigas*, at two different life stages. In the first chapter, larvae are exposed to elevated pCO_2 to assess how ocean acidification affects the earliest stages of development. Chapter 2 describes the development of shotgun proteomics tools that can facilitate the study of the mechanisms behind the oyster's response to ocean acidification and other environmental stressors. Chapter 3 details the effects of ocean acidification on the adult oyster proteomic response, fatty acid profiles, shell microstructural properties, and response to another stressor. Lastly, Appendix A describes an investigation of specific antioxidant response enzymes and their role in the response to elevated pCO_2 and

Appendix B includes results from a histological analysis of cuboidal metaplasia in response to ocean acidification and mechanical stress. The work as a whole represents novel investigations into the mechanisms behind the invertebrate response to elevated pCO_2. By combining analyses across different life stages and different scales (i.e. molecular to phenotypic) the results illustrate the integrative response of oysters to this environmental stress.

Works Cited

Applebaum, S.L., Ginsburg, D.W., Capron, C.S., and Manahan, D.T. (2013). Expression of amino acid transporter genes in developmental stages of adult tissues of Antarctic echinoderms. *Polar Biol*, *36*, 1257-1267.

Babson, A. L., Kawase, M., & MacCready, P. (2006). Seasonal and interannual variability in the circulation of Puget Sound, Washington: A box model study. *Atmosphere-Ocean*, *44*(1), 29–45. doi:10.3137/ao.440103

Bakun, A., Field, D. B., Redondo-Rodriguez, A., & Weeks, S. J. (2010). Greenhouse gas, upwelling-favorable winds, and the future of coastal ocean upwelling ecosystems. *Global Change Biology*, *16*(4), 1213–1228. doi:10.1111/j.1365-2486.2009.02094.x

Barkovskii, A.L., Green, C., and Hurley, D. (2010). The occurrence, spatial and temporal distrubiton, and environmental routes of tetracycline resistance and integrase genes in *Crassostrea virginica* beds. *Marine Pollution Bulletin*, *60*, 2215-2224.

Barros, P., Sobral, P., Range, P., Chícharo, L., & Matias, D. (2013). Effects of sea-water acidification on fertilization and larval development of the oyster Crassostrea gigas. *Journal of Experimental Marine Biology and Ecology*, *440*, 200–206. doi:10.1016/j.jembe.2012.12.014

Barton, A., Hales, B., Waldbusser, G. G., Langdon, C., & Feely, R. A. (2012). The Pacific oyster, Crassostrea gigas, shows negative correlation to naturally elevated carbon dioxide levels: Implications for near-term ocean acidification effects. *Limnology and Oceanography*, *57*(3), 698–710. doi:10.4319/lo.2012.57.3.0698

Beniash, E., Ivanina, a, Lieb, N., Kurochkin, I., & Sokolova, I. (2010). Elevated level of carbon dioxide affects metabolism and shell formation in oysters Crassostrea virginica (Gmelin). *Marine Ecology Progress Series*, *419*, 95–108. doi:10.3354/meps08841

Booth, J. A. T., McPhee-Shaw, E. E., Chua, P., Kingsley, E., Denny, M., Phillips, R., Bograd, S.J., Zeidberg, L.D., & Gilly, W. F. (2012). Natural intrusions of hypoxic,

low pH water into nearshore marine environments on the California coast. *Continental Shelf Research*, *45*, 108–115. doi:10.1016/j.csr.2012.06.009

Caldeira, K., & Wickett, M. E. (2005). Ocean model predictions of chemistry changes from carbon dioxide emissions to the atmosphere and ocean. *Journal of Geophysical Research*, *110*(C9), C09S04. doi:10.1029/2004JC002671

Clark, M. S., Thorne, M. a S., Amaral, A., Vieira, F., Batista, F. M., Reis, J., & Power, D. M. (2013). Identification of molecular and physiological responses to chronic environmental challenge in an invasive species: the Pacific oyster, Crassostrea gigas. *Ecology and evolution*, *3*(10), 3283–97. doi:10.1002/ece3.719

Colbourne, J. K., Pfrender, M. E., Gilbert, D., Thomas, W. K., Tucker, A., Oakley, T. H., Tokishita, S., Aerts, A., Arnold, G.J., Basu, M.K., et al. (2011). The ecoresponsive genome of Daphnia pulex. *Science*, *331*(6017), 555–61. doi:10.1126/science.1197761

Dean, B. (1902). Japanese Oyster-Culture. *Bull. US FISh. Comm.*, 17-38.

Dickinson, G. H., Ivanina, A. V, Matoo, O. B., Pörtner, H. O., Lannig, G., Bock, C., Beniash, E., & Sokolova, I. M. (2012). Interactive effects of salinity and elevated CO_2 levels on juvenile eastern oysters, Crassostrea virginica. *The Journal of experimental biology*, *215*(Pt 1), 29–43. doi:10.1242/jeb.061481

Dickinson, G. H., Matoo, O. B., Tourek, R. T., Sokolova, I. M., & Beniash, E. (2013). Environmental salinity modulates the effects of elevated CO_2 levels on juvenile hard-shell clams, Mercenaria mercenaria. *The Journal of experimental biology*, *216*(Pt 14), 2607–18. doi:10.1242/jeb.082909

Dineshram, R., Thiyagarajan, V., Lane, A., Ziniu, Y., Xiao, S., & Leung, P. T. Y. (2013). Elevated CO_2 alters larval proteome and its phosphorylation status in the commercial oyster, Crassostrea hongkongensis. *Marine Biology*, *160*(8), 2189–2205. doi:10.1007/s00227-013-2176-x

FAO (2012). *The State of the World Fisheries and Aquaculture*. Document prepared by the Food and Agriculture Orgnization of the United Nations. Technical Paper No. 564, FAO Fisheries and Aquaculture Deparment, Rome. 209 pp.

Fassbender, A. J., Sabine, C. L., Feely, R. a., Langdon, C., & Mordy, C. W. (2011). Inorganic carbon dynamics during northern California coastal upwelling. *Continental Shelf Research*, *31*(11), 1180–1192. doi:10.1016/j.csr.2011.04.006

Feely, R. A, Sabine, C. L., Lee, K., Berelson, W., Kleypas, J., Fabry, V. J., & Millero, F. J. (2004). Impact of anthropogenic CO_2 on the $CaCO_3$ system in the oceans. *Science*, *305*(5682), 362–6. doi:10.1126/science.1097329

Feely, R.A., Sabine, C.L., Hernandez-Ayon, J.M., Ianson, D., and Hales, B. (2008). Evidence for Upwelling of Corrosive "Acidified" Water onto the Continental Shelf. *Science*, *320*, 1490-1492. doi: 10.1126/science.1155676

Feely, R. A., Alin, S. R., Newton, J., Sabine, C. L., Warner, M., Devol, A., … Maloy, C. (2010). The combined effects of ocean acidification, mixing, and respiration on pH and carbonate saturation in an urbanized estuary. *Estuarine, Coastal and Shelf Science*, *88*(4), 442–449. doi:10.1016/j.ecss.2010.05.004

Feely, R. A., Sabine, C. L., Byrne, R. H., Millero, F. J., Dickson, A. G., Wanninkhof, R., Murata, A., Miller, L.A., & Greeley, D. (2012). Decadal changes in the aragonite and calcite saturation state of the Pacific Ocean. *Global Biogeochemical Cycles*, *26*(3), GB3001. doi:10.1029/2011GB004157

Galtsoff, P.S. (1930). The Role of Chemical Stimulation in the Spawning Reactions of *Ostrea virginica* and *Ostrea gigas*. *PNAS*, *16*(9), 555-559.

Gaylord, B., Hill, T. M., Sanford, E., Lenz, E.A., Jacobs, L.A., Sato, K. N., Russell, A.D., & Hettinger, A. (2011). Functional impacts of ocean acidification in an ecologically critical foundation species. *The Journal of experimental biology*, *214*(Pt 15), 2586–94. doi:10.1242/jeb.055939

Gazeau, F., Quiblier, C., Jansen, J. M., Gattuso, J.-P., Middelburg, J. J., & Heip, C. H. R. (2007). Impact of elevated CO 2 on shellfish calcification. *Geophysical Research Letters*, *34*(7), L07603. doi:10.1029/2006GL028554

Gruber, N., Hauri, C., Lachkar, Z., Loher, D., Frölicher, T. L., & Plattner, G.-K. (2012). Rapid progression of ocean acidification in the California Current System. *Science*, *337*(6091), 220–3. doi:10.1126/science.1216773

Hauri C, Gruber N, Plattner G-K, Alin S, Feely RA, Hales B, Wheeler PA (2009) Ocean acidification in the California Current System. Oceanography 22: 60-71

Hedgecock, D., Lin, J.-Z., DeCola, S., Haudenschild, C.D., Meyer, E., Manahan, D.T., and Bowen, B. (2006). Transcriptomic analysis of growth heterosis in larval Pacific oysters (*Crassostrea gigas*). *PNAS*, *104*(7), 2313-2318.

Hettinger, A., Sanford, E., Hill, T. M., Russell, A. D., Sato, K. N. S., Hoey, J., Forsch, M., Page, H.N., & Gaylord, B. (2012). Persistent carry-over effects of planktonic exposure to ocean acidification in the Olympia oyster. *Ecology*, *93*(12), 2758–68. Retrieved from http://www.ncbi.nlm.nih.gov/pubmed/23431605

Hönisch, B., Hemming, N. G., Archer, D., Siddall, M., & McManus, J. F. (2009). Atmospheric carbon dioxide concentration across the mid-Pleistocene transition. *Science*, *324*(5934), 1551–4. doi:10.1126/science.1171477

Hu, X., & Cai, W.-J. (2013). Estuarine acidification and minimum buffer zone-A conceptual study. *Geophysical Research Letters*, *40*(19), 5176–5181. doi:10.1002/grl.51000

Intergovernmental Panel on Climate Change (IPCC) (2007) Contribution of Working Groups I, II, and III to the Fourth Assessment Report of the Intergovernmental Panel on Climate Change. Pachauri, R.K., Reisinger, A. (Eds.), IPCC, Geneva, Switzerland, pp. 104

Jones, B. M., Iglesias-Rodriguez, M. D., Skipp, P. J., Edwards, R. J., Greaves, M. J., Young, J. R., Elderfield, H., & O'Connor, C. D. (2013). Responses of the Emiliania huxleyi proteome to ocean acidification. *PloS one*, *8*(4), e61868. doi:10.1371/journal.pone.0061868

Kaplan, D.M., Largier, J.L., Navarrete, S., Guiñez, R., Castilla, J.C. (2003). Large diurnal temperature fluctuations in the nearshore water column. *Estuarine Coastal and Shelf Science*, *57*, 385-398.

Kelly, M. W., Padilla-Gamiño, J. L., & Hofmann, G. E. (2013). Natural variation and the capacity to adapt to ocean acidification in the keystone sea urchin Strongylocentrotus purpuratus. *Global change biology*, *19*(8), 2536–46. doi:10.1111/gcb.12251

Kurihara, H., Kato, S., & Ishimatsu, A. (2007). Effects of increased seawater pCO_2 on early development of the oyster Crassostrea gigas. *Aquatic Biology*, *1*(1), 91–98. doi:10.3354/ab00009

Lannig, G., Eilers, S., Pörtner, H. O., Sokolova, I. M., & Bock, C. (2010). Impact of ocean acidification on energy metabolism of oyster, Crassostrea gigas--changes in metabolic pathways and thermal response. *Marine drugs*, *8*(8), 2318–39. doi:10.3390/md8082318

Letendre, J., Dupont-Rouzeyrol, M., Hanquet, A.-C., Durand, F., Budzinski, H., Chan, P., Vaudry, D., & Rocher, B. (2011). Impact of toxicant exposure on the proteomic response to intertidal condition in Mytilus edulis. *Comparative biochemistry and physiology. Part D, Genomics & proteomics*, *6*(4), 357–69. doi:10.1016/j.cbd.2011.08.002

Li, R., Zhang, L., Fang, Y., Han, B., Lu, X., Zhou, T., Feng, M. & Li, J. (2013). Proteome and phosphoproteome analysis of honeybee (Apis mellifera) venom collected from electrical stimulation and manual extraction of the venom gland. *BMC genomics*, *14*(1), 766. doi:10.1186/1471-2164-14-766

Lüchmann, K. H., Mattos, J. J., Siebert, M. N., Granucci, N., Dorrington, T. S., Bícego, M. C., Taniguchi, S., Sasaki, S.T., Daura-Jorge, F.G. & Bainy, A. C. D. (2011). Biochemical biomarkers and hydrocarbons concentrations in the mangrove oyster

Crassostrea brasiliana following exposure to diesel fuel water-accommodated fraction. *Aquatic toxicology*, *105*(3-4), 652–60. doi:10.1016/j.aquatox.2011.09.003

Malécot, M., Guével, B., Pineau, C., Holbech, B. F., Bormans, M., & Wiegand, C. (2013). Specific proteomic response of Unio pictorum mussel to a mixture of glyphosate and microcystin-LR. *Journal of proteome research*, *12*(11), 5281–92. doi:10.1021/pr4006316

Mann, R. (2983). The role of introduced bivalve mollusc species in mariculture. *J. World Maricul. Soc.*, *14*, 546-559.

Matoo, O. B., Ivanina, A. V, Ullstad, C., Beniash, E., & Sokolova, I. M. (2013). Interactive effects of elevated temperature and CO_2 levels on metabolism and oxidative stress in two common marine bivalves (Crassostrea virginica and Mercenaria mercenaria). *Comparative biochemistry and physiology. Part A, Molecular & integrative physiology*, *164*(4), 545–53. doi:10.1016/j.cbpa.2012.12.025

Matozzo, V., Chinellato, A., Munari, M., Finos, L., Bressan, M., & Marin, M. G. (2012). First evidence of immunomodulation in bivalves under seawater acidification and increased temperature. *PloS one*, *7*(3), e33820. doi:10.1371/journal.pone.0033820

Melzner, F., Stange, P., Trübenbach, K., Thomsen, J., Casties, I., Panknin, U., Gorb, S.N., & Gutowska, M. A. (2011). Food supply and seawater pCO2 impact calcification and internal shell dissolution in the blue mussel Mytilus edulis. *PloS one*, *6*(9), e24223. doi:10.1371/journal.pone.0024223

Meyer, E., and Manahan, D.T. (2010). Gene expression profiling of genetically determined growth variation in bivalve larvae (*Crassotrea gigas*). *The Journal of Experiemental Biology*, *213*, 749-758.

Michaelidis, B., Ouzounis, C., Paleras, A., & Pörtner, H. O. (2005). Effects of long-term moderate hypercapnia on acid – base balance and growth rate in marine mussels Mytilus galloprovincialis. *Marine Ecology Progress Series, 293*, 109–118.

Miller, A. W., Reynolds, A. C., Sobrino, C., & Riedel, G. F. (2009). Shellfish face uncertain future in high CO_2 world: influence of acidification on oyster larvae calcification and growth in estuaries. *PloS one*, *4*(5), e5661. doi:10.1371/journal.pone.0005661

Padilla, D.K. (2010). Context-dependent Impacts of a Non-native Ecosystem Engineer, the Pacific Oyster *Crassostrea gigas*. *Integrative and Comparative Biology*, *50*(2), 213-225. doi: 10.1093/icb/icq080

Papakostas, S., Vasemägi, A., Vähä, J.-P., Himberg, M., Peil, L., & Primmer, C. R. (2012). A proteomics approach reveals divergent molecular responses to salinity in

populations of European whitefish (Coregonus lavaretus). *Molecular ecology*, *21*(14), 3516–30. doi:10.1111/j.1365-294X.2012.05553.x

Parker, L. M., Ross, P. M., & O'Connor, W. A. (2010). Comparing the effect of elevated pCO_2 and temperature on the fertilization and early development of two species of oysters. *Marine Biology*, *157*(11), 2435–2452. doi:10.1007/s00227-010-1508-3

Parker, L. M., Ross, P. M., O'Connor, W. A., Borysko, L., Raftos, D.A., & Pörtner, H.-O. (2012). Adult exposure influences offspring response to ocean acidification in oysters. *Global Change Biology*, *18*(1), 82–92. doi:10.1111/j.1365-2486.2011.02520.x

Parker, L. M., Ross, P. M., Raftos, D., Thompson, E., & O'Connor, W. A. (2011). The proteomic response of larvae of the Sydney rock oyster, Saccostrea glomerata to elevated pCO2. *Australian zoologist*, *35*(4), 1011–1023.

Parker, R., Guarna, M. M., Melathopoulos, A. P., Moon, K.-M., White, R., Huxter, E., Pernal, S.F., & Foster, L. J. (2012). Correlation of proteome-wide changes with social immunity behaviors provides insight into resistance to the parasitic mite, Varroa destructor, in the honey bee (Apis mellifera). *Genome biology*, *13*(9), R81. doi:10.1186/gb-2012-13-9-r81

Pennington, J.T. and Chavez, F.P. (2000). Seasonal fluctuations of temperature, salinity, nitrate, chlorophyll and primary production at station H3/M1 over 1989-1996 in Monterey Bay, California. *Deep-Sea Research II*, *47*, 947-973.

Pespeni, M. H., Sanford, E., Gaylord, B., Hill, T. M., Hosfelt, J. D., Jaris, H. K., LaVigne, M., Lenz, E.A., Russell, A.D., Young, M.K., & Palumbi, S. R. (2013). Evolutionary change during experimental ocean acidification. *Proceedings of the National Academy of Sciences of the United States of America*, *110*(17), 6937–42. doi:10.1073/pnas.1220673110

Smith, A. S. V, & Key, G. S. (1975). Carbon Dioxide and Metabolism in Marine Environments. *Limnology and Oceanography, 20*(3), 493–495.

Talmage, S. C., & Gobler, C. J. (2011). Effects of elevated temperature and carbon dioxide on the growth and survival of larvae and juveniles of three species of northwest Atlantic bivalves. *PloS one*, *6*(10), e26941. doi:10.1371/journal.pone.0026941

Thomsen, J., Casties, I., Pansch, C., Körtzinger, A., & Melzner, F. (2013). Food availability outweighs ocean acidification effects in juvenile Mytilus edulis: laboratory and field experiments. *Global change biology*, *19*(4), 1017–27. doi:10.1111/gcb.12109

Thomsen, J., & Melzner, F. (2010). Moderate seawater acidification does not elicit long-term metabolic depression in the blue mussel Mytilus edulis. *Marine Biology*, *157*(12), 2667–2676. doi:10.1007/s00227-010-1527-0

Timmins-Schiffman, E., O'Donnell, M. J., Friedman, C. S., & Roberts, S. B. (2012). Elevated pCO_2 causes developmental delay in early larval Pacific oysters, Crassostrea gigas. *Marine Biology*, *160*(8), 1973–1982. doi:10.1007/s00227-012-2055-x

Tomanek, L., Zuzow, M. J., Ivanina, A. V, Beniash, E., & Sokolova, I. M. (2011). Proteomic response to elevated P_{CO2} level in eastern oysters, Crassostrea virginica: evidence for oxidative stress. *The Journal of experimental biology*, *214*(Pt 11), 1836–44. doi:10.1242/jeb.055475

Trimble, A.C., Ruesink, J.L., and Dumbauld, B.R. (2009). Factors preventing the recovery of a historically overexploited shellfish species, *Ostrea lurida* Carpenter 1864. *Journal of Shellfish Research*, *28*(1), 97-106. doi: 10.2983/035.028.0116

Waldbusser, G., Bergschneider, H., & Green, M. (2010). Size-dependent pH effect on calcification in post-larval hard clam Mercenaria spp. *Marine Ecology Progress Series*, *417*(x), 171–182. doi:10.3354/meps08809

Waldbusser, G. G., Brunner, E. L., Haley, B.A., Hales, B., Langdon, C. J., & Prahl, F. G. (2013). A developmental and energetic basis linking larval oyster shell formation to acidification sensitivity. *Geophysical Research Letters*, *40*(10), 2171–2176. doi:10.1002/grl.50449

Welladsen, H. M., Southgate, P. C., & Heimann, K. (2010). The effects of exposure to near-future levels of ocean acidification on shell characteristics of Pinctada fucata (Bivalvia : Pteriidae). *Molluscan Research, 30*(3), 125–130.

Wong, K. K. W., Lane, A. C., Leung, P. T. Y., & Thiyagarajan, V. (2011). Response of larval barnacle proteome to CO_2-driven seawater acidification. *Comparative biochemistry and physiology. Part D, Genomics & proteomics*, *6*(3), 310–21. doi:10.1016/j.cbd.2011.07.001

Zeebe, R. E. (2012). History of Seawater Carbonate Chemistry, Atmospheric CO_2 , and Ocean Acidification. *Annual Review of Earth and Planetary Sciences*, *40*(1), 141–165. doi:10.1146/annurev-earth-042711-105521

Zhang, G., Fang, X., Guo, X., Li, L., Luo, R., Xu, F., Pengcheng, Y., Zhang, L., Wang, X., Qi, H. et al. (2012). The oyster genome reveals stress adaptation and complexity of shell formation. *Nature*, *490*(7418), 49–54. doi:10.1038/nature11413

Chapter I: Elevated pCO_2 causes developmental delay in early larval Pacific oysters, *Crassostrea gigas*

A version of this chapter was published in Marine Biology as: Timmins-Schiffman, E., O'Donnell, M.J., Friedman, C.S., and Roberts, S.B. 2013. Elevated pCO_2 causes developmental delay in early larval Pacific oysters, *Crassostrea gigas*. Mar Biol, 160: 1973-1982. doi 10.1007/s00227-012-2055-x

Abstract

Increasing atmospheric CO_2 equilibrates with surface seawater, elevating the concentration of aqueous hydrogen ions. This process, ocean acidification, is a future and contemporary concern for aquatic organisms, causing failures in Pacific oyster (*Crassostrea gigas*) aquaculture. This experiment determines the effect of elevated pCO_2 on the early development of *C. gigas* larvae from a wild Pacific Northwest population. Adults were collected from Friday Harbor, Washington, USA (48°31'70N, 12°1'10W) and spawned in July 2011. Larvae were exposed to Ambient (400 µatm CO_2), MidCO_2 (700 µatm), or HighCO_2 (1,000 µatm). After 24 h, a greater proportion of larvae in the HighCO_2 treatment were calcified as compared to Ambient. This unexpected observation is attributed to increased metabolic rate coupled with sufficient energy resources. Oyster larvae raised at HighCO_2 showed evidence of a developmental delay by 3 days post-fertilization, which resulted in smaller larvae that were less calcified.

Introduction

Ocean acidification is expected to affect ecosystems at an accelerating pace over the next century (Caldeira and Wickett 2003; IPCC 2007). Seawater pH declines (acidifies) in association with the uptake of anthropogenic CO_2 and resultant increased H^+ ion concentration. Projected changes in atmospheric pCO_2 may have significant consequences for natural populations ranging from physiological changes to broad-scale range shifts (Talmage and Gobler 2011; O'Donnell et al. 2009; Wong et al. 2011; Tomanek et al. 2011; Banks et al. 2010; Perry et al. 2005). Acidification of nearshore waters can occur via a variety of processes, including equilibration with elevated pCO_2 in the atmosphere, upwelling events, terrestrial run-off, and respiration. The upper ocean acidification in the North Pacific is proportional to the anthropogenic increase in

atmospheric CO_2, enforcing that the present-day pH changes are outside the range of natural variability (Byrne et al. 2010a, b). In addition to atmospheric sources of CO_2, oceanic upwelling and nearshore respiration further reduce the pH of water in which larvae develop (as low as pH 7.4 along the west coast of North America) and increasingly result in waters undersaturated with respect to aragonite (Feely et al. 2008, 2010). During the spring and summer off the US west coast, upwelling of waters rich in CO_2 and respiration from nearshore biological activity can cause under saturation of nearshore waters (Feely et al. 2008, 2010; Fassbender et al. 2011). These contemporary processes occur in the same area where planktonic invertebrate larvae congregate. As CO_2 emissions continue to equilibrate with ocean surface water, these habitats that already experience low pH could see further and more sustained increases in pCO_2.

Numerous studies have examined developmental consequences of ocean acidification on marine bivalve larvae. Exposure to low-pH water early in development caused decreased mid-stage growth and survival in *C. gigas* (Barton et al. 2012). *C. gigas's* congener, *Crassostrea virginica*, grew more slowly and incorporated less $CaCO_3$ into their shells at elevated pCO_2 when compared to controls (Miller et al. 2009). Similarly, ocean acidification conditions decreased both shell integrity and tissue mass in larval mussels, *Mytilus californianus* (Gaylord et al. 2011). Larval Sydney rock oysters (*Saccostrea glomerata*) demonstrated reduced survival and slower growth and development when reared under conditions simulating future oceanic pCO_2 (Watson et al. 2009). Both clam (*Mercenaria mercenaria*) and scallop larvae (*Argopectens irrandians*) were impacted by elevated pCO_2 in their metamorphosis, growth, and lipid synthesis (Talmage and Gobler 2011). The effects of ocean acidification have been studied on populations of *C. gigas* from Japan (Kurihara et al. 2007), Australia (Parker et al. 2010, 2012), and Europe (Gazeau et al. 2011), but few studies to date look at these effects on populations of *C. gigas* from the United States. Due to differences in experimental design, it is difficult to directly compare the three aforementioned studies, but overall *C. gigas* larvae are smaller when raised at elevated pCO_2 (Kurihara et al. 2007; Parker et al. 2010; Gazeau et al. 2011), demonstrate a developmental delay (Kurihara et al. 2007), and have morphological and shell deformities (Kurihara et al. 2007; Parker et al. 2010; Gazeau et al. 2011).

Pacific oyster larvae are planktotrophs, spending an extended period of a few weeks in the plankton, where they undergo a variety of important morphological and physiological changes. Larval metamorphosis and settlement are frequently associated with external environmental cues (such as presence of suitable substrate) and with physiological cues triggered by neurotransmitters (Bonar et al. 1990), and their successful completion is necessary for larval metamorphosis into a settled juvenile oyster. Organismal responses to ocean acidification vary among and within taxa suggesting that ecological and evolutionary history may influence responses to ocean acidification. Thus, empirical studies are needed to understand the mechanistic responses of species to a specific environmental stress and how the stress corresponds to the species' or population's original ecological niche.

One of the primary means by which marine organisms are directly influenced by ocean acidification is through relative concentrations of H^+ and associated decreased availability of CO_3^{2-}. These changes in water chemistry impact calcifying organisms as they rely on CO_3^{2-} to form and maintain carbonate-based structures (Beniash et al. 2010; Thomsen and Melzner 2010), while greater H^+ concentration can cause acidosis of body fluids. Acidosis can result in dissolution of calcium carbonate structures, reducing shell thickness and releasing ions into the hemolymph. Many adult aquatic invertebrates can make use of dissolved calcified structures or possibly actively dissolve their shell, to make HCO_3^- more available as a buffer against internal acidosis. Excess HCO_3^- for buffering can also be acquired from the aquatic environment. This phenomenon has been observed in Dungeness crabs, *Cancer magister* (Pane and Barry 2007); blue crabs, *Callinectes sapidus* (Henry et al. 1981); limpets, *Patella vulgata* (Marchant et al. 2010); and urchins, *Psammechinus miliaris* (Miles et al. 2007); however, internal acidosis was not successfully avoided in oysters, *C. gigas* (Lannig et al. 2010). It is not clear to what degree larvae can utilize this mechanism to maintain homeostasis under elevated pCO_2 conditions, but some invertebrates that inhabit naturally CO_2-rich environments are able to reproduce and the larvae settle without apparent adverse effects (Thomsen and Melzner 2010).

Sustained environmental change, such as ocean acidification, can negatively affect both the ecosystem and economy. Shellfish, including oysters, provide important

ecosystem services such as improved water quality and benthic-pelagic coupling through the filtration of large volumes of water, release of feces to the benthos, and creation of habitat via reef formation (Coen and Luckenbach 2000). In addition to their ecological roles, mollusks are economically important to many coastal communities worldwide. In 2008, mollusks comprised 64.1 % (or 13.1 million tons) of worldwide aquaculture production, with oysters accounting for 31.8 % of the total production (FAO 2010). The global economic cost of ocean acidification to the mollusk fishery is unclear but has been estimated to increase with rising atmospheric CO_2 levels and terrestrial sources of acidification (Narita et al. 2012). Recently, in the Pacific Northwest of the US, concern has heightened over the already apparent effects of corrosive, acidified water on both natural and hatchery production of *C. gigas* larvae (Elston et al. 2008; Feely et al. 2010; Barton et al. 2012). Hatchery water supply comes from adjacent natural bays, and when upwelling events occur, the water that enters the hatchery can reach and exceed pCO_2 of 1,000 µatm (S. Alin, unpublished data; B. Eudeline, pers. comm.). These upwelling events have been linked to mortality episodes in the hatchery, perhaps due to a combination of acidic water and pathogens associated with the water masses (Elston et al. 2008). Acidification events are projected to become more frequent and sustained as atmospheric pCO_2 continues to rise.

This study characterized the effects of two elevated levels of pCO_2 on size, calcification, and development during early larval stages of the Pacific oyster, *Crassostrea gigas*. Oyster larvae were raised in two elevated levels of pCO_2 (700 and 1,000 µatm) and ambient (400 µatm) seawater through 72 h following fertilization. The chemistry scenarios simulated in this study are based on projections for the coming century, but these values of low pH and Ω are already occurring with increasing frequency in nearshore upwelling systems off the US West coast (Feely et al. 2010; Hauri et al. 2009).

Materials and methods

Seawater chemistry manipulation

Experimental conditions were maintained using a flowthrough seawater system in Friday Harbor, Washington, USA. Water entering the system was filtered (to 0.2-µm),

UV-sterilized, and CO_2-depleted using membrane contactors (Membrana, Charlotte, North Carolina, USA) under partial vacuum. Three experimental treatments were chosen to correspond with dissolved CO_2 levels of 400, 700, or 1,000 ppm in the atmosphere. These three treatments will be referred to throughout the manuscript as Ambient, MidCO_2, and HighCO_2. Set-point pH levels were determined with the program CO_2SYS (Robbins et al. 2010) using an average total alkalinity of 2,060 μmol kg^{-1} based on total alkalinity measurements taken the week prior to the experimental trial.

Larval *C. gigas* were held in 3-L microcosms within a large reservoir filled with the respective treatment water. Ambient air stripped of CO_2 by a CO_2 adsorption unit (Twin Tower Engineering, Broomfield, Colorado, USA) was used to aerate the seawater within the reservoirs through a Venturi injector into the larger reservoir of treatment water. This replaced oxygen lost through the degassing process. Reservoir pH was continuously monitored by a Durafet III pH probe (Honeywell, Morristown, New Jersey, USA). When the probe registered that the treatment's pH strayed from its set point, a solenoid would open or close to allow more or less pure CO_2 (Praxair, Danbury, Connecticut, USA) to be injected via the Venturi. The Durafet probe information was fed into a Honeywell UDA2182 pH controller, which also controlled the solenoids.

Seawater was pumped from the reservoir into larval microcosms through irrigation drippers (DIG Industries, Sun Valley, California, USA) at a rate of 1.9-L h^{-1}. An outflow tube at the top of the microcosms fitted with 35-μm mesh allowed water to exit the microcosms while retaining larvae. All systems were equilibrated to the correct treatment level 48 h prior to the start of the experiment. Water temperature was held at 20.4 ± 0.4°C.

Oysters

Ten female and four male adult *C. gigas* were collected from Argyle Creek in Friday Harbor, Washington, in July 2011. Oysters were strip-spawned into Ambient seawater with eggs and sperm pooled separately (day 0). Pooled eggs (approximately 2 million) were divided equally into 18 7.5-cm diameter containers. Sperm was diluted (so as to approximate a 1:1 sperm/egg ratio) in Ambient seawater and added to each container of eggs. After the addition of sperm, the eggs were gently agitated and incubated for 15 min to allow for fertilization.

Six containers of fertilized eggs were transferred to microcosms containing one of three treatment conditions. Initial densities post-hatching were approximately 1 larva mL^{-1}. On days 1 and 3 post-fertilization, larvae were randomly sampled to determine survival, size, developmental stage, and presence or absence of calcification. For each microcosm sampled, larvae were filtered onto 35-μm mesh screens and washed with the appropriate seawater. Approximately 100 larvae were removed for each sample, relaxed with 7.5 % $MgCl_2$, and fixed in 4% paraformaldehyde buffered in filtered seawater. The remaining larvae were returned to cleaned microcosms filled with new seawater. Larvae were fed *Dunaliellia* sp. and *Isochrysis* sp. at concentrations of 30,000 cells mL^{-1} each (concentrations for optimal larval growth) on day 2. During feeding, water flow was turned off in microcosms for 2 h. All microcosms were cleaned at each sampling event.

Larvae were examined using light microscopy to determine survival, size, developmental stage, and shell presence/absence. Survival was determined at 20–40x: larvae were counted as dead if there was a complete absence of ciliary movement. Larval hinge length and shell height were measured at 10x magnification with a Nikon Eclipse E600 and NIS Elements Basic Research software (Nikon, Tokyo, Japan). Larval developmental stage and shell presence were determined at 20x magnification using an inverted microscope and double polarized light. Larvae were scored as calcified on day 1 post-fertilization if calcified shell was observed at the hinge (Fig. I.1a). On day 3 post-fertilization, larvae were classified as fully calcified if polarized light produced a ‘‘Maltese cross’’ in the larval shell (Fig. I.1b; LaBarbera 1974).

Carbonate chemistry

Salinity was measured with a conductivity meter (Hach sensION5; Loveland, Colorado, USA), and temperature was measured using a Fluke 1523 thermometer (Fluke, Everett, Washington, USA). Seawater pH entering the microcosms was measured daily using the spectrophotometric technique outlined in SOP 6b by Dickson et al. (2007) to confirm pH measurements from the Durafet probe. When any discrepancies were observed, the Durafet probe was recalibrated. Seawater pH measurements were taken from two microcosms per treatment on days 0, 1, and 3. Final pH values reported here have been corrected for dye addition and temperature. Total alkalinity (A_T) was measured following the open cell titration of SOP 3b (Dickson et al. 2007). Samples for A_T were

taken from incoming water and from two microcosms in each treatment on days 0, 2, and 3. CO_2SYS (Robbins et al. 2010) was used to calculate calcium carbonate saturation state (Ω) of aragonite and calcite, carbonate ion concentration, and pCO_2 with A_T and pH as inputs using the following constants: Lueker et al. (2000) for CO_2 constants; Dickson (1990) for $KHSO_4$, total scale (mol kg^{-1} SW) for pH scale; and Wanninkhof (1992) for air–sea flux.

Statistics

Differences in larval size and mortality across treatments were examined using a two-way ANOVA with fixed effects of treatment and day followed by Tukey's Honestly Significant Difference test (Tukey's HSD). A one-way ANOVA was also used to test for differences in larval size among treatments using the combined fixed factor of daytreatment. Larval calcification and developmental stage were compared among treatments using a generalized linear model (GLM). Binomial error distributions were used for GLM analyses. The occurrence of a developmental delay was assessed by fitting the regression of shell height on hinge length to a linear model and testing for differences in the slopes of these lines across treatments. Developmental delay would be demonstrated if the larvae maintained the same allometry across treatments (the slopes of the lines were the same) but were different in size. At least two replicates within treatments and time points were used for all statistical analyses. All analyses were performed in R (R Development Core Team 2011).

Results

Carbonate chemistry

Throughout the experiment, seawater pH differed across treatments and A_T varied slightly but to the same degree across treatments (Table I.1). Mean seawater pH was consistent within but varied among treatments (Fig. I.2). Mean pH (±standard deviation), as measured by the Durafet pH probes (Fig. I.2), was 7.99 ± 0.04 in the Ambient treatment, 7.75 ± 0.06 in the MidCO_2 treatment, and 7.66 ± 0.09 in the HighCO_2 treatment. Aragonite and calcite saturation states were >1.0 for the duration of the experiment, except in the HighCO_2 treatment on days 1 and 2 (Table I.1). Carbonate ion concentration was lowest in the HighCO_2 treatment (average ± SD of 61.15 ± 4.05 µmol

kg^{-1} seawater, N = 4, Table I.1), intermediate in $MidCO_2$ (74.05 ± 6.43 µmol kg^{-1}, N = 4), and highest in the Ambient treatment (120.24 ± 11.52 µmol kg^{-1}, N = 4). Partial pressure of CO_2 in the seawater averaged 468 ± 63 µatm in the Ambient treatment, 847 ± 67 µatm in the $MidCO_2$ treatment, and 1,065 ± 58 µatm in the $HighCO_2$ treatment.

Size, development, and calcification

Survival was near 100 % in all treatments on day 1 (Ambient = 99.0 %, $MidCO_2$ and $HighCO_2$ = 99.7 %). On day 3, survival was 92.9 % in the Ambient treatment and was approximately 88.6 % in the $MidCO_2$ and 85.6 % in the $HighCO_2$ treatment. Mortality was similar across treatments ($F = 0.59$, $P > 0.05$) but different across days ($F = 17.7$, $P < 0.05$).

On day 1, a slightly greater proportion (0.977) of larvae at $HighCO_2$ were at the D-hinge stage (compared with those that were still trocophores), but this difference was not significant (z value = 1.016, P = 0.310; data not shown). The proportion of larvae at the D-hinge stage on day 1 in the Ambient treatment was 0.875 and in $MidCO_2$ was 0.833. Amount of larvae with shell was significantly different among treatments for days 1 and 3 post-fertilization. Following 24 h of treatment (day 1), the proportion of larvae with shell present was inversely proportional to pCO_2 level with the greatest number of larvae with shell in the $HighCO_2$ treatment (z value = 2.084, P = 0.0372, Fig. I.3). On day 3, fewer larvae at $HighCO_2$ conditions had full shell compared with the other two treatments (z value = -3.203, P = 0.00136).

Larval size (shell height and hinge length) was similar across experimental treatments after 24 h; however, by day 3, larvae grew significantly larger (height and length) in the Ambient and $MidCO_2$ as compared to the $HighCO_2$ treatment (Table I.2, Figs. I.4, I.5). Between days 1 and 3, larvae increased in size under Ambient conditions (shell height, P < 1e-7) and $MidCO_2$ conditions (shell height and hinge length, P < 1e-7 and P = 7.4e-6, respectively; Figs. I.4, I.5) but did not significantly increase in size under $HighCO_2$ conditions. By day 3, all larvae observed across treatments were at the D-hinge stage. The slope of the linear regression through shell height versus hinge length for the larvae raised at Ambient pCO_2 was 0.6459 (Fig. I.6), which was not significantly different from the slope of the regression line through the $MidCO_2$ data (0.8583, $P > 0.05$) or from the line through the $HighCO_2$ size data (0.3625, $P > 0.10$).

Discussion

Oyster larvae raised at HighCO_2 showed evidence of a developmental delay by 3 days post-fertilization, which caused them to be smaller and have less calcified material than controls. These results are consistent with other studies of *Crassostrea* spp. larvae in which elevated pCO_2 resulted in decreased growth and shell mineralization (Kurihara et al. 2007; Miller et al. 2009). Kurihara et al. (2007) raised *C. gigas* to 48 h post-fertilization at an elevated pCO_2 of about 2,268 µatm, much higher than pCO_2 projected for the coming century, and observed a negative effect on calcification as early as 24 h post-fertilization. The authors also observed a developmental delay in reaching the D-hinge stage at 48 h post-fertilization (Kurihara et al. 2007). Since we did not measure growth or calcification in our larvae at 48 h post-fertilization, we are not able to draw direct comparisons with this time point, but we did observe a developmental delay by 72 h post-fertilization. Similarly, *C. virginica* larvae raised from 72 h post-fertilization through competency at different pCO_2 grew more slowly at elevated pCO_2 (560 and 800 μatm) and biomineralized less $CaCO_3$ than controls; however, *Crassostrea ariakensis* showed no effect of pCO_2 treatment (Miller et al. 2009). It is likely the observed differences between the studies are related to the much higher pCO_2 level used by Kurihara et al. (2007) and species- and population-specific differences in acclimation to ocean acidification.

The developmental delay is evidenced by similar growth trajectories across treatments (Figs. I.3, I.6) coupled with the smaller size of larvae in the HighCO_2 treatment. This suggests that change in size is not a direct effect of ocean acidification on shell growth and maintenance. In a study comparing faster growing hybrid *C. gigas* larvae to slower growing inbred larvae, slower growth was attributed to reduced feeding rate and differing allocation of internal energy reserves for metabolic processes (Pace et al. 2006). The stress of elevated pCO_2 can induce similar physiological changes via effects on metabolic demands, resulting in a developmentally delayed phenotype (Stumpp et al. 2011a). It is difficult to detect developmental delay with complete confidence in studies that do not follow larvae through to settlement. In one such study, larval *Strongylocentrotus purpuratus* were exposed to elevated pCO_2 throughout their larval period, and from this perspective, it was apparent that ocean acidification caused a

delay in development, although at discrete time points, this delay could be interpreted as overall smaller size (Stumpp et al. 2011a). Developmental delay may give these species the energetic resources they need to survive stress and reach the later developmental stages of metamorphosis and settlement. However, a delay in development opens the possibility for a host of other complications for pelagic larvae, such as greater potential to be advected to unsuitable habitat (Strathmann 1985), greater chance of being exposed to predators (Underwood and Fairweather 1989), and an overall longer time in the water column where environmental conditions are variable and risky for a free-floating larva.

A greater percentage of the larvae in the HighCO_2 treatment had shell present by 24 h post-fertilization compared with both Ambient and MidCO_2. The impact of ocean acidification on larval invertebrates can change in direction and magnitude as the larvae switch from a non-feeding to a feeding stage. The larvae at HighCO_2 were most likely able to maintain a normal developmental rate and calcified structures early in development because an increased metabolic rate would have been supported by sufficient maternal energy resources. In early development, *C. gigas* depend on maternal lipid reserves, but after 24 h in the plankton, the larvae become dependent upon external resources (Gallager et al. 1986). Environmental stress frequently instigates an elevated metabolic rate (Lannig et al. 2010; Stumpp et al. 2011a). During the non-feeding stage, larvae may have enough maternal resources to support their increased metabolic rate and sustain normal or even accelerated growth and development. In the non-feeding lecithotrophic larvae of the common sun star (*Crossaster papposus*), larvae at low pH developed and grew faster than those in ambient conditions (Dupont et al. 2010). Once the metabolic switch to external resources occurs, the larvae may not be able to get enough resources to sustain the increased metabolic rate as well as normal development. A similar trend is seen in larval purple sea urchins, *S. purpuratus*. Ocean acidification had a larger impact on the feeding larval stage of *S. purpuratus* than it did on the non-feeding stage (Stumpp et al. 2011a). Similarly to *C. gigas*, *S. purpuratus* demonstrated a developmental delay starting with the onset of feeding (Stumpp et al. 2011a). At the same time, routine metabolic rate increased in both elevated pCO_2 and ambient treatment, but increased more at low pH (Stumpp et al. 2011a). The results from these studies suggest that the maintenance of homeostasis becomes more difficult under the energetic demands

of ocean acidification stress; however, the physiological stress is realized as developmental delay, with associated phenotypes of less shell and smaller size, only when larvae are in a feeding stage. Reallocation of resources associated with invertebrate responses to ocean acidification has been shown to affect several processes, including as soft tissue growth (Gaylord et al. 2011; Beniash et al. 2010), scope for growth (Stumpp et al. 2011a), and shell integrity (Gaylord et al. 2011; Melzner et al. 2011).

Larval shell formation is closely linked to development and begins by 24 h post-fertilization. Numerous species experience decreased calcification when water is undersaturated with respect to aragonite (Kurihara et al. 2007; Miller et al. 2009; Crim et al. 2011; Gazeau et al. 2011; Byrne et al. 2010a, b), although some species are still able to form apparently normal calcified structures in undersaturated conditions (Dupont et al. 2010; Catarino et al. 2011; Yu et al. 2011). Early *C. gigas* larval shells are made of amorphous calcium carbonate and aragonite (Weiss et al. 2002), two of the more soluble forms of $CaCO_3$ at low pH. Invertebrates are able to control calcification through amorphous mineral precursors and metabolites (Weiss 2011), thus decreasing the potential effects of a corrosive environment. On days 1 and 2, Ω_{Ar} was below 1.0, causing the seawater to be undersaturated with respect to aragonite. Calcification can become energetically costly due to scarcity of CO_3^{2-} ions in the environment and disruption of ionic gradients of the calcifying compartment from changes in H^+. If oyster larvae remove a fixed number of H^+ from their calcifying fluid versus maintaining a fixed ratio of extracellular/intracellular H^+, then their energy budget would be more taxed during environmental hypercapnia (Ries 2011). This added stress on the process of calcification could have contributed to the energy budget shifts that led to a developmental delay.

In this study, *C. gigas* tolerated the MidCO_2 treatment through 3 days post-fertilization. The lack of negative effects on shell formation and maintenance in the larvae from the MidCO_2 treatment suggests that a cut-off of $\Omega_{Ar} < 1.0$ is significant in terms of the ability of this population to biomineralize at this time point in development. It is also possible that the high level of food available to the larvae modulated the impact of ocean acidification and could have led to an underestimation its effect in this treatment (Melzner et al. 2011). An elevated pCO_2 of 750 µatm (Ω_{Ar} of about 1.0) had significant negative effects on hard clam (*Mercenaria mercenaria*) and bay scallop (*Argopecten*

irradians) larvae after about 3 weeks of exposure as evidenced by decreased survival, development, growth, and lipid synthesis (Talmage and Gobler 2011). The comparable exposure conditions in our study ($MidCO_2$) did not have a negative impact over the time period observed. Due to the similarities of carbonate chemistry parameters with Talmage and Gobler (2011), the differential responses observed across species are likely indicative of variability in species, developmental stage tolerances, or length of exposure. Longer experiments in larvae have demonstrated that the negative effects of ocean acidification persist and sometimes worsen in mussels *M. californianus* (Gaylord et al. 2011), urchins *S. purpuratus* (Stumpp et al. 2011a, b), abalone *Haliotis kamtschatkana* (Crim et al. 2011), and oysters, *Crassostrea ariakensis* and *C. virginica* (Miller et al. 2009). The compounding negative effects of ocean acidification during an experiment may be due to a species' decreasing ability to tolerate a specific environmental stress as their metabolic needs change throughout development.

Conclusions

In this study, we observed that an acute, 72-h exposure to the end-of-century projections of ocean acidification ($HighCO_2$) has a negative impact on development in oyster larvae. Additionally, this study revealed that moderate changes in seawater chemistry ($MidCO_2$, about 800 µatm, mean $\Omega_{Ar} > 1.19 \pm 0.10$) did not have an observed significant impact on larvae through 3 days post-fertilization. It appears the effects of an environmental stress, such as ocean acidification, vary depending on developmental and metabolic stage of *C. gigas* larvae. This is most likely directly associated with a switch in larval energy metabolism as the oysters develop from a non-feeding stage to a feeding stage. In order to effectively evaluate the possibility of acclimation or adaptation, future research should focus on characterizing larvae from diverse genotypes and locations as well as assessing any influences that might be experienced later in development.

Tables

Table I.1. Salinity, total alkalinity (A_T), and spectrophotometric pH are point measurements taken each day. Partial pressure CO_2, Ω, and CO_3^{2-} were calculated from

spectrophotometric pH and A_T. Mean and standard deviation (μ±SD) for the following parameters are given for all 3 days: temperature, salinity, A_T, pH, pCO_2, and CO_3^{2-}.

Treatment	Day	Temperature (°C)	Salinity (ppt)	Total Alkalinity (μmol/kg)	pH (Durafet)	pH (spec)	pCO_2 (μatm)	Ω (calcite)	Ω (aragonite)	CO_3^{2-} (μmol/kg)
	0	20.38	28.13	1998.72	7.95	7.90	557.22	2.62	1.67	104.27
	1	20.50	27.97	2005.28	7.99	7.97	466.27	2.14	1.36	120.26
Ambient	2	20.49	28.16	1965.59	7.96	8.00	420.92	3.15	2.01	125.38
	3	20.46	28.91	2021.96	8.00	8.00	428.43	3.27	2.10	131.03
	μ±SD	*20.46±0.05*	*28.29±0.42*	*1997.89±23.65*	*7.99±0.04*		*468±63*			*120.24±11.52*
	0	20.00	28.13	2003.25	7.75	7.73	860.92	1.83	1.17	72.79
	1	20.25	27.97	1983.64	7.73	7.75	812.40	1.90	1.21	75.48
$MidCO_2$	2	20.18	28.16	1969.06	7.78	7.69	935.39	1.66	1.06	66.21
	3	20.14	28.91	2022.46	7.77	7.77	780.96	2.04	1.31	81.73
	μ±SD	*20.14±0.11*	*28.29±0.42*	*1994.60±23.26*	*7.75±0.06*		*847±67*			*74.05±6.43*
	0	20.25	28.13	2001.57	7.67	7.66	1025.33	1.59	1.02	63.28
	1	20.47	27.97	1979.61	7.64	7.61	1149.99	1.42	0.91	56.46
$HighCO_2$	2	20.10	28.16	1966.46	7.70	7.64	1057.36	1.49	0.95	59.30
	3	20.41	28.91	2023.45	7.64	7.66	1030.70	1.64	1.05	65.54
	μ±SD	*20.31±0.17*	*28.29±0.42*	*1992.77±25.06*	*7.66±0.09*		*1065±58*			*61.15±4.05*

Table I.2. Results from post hoc Tukey's HSD following ANOVA for comparisons of hinge length and shell height among treatments.

		Hinge Length		Shell Height	
	Treatment	*$MidCO_2$*	*$HighCO_2$*	*$MidCO_2$*	*$HighCO_2$*
2-way ANOVA	*Ambient*	0.250	0.0362	0.985	<<0.001
	$MidCO_2$	-	<<0.001	-	<<0.001
1-way ANOVA Day 1	*Ambient*	0.849	0.984	0.585	0.885
	$MidCO_2$	-	0.993	-	0.992
1-way ANOVA Day 3	*Ambient*	0.565	0.0311	0.261	<<0.001
	$MidCO_2$	-	<<0.001	-	<<0.001

Figures

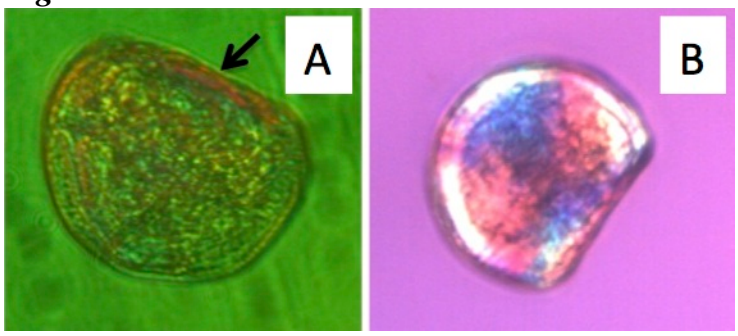

Figure I.1. D-hinge larvae under polarized light portraying calcification at the hinge without a Maltese cross in the shell (a) and full calcification as evidenced by the Maltese cross (b).

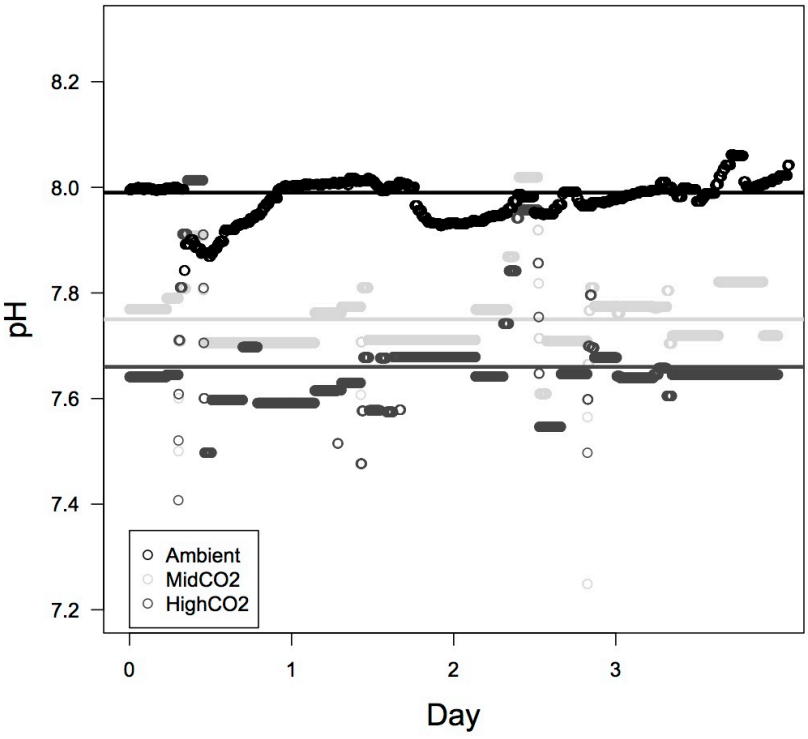

Figure I.2. Profiles of pH measurements in the three different treatments – Ambient (black), MidCO_2 (light gray), and HighCO_2 (dark gray). Average pH for the experiment

for each treatment is represented by solid lines. The DuraFET probes recorded pH measurements every minute.

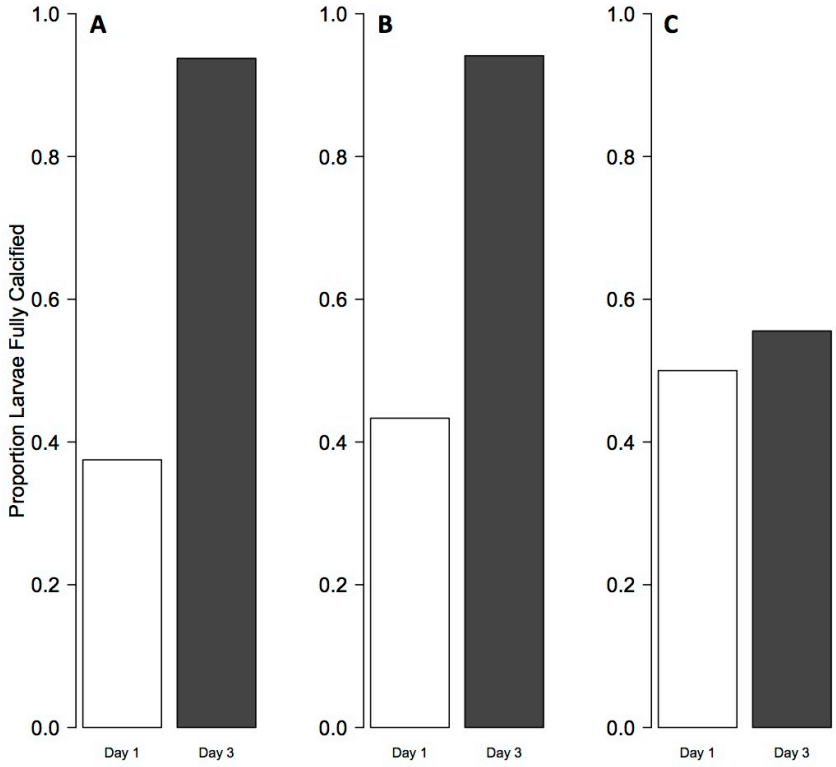

Figure I.3. Proportion of calcified larvae at different pCO_2 treatments. Bars represent calcification on day 1 (white) and day 3 (gray). Proportion of larvae calcified are provided from the Ambient treatment (panel A), MidCO_2 treatment (panel B), and HighCO_2 treatment (panel C). There is a significant difference in calcification among treatments, with the highest proportion of larvae calcified at HighCO_2 on day 1 and the fewest larvae calcified in HighCO_2 on day 3.

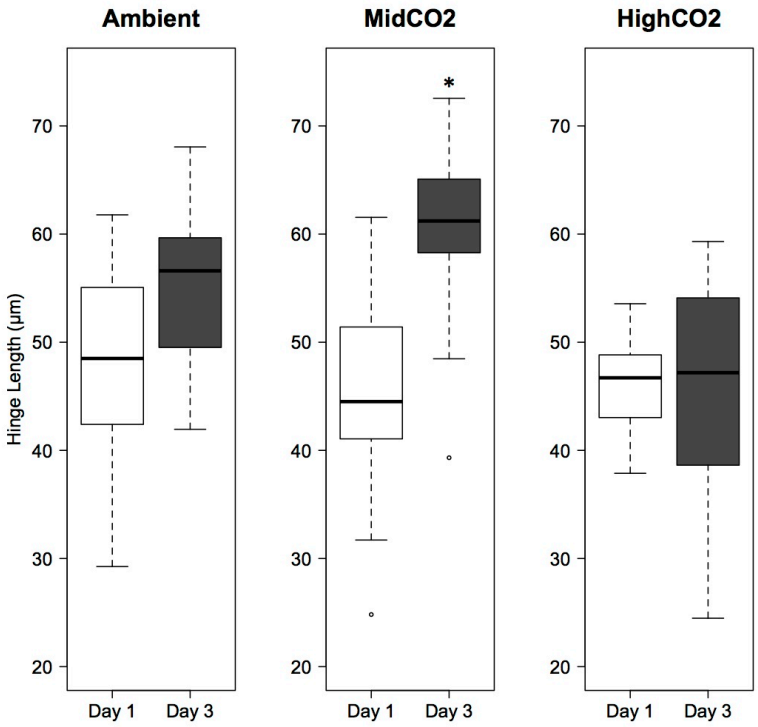

Figure I.4. Larval hinge length on day 1 (white boxplots) and day 3 (gray boxplots). Results are shown for the Ambient treatment, MidCO_2 treatment, and HighCO_2 treatment. Boxplots contain the middle 50% of the data and dashed lines encompass the data with 1.5x the spread of the middle 50%. Open circles represent outliers. Horizontal black bars indicate median values. An asterisk indicates significant differences within a treatment. On day 3, larvae in the HighCO_2 treatment were significantly smaller than those in the other two treatments ($P < 0.05$).

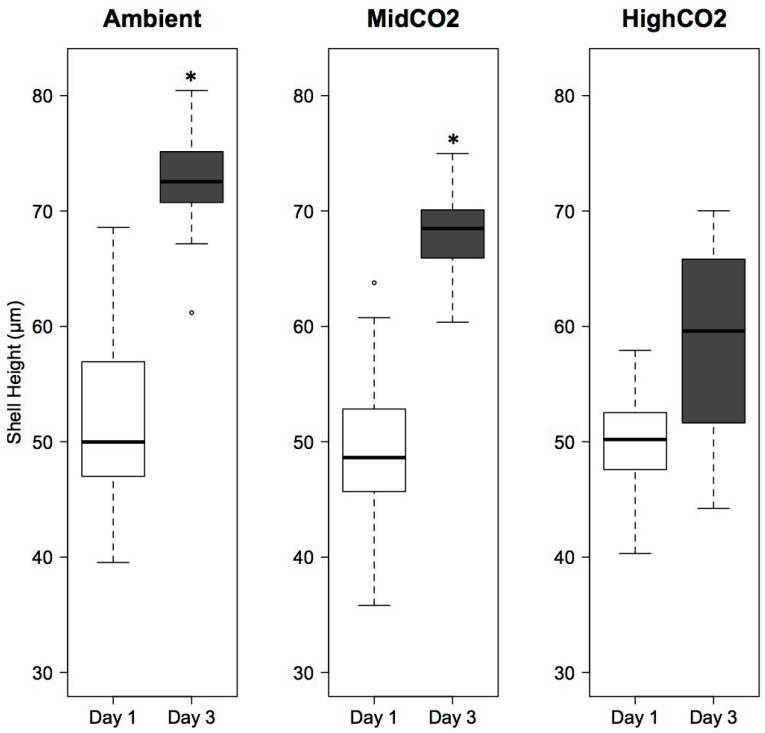

Figure I.5. Larval shell height on day 1 (white boxplots) and day 3 (gray boxplots). Results are shown for the Ambient treatment, MidCO_2 treatment, and HighCO_2 treatment. Boxplots contain the middle 50% of the data and dashed lines encompass the data with 1.5x the spread of the middle 50%. Open circles represent outliers. Horizontal black bars indicate median values. An asterisk indicates significant differences within a treatment. On day 3, shell height was reduced in larvae at HighCO_2 relative to those raised at Ambient and at MidCO_2 ($P < 0.01$).

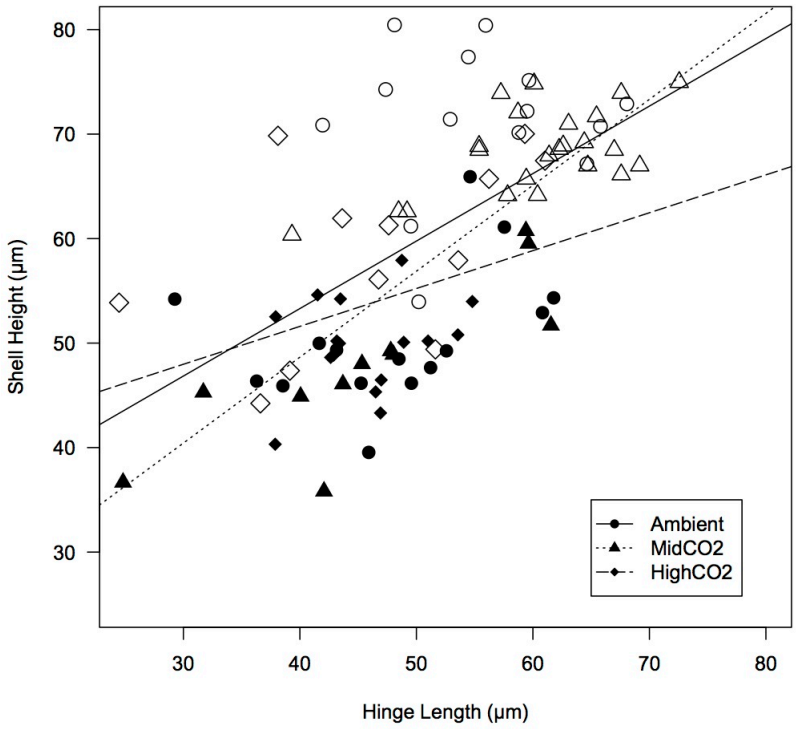

Figure I.6. Regression of larval shell height on hinge length by treatment and day. Data from larvae raised under Ambient pCO_2 conditions are represented by circles, MidCO_2 are triangles, and HighCO_2 are diamonds. Size data from day 1 are in black and day 3 are in white. The solid line is the regression line for Ambient data (intercept = 27.47, slope = 0.65), dotted for MidCO_2 (intercept = 15.76, slope = 0.82), and dashed for HighCO_2 (intercept = 37.10, slope = 0.36). The slopes of all lines are statistically the same ($P > 0.05$).

Acknowledgements

We would like to thank Drs. Ken Sebens and Emily Carrington for use of lab space and facilities at Friday Harbor Labs. Support from National Science Foundation grant EF1041213 to Dr. Carrington funded the construction of the ocean acidification system and analytical equipment used in this study. National Oceanographic and Atmospheric Administration Saltonstall-Kennedy Program grant # NA09NMF4270093 to Dr. Steven Roberts and Dr. Carolyn Friedman also supported this research project. Matt George, Laura Newcomb, and Michelle Herko provided help with maintenance of the ocean acidification system, larval care, and water chemistry analysis, respectively. Thank you to Dr. Richard Strathmann for his advice on larval care and to Dr. Billie Swalla for advice on fixation and for use of her lab space. Dr. Brent Vadopalas and Dr. Loveday Conquest

were incredibly helpful with advice on statistical analysis. Lisa Crosson, Mackenzie Gavery, Caroline Storer, and Sam White provided valuable, critical feedback during the writing process. We are very appreciative of the thorough and helpful comments from two anonymous reviewers and from the editor of this issue, Dr. Sam Dupont.

Works Cited

Banks SC, Ling SD, Johnson CR, Piggott MP, Williamson JE, Behergegaray LB (2010) Genetic structure of a recent climate change-driven range extension. Molecular Ecology 19: 2011-2024

Barton A, Hales B, Waldbusser G, Langdon C, Feely RA (2012) The Pacific oyster, Crassostrea gigas, shows negative correlation to naturally elevated carbon dioxide levels: Implications for near-term ocean acidification impacts. Limnology and Oceanography 57: 698-710

Beniash E, Ivanina A, Lieb NS, Kurochkin Il, Sokolova IM (2010) Elevated levels of carbon dioxide affects metabolism and shell formation in oysters Crassostrea virginica. Marine Ecology Progress Series 419: 95-108

Bonar DB, Coon SL, Walch M, Weiner RM, Fitt W (1990) Control of oyster settlement and metamorphosis by endogenous and exogenous chemical cues. Bulletin of Marine Science 46: 484-498.

Byrne M, Ho M, Wong E, Soars NA, Selyakumaraswamy P, Shepard-Brennand H, Dworjanyn SA, David AR (2010). Unshelled abalone and corrupted urchins: development of marine calcifiers in a changing ocean. Proc R Soc B. doi:10.1098/rspb.2010.2404.

Byrne RH, Mecking S, Feely RA, Liu X (2010). Direct observations of basin-wide acidification of the North Pacific Ocean. Geophysical Research Letters. doi:10.1029/2009GL040999

Caldeira K, Wickett ME (2003) Anthropogenic carbon and ocean pH. Nature 425:365.

Catarino AI, De Ridder C, Gonzalez M, Gallardo P, Dubois P (2011) Sea urchin Arbacia dufresnei (Blainville 1825) larvae response to ocean acidification. Polar Biology. doi: 10.1007/s00300-011-1074-2

Coen LD, Luckenbach MW (2000) Developing success criteria and goals for evaluating oyster reef restoration: Ecological function or resource exploitation? Ecological Engineering 15: 323-343

Crim RN, Sunday JM, Harley CDG (2011) Elevated seawater CO2 concentrations impair larval development and reduce larval survival in endangered northern abalone (Haliotis kamtschatkana). Journal of Experimental Marine Biology and Ecology 400: 272-277

Dickson AG, Sabine CL, Christian JR (2007) Guide to best practices for ocean CO2 measurements. Sidney, British Columbia, North Pacific Marine Science Organization, 176 pp.

Dupont S, Lundve B, Thorndyke M (2010) Near future ocean acidification increases growth rate of the lecithotrophic larvae and juveniles of the sea star Crossaster papposus. J Exp Zool (Mol Dev Evol) 314B: 382-389

Elston RA, Hasegawa H, Humphrey KL, Polyak IK, Häse CC (2008) Re-emergence of Vibrio tubiashii in bivalve aquaculture: severity, environmental drivers, geographic extent, and management. Dis Aquat Org 82: 119-134

FAO Fisheries and Aquaculture Department (2010) World aquaculture 2010. FAO Fisheries and Aquaculture Department. Technical Paper. No. 500/1. Rome, FAO. 2011. 105 pp.

Fassbender AJ, Sabine CL, Feely RA, Langdon C, Mordy CW (2011) Inorganic carbon dynamics during northern California coastal upwelling. Continental Shelf Research 31: 1180-1192

Feely RA, Alin SR, Newton J, Sabine CL, Warner M, Devol A, Krembs C, Maloy C (2010) The combined effects of ocean acidification, mixing, and respiration on pH and carbonate saturation in an urbanized estuary. Estuarine, Coastal and Shelf Science 88: 442-449

Feely RA, Sabine CL, Hernandez-Ayon JM, Ianson D, Hales B (2008) Evidence for upwelling of corrosive "acidified" water onto the continental shelf. Science 320: 1490-1492

Gallager SM, Mann R, Sasaki GC (1986) Lipid as an index of growth and viability in three species of bivalve larvae. Aquaculture 56: 81-103

Gaylord B, Hill TM, Sanford E, Lenz EA, Jacobs LA, Sato KN, Russell AN, Hettinger A (2011) Functional impacts of ocean acidification in an ecologically critical foundation species. J Exp boil 214: 2586-2594

Gazeau F, Gattuso J-P, Greaves M, Elderfield H, Peene J, Heip CHR, Middelburg JJ (2011) Effects of carbonate chemistry alteration on early embryonic development of the Pacific oyster (Crassostrea gigas). PLoS One doi:10.1371/journal.pone.0023010

Hauri C, Gruber N, Plattner G-K, Alin S, Feely RA, Hales B, Wheeler PA (2009) Ocean acidification in the California Current System. Oceanography 22: 60-71

Henry RP, Kormanik GA, Smatresk NJ, Cameron JN (1981) The role of $CaCO_3$ dissolution as a source of HCO_3^- for the buffering of hypercapnic acidosis in aquatic and terrestrial decapod crustaceans. J Exp Biol 94: 269-273.

Intergovernmental Panel on Climate Change (IPCC) (2007) Contribution of Working Groups I, II, and III to the Fourth Assessment Report of the Intergovernmental Panel on Climate Change. Pachauri, R.K., Reisinger, A. (Eds.), IPCC, Geneva, Switzerland, pp. 104

Kurihara H, Kato S, Ishimatsu A. (2007) Effects of increased seawater pCO_2 on early development of the oysters Crassostrea gigas. Aquatic Biology 1: 91-98

LaBarbera M (1974) Calcification of the first larval shell of Tridacna squamosa (Tridacnidae: Bivalvia). Mar Biol 25: 233-238

Lannig G, Eilers S, Pörtner HO, Sokolova IM, Bock C (2010) Impact of ocean acidification on energy metabolism of Oyster, Crassostrea gigas-Changes in metabolic pathways and thermal response. Mar Drugs 8: 2318-2339

Marchant HK, Calosi P, Spicer JI (2010) Short-term exposure to hypercapnia does not compromise feeding, acid-base balance or respiration of Patella vulgata but surprisingly is accompanied by radula damage. Journal of the Marine Biological Association of the United Kingdom 90: 1379-1384

Melzner F, STange P, Trubenbach K, Thomsen J, Casties I, Panknin U, Gorb SN, Gutowska MA (2011) Food supply and seawater pCO_2 impact calcification and internal shell dissolution in the blue mussel Mytilus edulis. PLoS ONE 6: e24223. doi:10.1371/journal.pone.0024223

Miller AW, Reynolds AC, Sobrino C, Riedel GF (2009) Shellfish face uncertain future in high CO_2 world: Influence of acidification on oyster larvae calcification and growth in estuaries. PLoS ONE 4: e5661. doi:10.1371/journal.pone.0005661

Miles H, Widdicombe S, Spicer JI, Hall-Spencer J (2007) Effects of anthropogenic seawater acidification on acid-base balance in the sea urchin Psammechinus miliaris. Marine Pollution Bulletin 54: 89-96

Narita D, Rehdanz K, Tol RSJ (2012) Economic costs of ocean acidification: a look into the impacts on global shellfish production. Climatic Change. doi:10.1007/s10584-011-0383-3

O'Donnell MJ, Hammond LM, Hofmann GE (2009) Predicted impact of ocean acidification on a marine invertebrate: elevated CO_2 alters response to thermal stress in sea urchin larvae. Mar Biol 156: 439-446

Pace DA, Marsh AG, Leong PK, GreenAJ, Hedgecock D, Manahan DT (2006) Physiological bases of energetically determined variation in growth of marine invertebrate larvae: A study of growth heterosis in the bivalve Crassostrea gigas. Journal of Experimental Marine Biology and Ecology 335: 188-209.

Pane EF, Barry JP (2007) Extracellular acid-base regulation during short-term hypercapnia is effective in a shallow-water crab, but ineffective in a deep-sea crab. Mar Ecol Prog Ser 334: 1-9

Parker LM, Ross PM, O'Connor WA (2010) comparing the effect of elevated pCO_2 and temperature on the fertilization and early development of two species of oysters. Mar Biol 157: 2435-2452

Parker LM, Ross PM, O'Connor WA, Borysko L, Raftos DA, Portner H-O (2012) Adult exposure influences offspring response to ocean acidification in oysters. Global Change Biology 18: 82-92

Perry A, Low PJ, Ellis JR, Reynolds JD (2005) Climate change and distribution shifts in marine fishes. Science 308:1912-1915

Ries JB (2011) A physicochemical framework for interpreting the biological calcification response to CO_2-induced ocean acidification. Geochimica et Cosmochimica Acta 75: 4053-4064.

Robbins LL, Hansen ME, Kleypas JA,Meylan SC (2010) CO2calc: A User-Friendly Carbon Calculator for Windows, Mac OS X, and iOS (iPhone): U.S. Geological Survey Open File Report 2010-1280, 42pp.

Strathmann RR (1985) Feeding and nonfeeding larval development and life-history evolution in marine invertebrates. Ann. Rev. Ecol. Syst. 16: 339-361

Stumpp M, Wren J, Melzner F, Thorndyke MC, Dupont ST (2011a) CO_2 induced seawater acidification impacts sea urchin larval development I: Elevated metabolic rates decrease scope for growth and induce developmental delay Comparative Biochemistry and Physiology – Part A: Molecular and Integrative Physiology 160: 331-340

Stumpp M, Dupont ST, Thorndyke MC, Melzner F (2011b) CO_2 induced seawater acidification impacts sea urchin larval development II: Gene expression patterns in pluteus larvae. Comparative Biochemistry and Physiology – Part A: Molecular and Integrative Physiology 160: 320-330

Talmage SC, Gobler CJ (2011) Effects of elevated temperature and carbon dioxide on the growth and survival of larvae and juveniles of three species of northwest Atlantic bivalves. PLoS One doi: 10.1371/journal.pone.0026941

Thomsen J, Melzner F (2010) Moderate seawater acidification does not elicit long-term metabolic depression in the blue mussel Mytilus edulis. Mar Biol 157: 2667-2676

Tomanek L, Zuzow MJ, Ivanina AV, Beniash E, Sokolova IM (2011) Proteomic response to elevated P_{CO2} level in eastern oysters, Crassostrea virginica: evidence for oxidative stress. J Exp Biol 214: 1836-1844

Underwood AJ, Fairweather PG (1989) Supply-side ecology and benthic marine assemblages. Trends in Ecology and Evolution 4: 16-20

Watson S-A, Southgate PC, Tyler PA, Peck LS (2009) Early larval development of the Sydney rock oyster *Saccostrea glomerata* under near-future predictions of CO_2-driven ocean acidification. Journal of Shellfish Research 28: 431-437

Weiss IM (2011) Biomaterials: Metabolites empowering minerals. Nature Chemical Biology 7: 192-193.

Weiss IM, Tuross N, Addadi L, Weiner S (2002) Mollusc larval shell formation: Amorphous calcium carbonate is a precursor phase for aragonite. J Exp Zool 293: 478-491

Wong KKW, Lane AC, Leung PTY, Thiyagarajan V (2011) Response of larval barnacle proteome to CO_2-driven seawater acidification. Comparative Biochemistry and Physiology Part D: Genomics and Proteomics 6: 310-321

Yu PC, Matson PG, Martz TR, Hofmann GE (2011) The ocean acidification seascape and its relationship to the performance of calcifying marine invertebrates: Laboratory experiments on the development of urchin larvae framed by environmentally-relevant pCO_2/pH. Journal of Experimental Marine Biology and Ecology 400: 288-295

Chapter II: Shotgun proteomics as a viable approach for biological discovery in the Pacific oyster

Published in Conservation Physiology as: Timmins-Schiffman, E., Nunn, B.L., Goodlett, D.R., and Roberts, S.B. 2013. Shotgun proteomics as a viable approach for biological discovery in the Pacific oyster. Conserv Physiol, 1. doi 10.1093/conphys/cot009

Abstract

Shotgun proteomics offers an efficient means to characterize proteins in a complex mixture, particularly when sufficient genomic resources are available. In order to assess the practical application of shotgun proteomics in the Pacific oyster (*Crassostrea gigas*), liquid chromatography coupled with tandem mass spectrometry was used to characterize the gill proteome. Using information from the recently published Pacific oyster genome, 1043 proteins were identified. Biological samples ($n = 4$) and corresponding technical replicates (three) were similar in both specific proteins identified and expression, as determined by normalized spectral abundance factor. A majority of the proteins identified (703) were present in all biological samples. Functional analysis of the protein repertoire illustrates that these proteins represent a wide range of biological processes, supporting the dynamic function of the gill. These insights are important for understanding environmental influences on the oyster, because the gill tissue acts as the interface between the oyster and its environment. *In silico* analysis indicated that this sequencing effort identified a large proportion of the complete gill proteome. Together, these data demonstrate that shotgun sequencing is a viable approach for biological discovery and will play an important role in future studies of oyster physiology.

Introduction

Fluctuations in gene and protein expression can be sensitive and specific indicators of biological processes. At the transcript level, several methodologies can be used to characterize expression from the gene-centric to systems level, including quantitative PCR (e.g. Griffitt *et al*., 2006; Stumpp *et al*., 2011), microarrays (e.g. Todgham and Hofmann, 2009; Lockwood *et al*., 2010), and high-throughput sequencing (e.g. Polato *et al*., 2011; Philipp *et al*., 2012). The use of high-throughput sequencing technology has exponentially increased available genome and transcript information for

taxa of ecological interest in recent years. While these results provide an accurate portrayal of changes at the molecular level, it is common that proteins have a more direct role in regulating physiological processes and responding to environmental change.

Historically, there have been several technical and analytical challenges in characterizing global protein expression. One challenge is the need to have sufficient genomic resources available to describe proteins of interest. Specifically, protein sequencing generally produces short amino acid fragments that require a known corresponding gene for identification and annotation purposes. However, lack of genomic resources has not completely hampered proteomic studies. For example, researchers characterized the physiological response of *Gillichthys mirabilis* gill tissue exposed to osmotic and temperature stress using two-dimensional gel electrophoresis without sequencing proteins (Kültz and Somero, 1996). In another study, researchers used surface enhanced laser desorption/ionization and identified 11 differentially expressed proteins in the gill tissue of *Oncorhynchus mykiss* exposed to zinc stress (Hogstrand *et al*., 2002). Four proteins were identified based on a combination of their physical properties (i.e. mass and binding) coupled with sequence similarity comparisons with the limited number of teleost protein sequences in the SwissProt database (Hogstrand *et al*., 2002).

The use of predicted protein sequences in closely related species can assist in annotation, but species-specific information will provide more accurate results. This is evident in a study on protein expression in pea (*Pisum sativum*) chloroplasts, where concurrent complementary DNA sequencing facilitated the identification of a greater number of proteins compared with identification through homology searches with closely related model species (Bräutigam *et al*., 2008). The reason that species-specific information provides such an advantage is due to how modern-day protein sequence identification is executed. The vast majority of high-throughput mass spectrometry (MS) proteomics is accomplished by matching observed peptide fragmentation patterns (tandem mass spectra) to theoretical spectra. This is possible because peptides fragment in a predictable manner, allowing for theoretical tandem mass spectra to be created *in silico* from a given protein sequence, stressing the importance of the database used. These correlation-based algorithms require the peptide mass (precursor mass) and peptide

fragmentation (tandem mass spectrum). Even when employing databases of closely related species, a large number of viable tandem mass spectra of peptides might not be assigned accurately to a protein, because a single amino acid mutation could significantly alter the peptide mass and resulting fragmentation pattern.

As technological advances have continued to increase the accessibility of whole transcriptomes and genomes to researchers, there is increasing interest in leveraging these data to carry out proteomic studies for both biological discovery and for better characterizing physiological responses to environmental change. Recently, the Pacific oyster (*Crassostrea gigas*) genome was sequenced (Zhang *et al*., 2012). Given the availability of this resource, our objective was to quantify the level of information (and respective variability) attainable in proteomic studies in oysters. There have been several prior studies examining protein expression in oysters using liquid chromatography coupled with tandem mass spectrometry (LC-MS/MS) with samples separated by two-dimensional gel electrophoresis (2-DE) beforehand. In larval oysters, these proteomic techniques have identified specific proteins that are responsible for early developmental changes in *C. gigas* (Huan *et al*., 2012) and the larval *C. gigas* response to elevated partial pressures of CO_2 (ocean acidification; Dineshram *et al*., 2012). These methods have also been used to identify and sequence proteins that are differentially regulated in a range of physiological situations in adult oyster species. The discoveries include the following: the up-regulation of antioxidant proteins in response to ocean acidification (Tomanek *et al*., 2011); expression profiles denoting high-quality oocytes (Corporeau *et al*., 2012); differing proteomic profiles between disease-resistant and disease-susceptible oysters (Simonian *et al*., 2009); and specific responses to metal exposure (Thompson *et al*., 2011, 2012a, 2012b; Liu and Wang, 2012) and acid sulfate run-off (Amaral *et al*., 2012). These seminal studies in marine invertebrate proteomics demonstrate that analysis of global protein expression is a powerful tool to facilitate our understanding of the molecular physiological response to environmental stressors.

An alternative to 2-DE approaches is to perform shotgun proteomics. Shotgun proteomics is the sequencing of a complex mixture of peptides using LC-MS/MS without prior separation (i.e. 2-DE). One of the main advantages of using 2-DE methods is that information on the physical properties of the proteins (mass and isoelectric point) can be

used in the protein identification, whereas these empirical data are lost in the strictly tandem MS approaches. However, tandem MS has significantly greater data efficiency than gel-based approaches. The use of shotgun proteomics allows for a greater number of proteins to be identified rapidly from a single sample, providing a more complete metabolic picture of cellular function and physiology. This method has been demonstrated by Muralidharan *et al*. (2012), who used shotgun proteomics to uncover *Saccostrea glomerata* haemocyte proteomic responses to metal contamination, and by Dheilly *et al*. (2012, 2013), who explored the proteomic response of coelomocytes to immune challenge in two urchin species.

In this study, we used shotgun proteomics to sequence the gill proteome of the Pacific oyster, *Crassostrea gigas*. The gill is the interface between bivalves and their environment, necessitating that the tissue performs a variety of physiological functions in response to the environment (e.g. David *et al*., 2007; Wang *et al*., 2010). The identification of proteins that are expressed in gill tissue supports the development of tools that can help to guide future research on the molecular physiology of molluscs faced with stresses such as climate change and disease. The goal of this study was to determine the effectiveness of using a shotgun proteomics approach and to carry out functional characterization of proteins expressed in gill tissue.

Methods

Oysters

Pacific oysters (*C. gigas*, 11 months old) were collected in Shelton, WA, USA. Oysters were transferred to Friday Harbor Laboratories (Friday Harbor, WA, USA) into a flow-through system at 13°C for 6 weeks. Eight 4 L vessels containing six oysters each were kept in a water bath with seawater flowing through at 57.5 ml min^{-1}. Vessels were cleaned every other day with fresh-water and salt-water rinses. Oysters were fed Shellfish Diet 1800 (Reed Mariculture, Campbell, CA, USA). At the end of six weeks, gill tissue was removed from four oysters and immediately flash frozen in liquid nitrogen for proteomic analysis.

Protein digestion and desalting

Gill tissue samples (50–100 mg) were homogenized in 50 mM NH_4HCO_3 (100 µl) using RNAse-free plastic pestles. Each homogenized gill sample was sonicated four times with a probe sonicator and stored on dry ice between sonications. After sonication, protein concentrations were measured using the Bradford assay, following the manufacturer's protocol (Pierce, Thermo Fisher Scientific, Rockford, IL, USA). Urea (36 mg) was added to each sample (for a total concentration of 6 M) to denature and solubilize peptides. Next, 1.5 M Tris (pH 8.8; 6.6 µl) was added, followed by 200 mM (*tris*(2-carboxyethyl)phosphine) (2.5 µl). Samples were incubated for 1 h at 37°C on a shaker. To alkylate the proteins, 200 mM iodoacetamide (20 µl) was added. Samples were then vortexed, and incubated for 1 h at room temperature in the dark. To absorb excess iodoacetamide, 200 mM dithiolthreitol (20 µl) was added, followed by vortexing and incubation at room temperature for 1 h. A volume equal to approximately 100 µg was removed, and the remainder was discarded. Ammonium bicarbonate (200 µl of 25 mM) was added to dilute the urea, and then high-pressure liquid chromagography (HPLC) grade MeOH (50 µl) was added to each tube. Trypsin was solubilized in a trypsin dilution buffer (20 µl) to a concentration of 1 µg/µl (Promega, Madison, WI, USA), and 3 µl of this solution was added to each sample to digest the proteins enzymatically. The samples were incubated overnight at 37°C. The next day, dilute formic acid was added, and the samples were evaporated on the speed vac to near dryness. Samples were reconstituted in 200 µl of 5% acetonitrile and 0.1% trifluoroacetic acid.

Samples were desalted by passage through a pre-prepared MacroSpin column, following the manufacturer's specifications (The Nest Group, Southborough, MA, USA). After desalting, the remaining solvent was evaporated using a speed vac.

Liquid chromatography and tandem mass spectrometry

Mass spectrometry was performed at the University of Washington Proteomics Resource (Seattle, WA, USA). Samples were resuspended in 2% acetonitrile and 0.1% formic acid in water (100 µl). Samples were then vortexed to mix and spun down at 21130 × g for 10 min. The supernatant was aliquoted to autosampler vials. Nano LC separation was performed with a nanoACUITY system (Waters, Milford, MA, USA) interfaced to an LTQ Orbitrap XL mass spectrometer (Thermo Scientific, San Jose, CA,

USA). Peptides were trapped on a 100 μm i.d. × 20 mm long pre-column packed with 200 Å (5 μm) Magic C18 particles (C18AQ; Michrom, Auburn, CA, USA). For separation, a 75 μm i.d. × 250 mm long analytical column with a laser pulled emitter tip packed with 100 Å (5 μm) Magic C18 particles (C18Q; Michrom) was used and analysed in positive ion mode. For each LC-MS/ MS analysis, an estimated amount of 0.5 μg of peptides was loaded onto the pre-column at 2 μl min^{-1} in water/acetonitrile (98%/2%), with 0.1% (v/v) formic acid. Peptides were eluted using an acetonitrile gradient flowing at 240 nl min^{-1}, using a mobile phase consisting of the following components: Solvent C (water, 0.1% formic acid) and Solvent D (acetonitrile, 0.1% formic acid). The gradient programme was as follows: 0–1 min, Solvent C (98%) and Solvent D (2%); 1 min, Solvent C (90%) and Solvent D (10%); 90 min, Solvent C (65%) and Solvent D (35%); 91–101 min, Solvent C (20%) and Solvent D (80%); and 102–120 min, Solvent C (98%) and Solvent D (2%). Peptide spectra were acquired by scans in the Orbitrap followed by the ion trap.

Data acquisition

High-resolution full precursor ion scans were acquired at 60 000 resolution in the Orbitrap over 400–2000 *m/z* while six consecutive tandem mass spectra were acquired by collision-induced dissociation in the linear ion trap (LTQ). The data-dependent ion threshold was set at 5000 counts for MS/ MS, and the maximum allowed ion accumulation times were 400 ms for full scans and 100 ms for MS/MS measurements. The number of ions accumulated was set to 1E6 for Orbitrap scans and 1E4 for linear ion trap MS/MS scans. An angiotensin and neurotensin standard was run after every eight injections. Each sample was injected in triplicate in a novel randomized order.

Protein identification and data analysis

Peptide sequence and corresponding protein identification for all mass spectra was carried out using SEQUEST (Eng *et al*., 1994) and the *C. gigas* proteome version 9 (Zhang *et al*., 2012, http://dx.doi.org/10.5524/100030). A DECOY database was created by reversing the *C. gigas* proteome and adding it to the forward database. This was completed in order to determine false positive matches of peptide spectra matching, and

yielded a false discovery rate of ~0.6%. Search parameters included trypsin as the assigned enzyme and a precursor mass accuracy of ±3 Da. SEQUEST results were analysed using PeptideProphet and ProteinProphet in order to evaluate peptide matches statistically and assign protein probabilities (Nesvizhskii *et al*., 2003). Only proteins with a probability of ≥0.9 (estimated false discovery rate of 0.6%), a minimum of two unique peptide hits within a single replicate, and a minimum of four total tandem mass spectral assignments in the combined technical and biological replicates were used in further characterizations described below.

In order to annotate corresponding proteins, the *C. gigas* proteome (version 9) was compared with the UniProtKB/ Swiss-Prot database (www.uniprot.org) using Blastp with an e-value limit of 1E-10. Associated gene ontology (GO) terms were used to classify sequences based on biological process, as well as to categorize genes into parent categories (GO Slim). Enrichment analysis was used to identify over-represented biological processes in the gill proteome compared with the entire proteome [Database for Annotation, Visualization and Integrated Discovery (DAVID), version 6.7; Huang *et al*., 2009a, 2009b, http://david.abcc.ncifcrf. gov/]. The results of the enrichment analysis were visualized in REViGO (Reduce and Visualize Gene Ontology; Supek *et al*., 2011, http://revigo.irb.hr/). Normalized spectral abundance factor (NSAF; Florens *et al*., 2006) was used to calculate expression for each protein in each oyster. Technical replicates were pooled by taking the sum of total independent tandem mass spectra for each protein (SpC). For each protein, SpC was divided by protein length (*L*). The NSAF is calculated from SpC/*L* divided by the sum of all SpC/*L* values for the proteins for a particular oyster. Comparisons of proteins identified across biological samples were visualized using Venny (Oliveros, 2007).

The minimum number of peptides needed to be sequenced to optimize unique protein identifications was determined using an *in silico* approach. A list was constructed of all sequenced peptides and their matching protein identification. Redundancies were maintained in this list, so that if a certain peptide was sequenced multiple times it was included multiple times in the list. Randomized subsets of this list were generated using the sample function in R (R Development Core Team, 2009). The number of hypothetically sequenced peptides in these lists ranged from 500 to 70 000. A plot was

generated to visualize the relationship between each sample size of randomly chosen peptides and the number of unique proteins identified.

Results

A combined total of 175 818 tandem MS spectra were generated across all four biological and three technical replicates using the Orbitrap mass spectrometer (Table II.1). Expression values were comparable between biological replicates, with r^2 ranging from 0.800 to 0.889 (Supplementary Data II.1). A total of 54 521 unique peptides contributed to the identification of 2850 proteins, with a probability score threshold of 0.9 (Supplementary Data II.2). Of these proteins, 1043 had at least two unique peptide hits and four tandem mass spectra in the combined replicates. The mean coverage of proteins by sequenced amino acids was 13.3%. Protein identifications for each injection, including protein probability scores, number of total and unique spectra, and peptide sequences, are provided in Supplementary Data II.3. The NSAF values for each protein are provided in Supplementary Data II.4.

For all biological samples, the number of proteins identified in each technical replicate was consistent with minimal standard deviation (1.2–3.5%). In each biological replicate, the proteins were identified from between 43 275 and 44 720 sequenced peptides (standard deviation as a percentage of the mean ranged from 4.8 to 7.4%). For each oyster, 54–55% of the identified proteins were present in all three technical replicates. Using spectral counts as a proxy for relative expression, protein expression levels were consistent across technical replicates (Fig. II.1).

The number of proteins identified in each oyster (after pooling technical replicates; see Methods) was 923, 959, 883, and 875 (Table II.1). Most proteins (n = 703) were identified across all biological samples (Fig. II.2).

In order to evaluate general protein expression and assess sample variability, the 10 most highly expressed proteins in each oyster were identified. There was not complete overlap in this group of proteins among the four oysters, so that a total of 12 proteins represent the most highly expressed for the entire dataset (Table II.2). The 12 most abundant proteins across the four oysters analysed represent core cell structure and function, such as nucleosome assembly, cytoskeleton structure, muscle components,

turnover of intracellular proteins, and protection against oxidative stress. Eight of these 12 proteins (arginine kinase, actin, histone H2A, histone H2B.3, histone H4, peptidyl-prolyl *cis-trans* isomerase, extracellular superoxide dismutase, and cytosol aminopeptidase) were identified in the top 10 most expressed proteins in all four oysters.

Of the 1043 proteins expressed across all samples, 1033 were annotated using the UnitProt-KB/SwissProt database. Of the annotated proteins, 888 were associated with Gene Ontology classifications. A majority of proteins were associated with the biological process of protein metabolism (n = 273), followed by cell organization and biogenesis (n = 201), and transport (n = 165) (Fig. II.3).

Enrichment analysis was carried out to determine which biological processes were over-represented in gill tissue in comparison to the entire proteome. Several of the functional groups identified were associated with the abundant proteins involved in metabolism and transport, as well as structural processes (i.e. actin-filament and microtubule) and oxidation–reduction. The most significantly enriched biological process was generation of precursor metabolites and energy. Protein IDs (accession numbers starting with "CGI") corresponding to the proteins that contributed to GO term enrichment are listed in Supplementary Data II.5.

The number of unique proteins identified with different numbers of sequenced peptides created an exponential curve (Fig. II.4). The plateau began around 30 000–40 000 sequenced peptides, with a total of 2400–2516 unique peptides identified. New unique peptides were still identified in larger sample sizes of peptides, but the return per sequenced peptide diminished.

Discussion

Technical and analytical challenges have resulted in limited focus on quantitative proteomics approaches in environmental physiology. Given the recent technological advances in the proteomics field (Yates *et al*., 2009) and release of the Pacific oyster genome (Zhang *et al*., 2012), we set out to assess the practical use of quantitative proteomics in this model species. For all biological samples, a majority of the proteins identified (54–55%) were present in all respective technical replicates. Relative expression across technical and biological replicates was also consistent (Fig. II.1,

Supplementary Data II.1). However, there were some proteins not identified in all technical replicates. Thus, proteins with limited expression might not be detected and/or expression levels might not be reflected accurately. It should be noted that the inclusion of proteins in our analysis is highly dependent on threshold selection. In the present study, a protein was included only if it had two unique spectral hits within a replicate and had four total spectra across the combined technical replicate data. If the threshold were adjusted to be more conservative (i.e. a greater total spectral count threshold), variability would be reduced. With a total spectral count threshold of five, 983 proteins are identified and 56–57% of the proteins are in all three technical replicates; with a threshold of 10, 845 proteins are identified and 61–63% of the proteins are in all technical replicates (data not shown).

The number of proteins identified and subsequently annotated can vary tremendously based on experimental design, target tissue, match thresholds, and genomic resources available. In the present study, the majority of the proteins (703) were identified in all biological samples. Based on *in silico* analysis (Fig. II.4), we have sequenced a relatively complete proteome for oyster gill tissue. In a study of European whitefish, *Coregonus lavaretus*, proteomics on fish larvae yielded sequencing of peptides corresponding to 1500 proteins (Papakostas *et al*., 2012). The similar number of protein identifications in whitefish compared with our study (1043) is likely to be associated with the tissue complexity. In the whitefish study, whole body tissue was examined. In a meta-proteomics study of marine microbes, 2273 distinct proteins were identified across 10 samples (Morris *et al*., 2010). The large number of proteins identified by Morris *et al*. (2010) is evidence of the large number of organisms and ecological niches that were sampled in their study. Previous proteomics studies on Sydney rock oyster haemolymph have found relatively few proteins compared with the present study in gill tissue, with the number of identified proteins ranging from 49 to 514 (Simonian *et al*., 2009; Thompson *et al*., 2011, 2012a, 2012b; Muralidharan *et al*., 2012). The identification of fewer proteins in haemolymph is probably because there are fewer cell types present in haemolymph compared with the gill.

In addition to assessing the feasibility of shotgun proteomics in the Pacific oyster,

we were also able to provide a functional characterization of the gill proteome. Gene ontology characterization identified a majority of proteins associated with protein metabolism, cell organization and biogenesis, and transport (Fig. II.3). These biological functions would be expected, because gill tissue is the primary interface between the oyster and the environment (water), where the tissue's major functions include ion regulation, respiration, and sorting of food particles. The high number of proteins involved in these GO categories is not necessarily unique to gill tissue but is likely to reflect the multifunctional nature of a tissue that responds to variable environments.

Enrichment analysis was performed to identify which functional groups of proteins expressed in gill tissue were over-represented in comparison to the complete protein repertoire. Several of the functional groups identified were associated with the abundant proteins involved in metabolism and transport, as well as cellular structure. These enrichment analysis findings are consistent with a previous transcriptomic comparison between *C. gigas* gill tissue and other tissues, with genes predominantly expressed in the gill being involved in epithelia morphogenesis, cilia movement, and detoxification and defense (Dheilly *et al.*, 2011). Some of the cytoskeletal proteins identified in gill were tektin-3, microtubule-associated protein futsch, and actin. Tektin is part of cilia and flagellar microtubules and has been found to change expression in response to an elevated partial pressure of CO_2 (Dineshram *et al.*, 2013), and has also been identified in Sydney rock oyster haemolymph (Thompson *et al.*, 2012b). Transport proteins included ATP synthases and v-type proton ATP synthase. ATP synthase is a good marker of environmental stress in *C. gigas*, because its transcript expression is altered in response to hypoxia (David *et al.*, 2005) and pesticide exposure (Tanguy *et al.*, 2005). The most significantly enriched biological process was generation of precursor metabolites and energy. Many of the proteins that contributed to the over-representation of this GO category in the gill tissue are involved in metabolic processes, such as 2-oxoglutarate dehydrogenase, dihydroplipoyllisin-residue acetyltransferase, glycogen phosphorylase, triose phosphate isomerase, and hexokinase. These enzymes are all involved in the breakdown of carbohydrates and other food inputs, and thus underline the important metabolic processes that occur in the gill.

Proteins involved in oxygen metabolism and reactive oxygen species defense

were also enriched in gill tissue, providing further support for the importance of gill tissue in response to environmental change. Previous transcriptomics-based studies of oysters support that the oxidative stress response plays an important role in the gill tissue (e.g. David *et al*., 2007; Fleury and Huvet, 2012). Genes and proteins responding to production of reactive oxygen species increase in oysters in many instances of environmental stress, such as exposure to contaminants (e.g. David *et al*., 2007; Muralidharan et al., 2012), as well as exposure to ocean acidification (Tomanek *et al*., 2011) and temperature stress (Meistertzheim *et al*., 2007). Specific proteins that contribute to reactive oxygen species defense are enzymes instrumental in the physiological response to oxidative stress, such as the antioxidants superoxide dismutase, peroxiredoxin, and catalase.

The success of the shotgun sequencing effort was due in part to the recent publication of the *C. gigas* genome, emphasizing that the dissemination of genomic resources provides invaluable opportunities for advancement for the scientific community. The sharing of these large data sets, such as the genome and the gill proteome, will support further research into the effects of environmental changes on the oyster in terms of both acclimatization and adaptation. The characterization of the scope of acclimatization and adaptation are instrumental in understanding how the Pacific oyster, an ecologically and economically important species, can respond to climate change at the physiological and population levels. These research results demonstrate that shotgun sequencing of oyster gill tissue is a viable approach for biological discovery and that it will be likely to play an important role in future studies on oyster physiology.

Tables

Table II.1. Summary of the number of peptides sequenced and proteins identified for each oyster (labeled A-D).

	Oyster			
	A	**B**	**C**	**D**
Peptides sequenced (total)	44720	43646	44177	43275
technical replicate #1	16112	15390	15611	15180
technical replicate #2	14645	14329	14592	14290
technical replicate #3	13963	13927	13974	13805
Proteins identified (total)	923	959	883	875
technical replicate #1	731	730	704	683
technical replicate #2	722	729	685	667
technical replicate #3	694	771	657	677
Proteins identified in all replicates	509	514	484	478

Table II.2. The 12 most abundant proteins in the gill proteome as determined by identifying the 10 most abundant proteins in each oyster.

Protein ID	Protein Description	Accession	Oysters
CGI_10021481	Arginine kinase	O15990	A,B,C,D
CGI_10022730	Actin	O17320	A,B,C,D
CGI_10008058	Histone H2A	P02269	A,B,C,D
CGI_10008057	Histone H2B.3	P35069	A,B,C,D
CGI_10008056	Histone H4	Q28DR4	A,B,C,D
CGI_10025180	Peptidyl-prolyl cis-trans isomerase	P54985	A,B,C,D
CGI_10004092	Extracellular superoxide dismutase	Q08420	A,B,C,D
CGI_10006610	Cytosol aminopeptidase	Q65FE6	A,B,C,D
CGI_10013347	ATP synthase subunit beta	Q05825	A,B,D
CGI_10012330	Tubulin beta chain	P11833	B,C
CGI_10000082	Barrier-to-autointegration factor	Q6P026	C,D
CGI_10010974	Glyceraldehyde-3-phosphate dehydrogenase	P56649	A

Figures

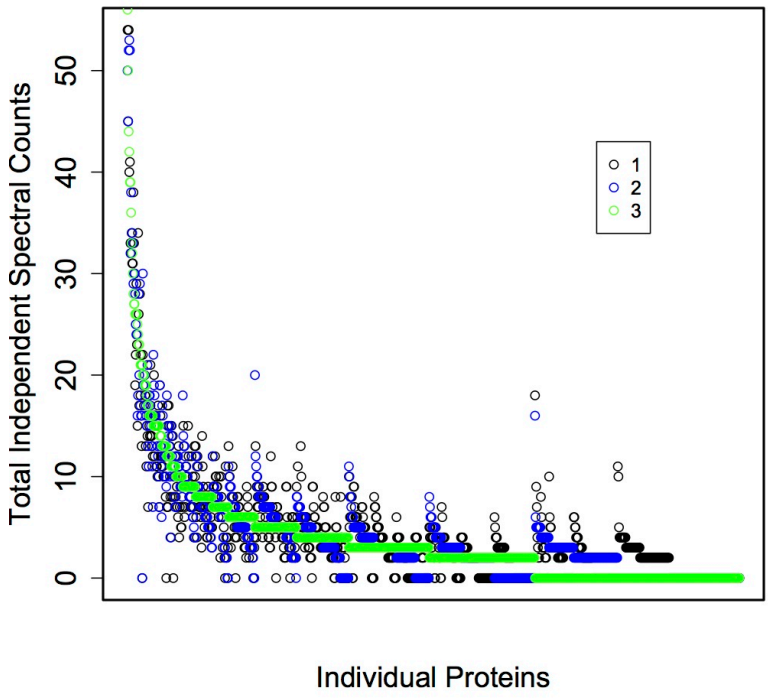

Figure II.1. Total independent spectral counts for three technical replicates for oyster A plotted for each protein (n = 1500). Similar patterns were observed for the other three oysters (data not shown).

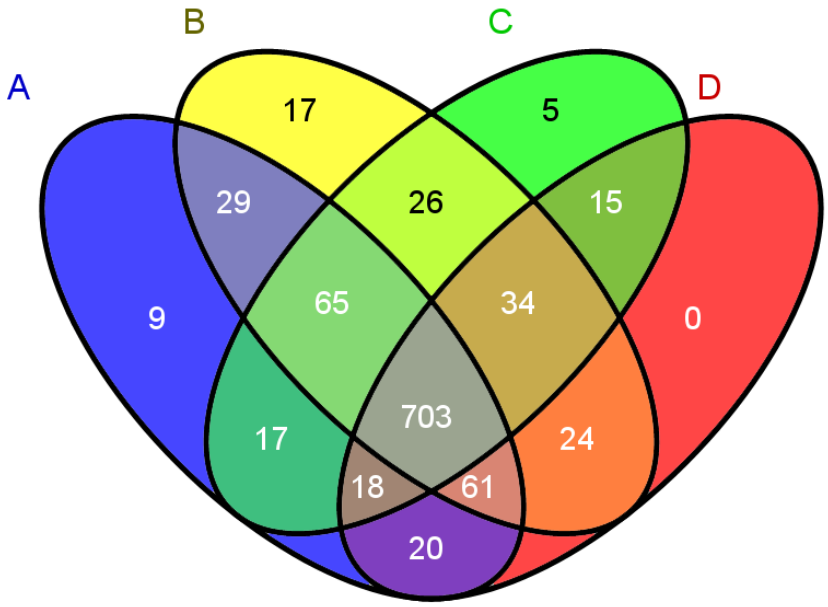

Figure II.2. Venn diagram of proteins identified among biological samples. Proteins identified in oyster A are in the blue ellipse, B in the yellow, C in green, and oyster D proteins are in the red ellipse.

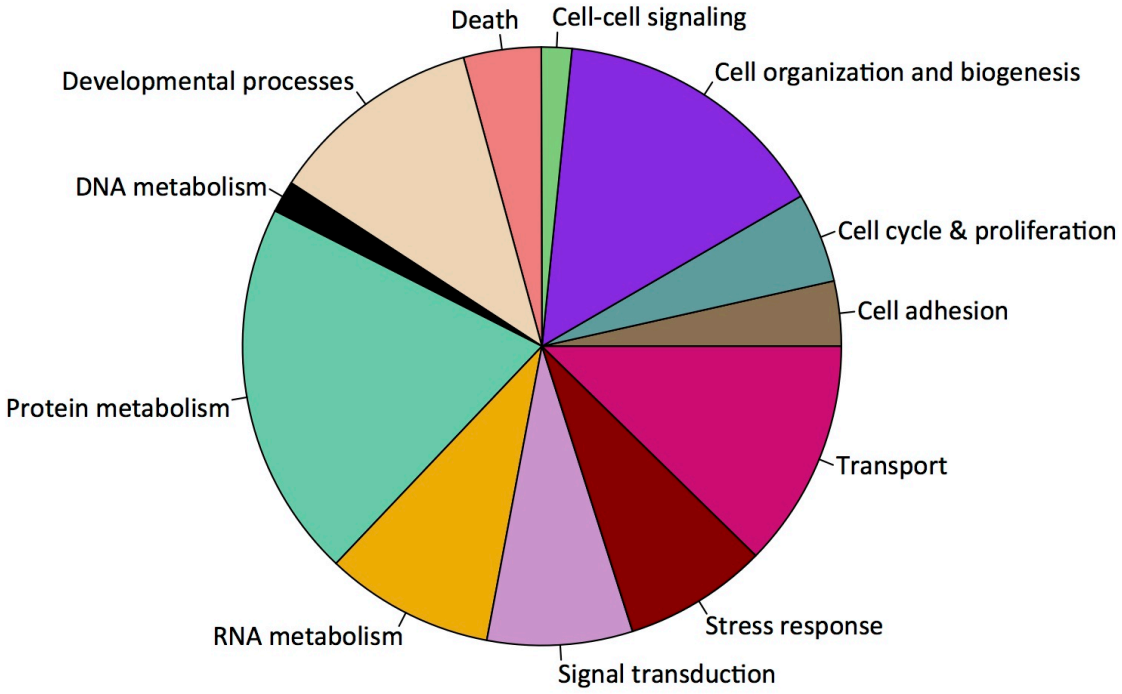

Figure II.3. Representation of biological processes corresponding to the proteins identified from oyster gill tissue.

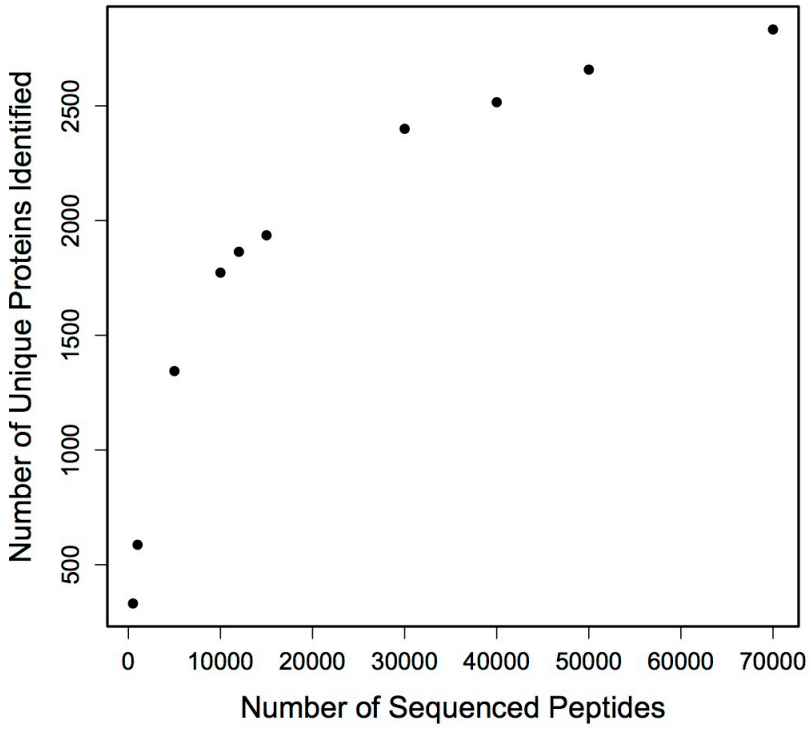

Figure II.4. Predicted number of unique proteins that would be identified based on a sequential increase in peptide sequences.

Supplementary Information

Supplementary information can be found in the online, published version of this article at http://conphys.oxfordjournals.org/content/1/1/cot009/suppl/DC1

doi: 10.1093/conphys/cot009

Supplementary Data 1: Correlations of protein expression values between biological replicates.

Supplementary Data 2: SwissProt-KB/Uniprot Annotations and spectral counts across biological replicates for all 2 850 proteins identified.

Supplementary Data 3: Protein identifications for each technical replicate, including protein probability scores, number of total and unique spectra, and peptide sequences.

Supplementary Data 4: Normalized spectral abundance factors (NSAF) for each protein in each biological replicate.

Supplementary Data 5: Gene Ontology (GO) annotations for each protein.

Acknowledgements
We would like to thank Taylor Shellfish for donating the oysters used for this study, Emily Carrington and Ken Sebens for providing laboratory space, and Ronen Elad who assisted with oyster care. Priska von Haller helped with experimental design for the LC-MS/MS and provided technical assistance. Jimmy Eng and Tahmina 'Eva' Jahan ran the database searches for protein identification. This work was supported by National Oceanographic and Atmospheric Administration Saltonstall-Kennedy Program (grant no. NA09NMF4270093).

Works Cited
Amaral V, Thompson EL, Bishop MJ, Raftos DA. (2012) The proteomes of Sydney rock oysters vary spatially according to exposure to acid sulfate runoff. Marine & Freshwater Research. 63: 361-369.

Bräutigam A, Shrestha RP, Whitten D, Wilkerson CG, Carr KM, Froehlich JE, Weber APM. (2008) Low-coverage massively parallel pyrosequencing of cDNAs enables proteomics in non-model species: Comparison of a species-specific database generated by pyrosequencing with databases from related species for proteome analysis of pea chloroplast envelopes. Journal of Biotechnology Biotechnol. 136: 44-53.

Corporeau C, Vanderplancke G, Boulais M, Suquet M, Quéré C, Boudry P, Huvet A, Madec S. (2012) Proteomic identification of quality factors for oocytes in the Pacific oyster *Crassostrea gigas*. Journal of Proteomics. 75: 5554-5563.

David E, Tanguy A, Pichavant K, Moraga D. (2005) Response of the Pacific oyster *Crassostrea gigas* to hypoxia exposure under experimental conditions. The FEBS Journal. 272: 5635-5652.

David E, Tanguy A, Moraga D. (2007) Peroxiredoxin 6 gene: A new physiological and genetic indicator of multiple environmental stress response in Pacific oyster *Crassostrea gigas*. Aquatic Toxicology. 84: 389-398.

Dheilly NM, Haynes PA, Raftos DA, Nair SV. (2012) Time course proteomic profiling of cellular repsonses to immunological challenge in the sea urchin, *Heliocidaris erythrogramma*. Developmental & Comparative Immunology. 37: 243-256.

Dheilly NM, Lelong C, Huvet A, Favrel P. (2011) Development of a Pacific oyster (*Crassostrea gigas*) 31,918-feature microarray: identification of reference genes and tissue-enriched expression patterns. BMC Genomics. 12: 468.

Dheilly NM, Raftos DA, Haynes PA, Smith LC, Nair SV. (2013) Shotgun proteomics of coelomic fluid from the purple sea urchin, *Strongylocentrotus purpuratus*. Developmental & Comparative Immunology. In press.

Dineshram R, Thiyagarajan V, Lane A, Ziniu Y, Xiao S, Leung PTY. (2013) Elevated CO_2 alters larval proteome and its phosphorylation status in the commercial oyster, *Crassostrea hongkongensis*. Marine Biology. In press.

Dineshram R, Wong KKW, Xiao S, Yu Z, Qian PY, Thiyagarajan V. (2012) Analysis of Pacific oyster larval proteome and its response to high-CO_2. Marine Pollution Bulletin. 64: 2160-2167.

Eng JK, McCormack AL, Yates JR. (1994) An Approach to Correlate Tandem Mass Spectral Data of Peptides with Amino Acid Sequences in a Protein Database. Journal of the American Society for Mass Spectrometry. 5: 976-989.

Fleury E, Huvet A. (2012) Microarray analysis highlights immune response of Pacific oysters as a determinant of resistance to summer mortality. Marine Biotechnology. 14: 203-217.

Florens L, Carozza MJ, Swanson SK, Fournier M, Coleman MK, Workman JL, Washburn MP. (2006) Analyzing Chromatin Remodeling Complexes Using Shotgun Proteomics and Normalized Spectral Abundance Factors. Methods. 4: 303-311.

Griffitt RJ, Chandler GT, Greig TW, Quattro JM. (2006) Cathepsin B and glutahione peroxidase show differing transcriptional responses in the grass shrimp, *Palaemonetes pugio* following exposure to three xenobiotics. Environmental Science & Technology. 40: 3640-3645.

Hogstrand C, Balesaria S, Glover CN. (2002) Application of genomics and proteomics for study of the integrated response to zinc exposure in a non-model fish species, the rainbow trout. Comparative Biochemistry and Physiology Part B: Biochemistry and Molecular Biology. 133: 523-535.

Huan P, Wang H, Dong B, Liu B. (2012) Identification of differentially expressed proteins involved in the early larval development of the Pacific oyster *Crassostrea gigas*. Journal of Proteomics. 75: 3855-3865.

Huang DW, Sherman BT, Lempicki RA. (2009a) Systematic and integrative analysis of large gene lists using DAVID Bioinformatics Resources. Nature Protocols. 4: 44-57.

Huang DW, Sherman BT, Lempicki RA. (2009b) Bioinformatics enrichment tools: paths toward the comprehensive functional analysis of large gene lists. Nucleic Acids Research. 37: 1-13.

Kültz D, Somero GN. (1996) Differences in protein patterns of gill epithelial cells of the fish *Gillichthys mirabilis* after osmotic and thermal acclimation. Journal of Comparative Physiology B: Biochemical, Systemic, and Environmental Physiology. 166: 88-100.

Liu F, Wang W (2012) Proteome pattern in oysters as a diagnostic tool for metal pollution. Journal of Hazardous Materials. 239-240: 241-248.

Lockwood BL, Sanders JG, Somero GN. (2010) Transcriptomic responses to heat stress in invasive and native blue mussels (genus *Mytilus*): molecular correlates of invasive success. The Journal of Experimental Biology. 213: 3548-3558.

Meistertzheim AL, Tanguy A, Moraga D, Thébault MT. (2007) Identification of differentially expressed genes of the Pacific oyster *Crassostrea gigas* exposed to prolonged thermal stress. The FEBS Journal. 274: 6392-6402.

Morris RM, Nunn BL, Frazer C, Goodlett DR, Ting YS, Rocap G. (2010) Comparative metaproteomics reveals ocean-scale shifts in microbial nutrient utilization and energy transduction. The ISME Journal. 4: 673-685.

Muralidharan S, Thompson E, Raftos D, Birch G, Haynes PA. (2012) Quantitative proteomics of heavy metal stress responses in Sydney rock oysters. Proteomics. 12: 906-921.

Nesvizhskii AI, Keller A, Kolker E, Aebersold R. (2003) A Statistical Model for Identifying Proteins by Tandem Mass Spectrometry. Analytical Chemistry. 75: 4646-4658.

Oliveros JC (2007) VENNY. An interactive tool for comparing lists with Venn Diagrams. http://bioinfogp.cnb.csic.es/tools/venny/index.html (last accessed 29 October 2012).

Papakostas S, Vasemägi A, Vähä JP, Himberg M, Peil L, Primmer CR. (2012) A proteomics approach reveals divergent molecular responses to salinity in populations of European whitefish (*Coregonus lavaretus*). Molecular Ecology. 21: 3516-3530.

Philipp EER, Kraemer L, Melzner F, Poustka AJ, Thieme S, Findeisen U, Schreiber S, Rosenstiel P. (2012) Massively Parallel RNA Sequencing Identifies a Complex Immune Gene Repertoire in the lophotrochozoan *Mytilus edulis*. PLoS One. 7: e33091.

Polato NR, Vera JC, Baums IB. (2011) Gene Discovery in the Threatened Elkhorn Coral: 454 Sequencing of the *Acropora palmata* Transcriptome. PLoS One 6: e28634.

R Development Core Team (2009) R: A language and environment for statistical computing. R Foundation for Statistical Computing, Vienna, Austria. ISBN 3-900051-07-0, URL http://www.R-project.org.

Simonian M, Nair SV, Neil JA, Raftos DA. (2009) Proteomic clues to the identification of QX disease-resistance biomarkers in selectively bred Sydney rock oysters, *Saccostrea glomerata*. Journal of Proteomics. 73: 209-217.

Stumpp M, Dupont S, Thorndyke MC, Melzner F. (2011) CO_2 induced seawater acidification impacts sea urchin larval development II: Gene expression patterns in pluteus larvae. Comparative Biochemistry and Physiology Part A: Molecular & Integrative Physiology. 160: 320-330.

Supek F, Bošnjak M, Škunca N, Šmuc T. (2011) REVIGO summarizes and visualizes long lists of Gene Ontology terms. PLoS One. 6: e21800.

Tanguy A, Boutet I, Laroche J, Moraga D. (2005) Molecular identification and expression study of differentially regulated genes in the Pacific oyster *Crassostrea gigas* in response to pesticide exposure. The FEBS Journal. 272: 390-403.

Thompson EL, Taylor DA, Nair SV, Birch G, Haynes PA, Raftos DA. (2011) A proteomic analysis of the effects of metal contamination on Sydney Rock Oyster (*Saccostrea glomerata*) haemolymph. Aquatic Toxicology. 103: 241-249.

Thompson EL, Taylor DA, Nair SV, Birch G, Hose GC, Raftos DA. (2012a) Proteomic analysis of Sydney Rock oysters (*Saccostrea glomerata*) exposed to metal contamination in the field. Environmental Pollution. 170: 102-112.

Thompson EL, Taylor DA, Nair SV, Birch G, Haynes PA, Raftos DA. (2012b) Proteomic discovery of biomarkers of metal contamination in Sydney Rock oysters (*Saccostrea glomerata*). Aquatic Toxicology. 109: 202-212.

Todgham AE, Hofmann GE. (2009) Transcriptomic response of sea urchin larvae *Strongylocentrotus purpuratus* to CO_2-driven seawater acidification. Journal of Experimental Biology. 212: 2579-2594.

Tomanek L, Zuzow MJ, Ivanina AV, Beniash E, Sokolova IM. (2011) Proteomic response to elevated P_{CO2} level in eastern oysters, *Crassostrea virginica*: evidence for oxidative stress. Journal of Experimental Biology. 214: 1836-1844.

Wang S, Peatman E, Hong L, *et al*. (2010) Microarray analysis of gene expression in eastern oyster (*Crassostrea virginica*) reveals a novel combination of antimicrobial and oxidative stress host responses after dermo (*Perkinsus marinus*) challenge. Fish & Shellfish Immunology. 29: 921-929.

Yates JR, Ruse CI, Nakorchevsky A. (2009) Proteomics by Mass Spectrometry: Approaches, Advances, and Applications. Annual Review of Biomedical Engineering. 11: 49-79.

Zhang G, Fang X, Guo X, *et al*. (2012) The oyster genome reveals stress adaptation and complexity of shell formation. Nature. 490: 49-54.

Chapter III: From shell deposition to protein expression: An integrative assessment of ocean acidification impacts on a marine invertebrate

Submitted for publication

Abstract

Ocean acidification as a result of increased anthropogenic CO_2 emissions is occurring in marine and estuarine environments worldwide. The coastal ocean experiences additional daily and seasonal fluctuations in pH that attain and exceed projected end of century open ocean pH reductions. In order to assess the impact of ocean acidification on marine invertebrates, Pacific oysters (*Crassostrea gigas*) were exposed to one of four different pCO_2 levels for four weeks: 400 μatm (pH 8.0), 800 μatm (pH 7.7), 1000 μatm (pH 7.6), or 2800 μatm (pH 7.3). Oysters in all four pCO_2 environments deposited new shell during the experiment, but growth rate was not different among the treatments. However, micromechanical properties of the new shell were compromised by elevated pCO_2. Elevated pCO_2 affected neither whole body fatty acid composition, nor glycogen content, nor mortality rate associated with acute heat shock. Shotgun proteomics revealed that several physiological pathways were significantly affected by ocean acidification, including antioxidant response, carbohydrate metabolism, and transcription and translation. Additionally, the proteomic response to a second stress differed with pCO_2, with numerous processes significantly affected by mechanical stimulation at high versus low pCO_2. These data contribute to an integrative view of the effects of ocean acidification on oysters as well as physiological trade-offs during environmental stress. The data have been deposited to the ProteomeXchange with identifier PXD000835.

Introduction

Current measurements of surface ocean pH have revealed decreases that are in accordance with modeled predictions of a pH decline of at least 0.3 units corresponding to atmospheric pCO_2 of 650-970 ppm by the year 2100 (Caldeira and Wickett, 2005; Feely et al., 2010, 2012; Friedrich et al., 2012; Gruber et al., 2012; Orr et al., 2005). The coastal ocean, home to productive fisheries and diverse ecosystems, may see even greater

changes in pH due to natural processes (i.e. hydrography, freshwater input, and biological activity) and a plethora of anthropogenic effects (i.e. deforestation, agriculture, mining, increasing population sizes) (reviewed in Duarte et al., 2013). Although some species that live in the coastal ocean show a degree of adaptation to variable pH (see Kelly et al., 2013; Pespeni et al., 2013), sessile invertebrates are sensitive to acute low pH exposures across life stages. In bivalves, low pH results in significant changes to larval development (e.g. Barton et al., 2012), reduced shell deposition in most species (e.g. Gazeau et al., 2007; Melzner et al., 2011), decreased integrity of the shell (Dickinson et al., 2012; Dickinson et al., 2013) and weakened attachment of byssal threads (O'Donnell et al., 2013). In addition to phenotypic impacts, elevated pCO_2 can result in significant shifts in marine invertebrate metabolism and resource utilization (e.g. Stumpp et al., 2011).

The Pacific oyster, *Crassostrea gigas*, is a marine invertebrate that has been well studied in terms of its response to ocean acidification. Larvae experience developmental delay and shell malformations in response to low pH (Barton et al., 2012; Gazeau et al., 2011; Kurihara et al., 2007; Parker et al., 2010; Timmins-Schiffman et al., 2013a). Adults are also affected negatively by ocean acidification. Fertilization success is reduced at moderately elevated pCO_2 (600 μatm) (Parker et al., 2010). Calcification rates for adult *C. gigas* decrease linearly with increasing pCO_2 (Gazeau et al., 2007). Reduced pH also alters response to other environmental variables. The standard metabolic rate of Pacific oysters at low pH was significantly elevated in response to increasing temperature compared to oysters at ambient pH (Lannig et al., 2010). Such studies illustrate that ocean acidification causes profound physiological changes in *C. gigas* that may have long-term consequences on fitness.

To examine the underlying processes associated with the biological impacts of ocean acidification on marine invertebrates, the current study takes an integrative approach in examining the response of adult oysters from alterations in protein expression to shell deposition rates. Oysters were exposed to one of four pCO_2 levels for one month: 400, 800, 1000, or 2800 μatm. The pCO_2 values represent approximate current-day surface ocean pCO_2 (400 μatm) and three elevated values reflecting potential end-of-century scenarios as well as pCO_2 variation that is currently experienced in the

nearshore environment. At the end of one month the impacts of elevated pCO_2 on shell growth, shell micromechanical properties, lipid metabolism, glycogen metabolism, response to acute heat shock, and response to mechanical stress were assessed.

By taking this integrative approach, these data highlight the complex nature of phenotypic impacts of ocean acidification, while at the same time uncovering the less accessible underlying physiological processes. The latter was made possible by the use of shotgun proteomics, applied for the first time in an investigation of the effects of ocean acidification. Shotgun proteomics is a powerful non-biased approach in the investigation of biological responses, which also offers insight into underlying mechanisms that could lead to phenotypic effects. Together these data demonstrate the scope of effects that ocean acidification can have on a marine invertebrate.

Methods

Ocean acidification system

This experiment was conducted at the Friday Harbor Labs Ocean Acidification Environmental Laboratory, Friday Harbor, Washington, USA where oysters were exposed to pCO_2 values of 400 μatm, 800 μatm, 1000 μatm, or 2800 μatm. The system and control of water chemistry has been previously described in detail (O'Donnell et al., 2013; Timmins-Schiffman et al., 2013a). Briefly, incoming water was filtered (0.2 μm) and stripped of CO_2. As the water flowed into the different treatment tanks, CO_2-free air and CO_2 were added back to reach set points that were continuously monitored by a DuraFET III pH probe (Honeywell, Morristown, NJ, USA). From the treatment tanks, water flowed into the eight replicate chambers for each of the four treatment levels at 57.5 mL/min. For this experiment, set points were calculated for 13°C and estimated total alkalinity (A_T) of 2100 μmol/kg for pCO_2 values of 400 μatm (pH 8.03), 800 μatm (pH 7.76), 1000 μatm (pH 7.67), and 2800 μatm (pH 7.24).

Seawater Chemistry Analysis

Spectrophotometric pH was measured for all treatments 19 out of the 29 days of the experiment as described in SOP 6b by Dickson et al. (2007). On days 5, 7, 11, 14, 20, 24, and 26 spectrophotometric pH was used to measure the pH of the water inside two of

the eight experimental chambers per treatment to ensure consistency with set points. Salinity was recorded with a conductivity meter (Hach sensION5, Loveland, CO, USA) and treatment temperature was verified with a Fluke 1523 thermometer (Fluke, Everett, WA, USA) whenever spectrophotometric pH was measured. Total alkalinity (A_T) was measured using an open cell titration as described in SOP 3b (Dickson et al. 2007) for the treatment reservoir water and for two chambers on days 5, 11, 20, and 26. If the A_T titration was not done on the day of collection, the water sample was poisoned with mercuric chloride and stored in a sealed borosilicate glass jar. CO_2calc (Robbins et al. 2010) was used to calculate calcium carbonate saturation state of aragonite and calcite, carbonate ion concentration, and pCO_2 with A_T and pH as inputs and using the following constants: Lueker et al. (2000) for CO_2 constants; Dickson (1990) for KHSO4; total scale (mol/kg SW) for pH scale; and Wanninkhof (1992) for air-sea flux.

Experimental design

Adult oysters (average shell length ± s.d. = 51± 5 mm, average width = 38 ± 6 mm) collected from Oyster Bay, Washington were maintained in 3.5 L chambers (n = 6 oysters per container) and acclimated for two weeks (T = 13°C, pH = 8). The oysters originated from the same spawning event in March 2011 from approximately 25 broodstock oysters. Oysters were fed 120,000 cells per mL per day of Shellfish Diet 1800 (Reed Mariculture, Campbell, CA, USA). Containers were cleaned every other day with freshwater to prevent fouling. At the beginning and end of the experiment, buoyant weight was measured. Relative growth rate of oyster cohorts within each treatment was calculated for buoyant weight based on Hoffmann and Poorter (2002). For each treatment, the difference in means of natural log-transformed mass data was divided by 29 days. Analysis of variance was used to determine the main effects and interactions of time and pCO_2 on buoyant weight, using the model:

$$\boldsymbol{bw \sim t \times pCO2} \qquad (1)$$

where *bw* is the measured buoyant weight for an oyster, *t* is time point (either start or end of the experiment) and pCO_2 is the treatment condition. Growth rate analyses were performed in R (R Core Team, 2013).

Oysters were held in one of four treatments for 29 days. At the end of the treatment period oysters were either immediately sampled (n =16), subjected to mechanical stress by centrifugation in a standard salad spinner (5min, ~100rpm) and sampled (n = 8), or subjected heat shock for one hour and sampled (n = 24). Centrifugation has previously been shown to stimulate a stress response in oysters as evidenced by increased circulating noradrenaline and impacts on hemocyte function (Lacoste et al., 2001a; Lacoste et al., 2001b). In this study, mechanical stimulation was used to characterize how elevated pCO_2 impacts the physiological response to an additional stressor.

For sampling, a section of the posterior gill lamellae was dissected and immediately flash frozen in liquid nitrogen for protein expression analysis. Only samples held at 400 μatm (control) and 2800 μatm, both mechanically stressed and without additional stress, were considered for protein analysis. Remaining viscera from all oysters were put in a separate tube and flash frozen for fatty acid analysis. Both shell valves were gently cleaned of remaining tissue and left to air dry for characterization of shell mechanical properties.

Shell micromechanical properties

Micromechanical testing was conducted on left shell valves of *C. gigas* that had been exposed to 400, 1000 or 2800 μatm. All reagents, supplies and equipment for sample preparation were purchased from Allied High Tech Products, Inc. (Rancho Dominguez, CA, USA) unless otherwise stated. Micromechanical testing was conducted within the outermost 3 mm of the shell posterior, the region of the shell where growth occurs most rapidly. Although we could not definitively differentiate shell grown during the experimental exposure from pre-existing shell, observations of growth during the course of the experiment were consistent with a 3 mm deposition of new shell.

To prepare samples, shell valves were first cut across their width using a water-cooled diamond tile saw (Skilsaw, #3540), separating the anterior from the posterior portion of the shell. The posterior segment of valves (approximately 35 mm in length) was then cleaned using Micro Organic Soap and a cotton ball to remove oil and debris and mounted on a glass microscope slide using mounting wax. Slides with mounted

shells were secured to the cutting arm of a low speed diamond saw (TechCut 4, cooled with proprietary cutting fluid) and the shell segment was cut longitudinally, transecting the most posterior edge. Sectioned shell valves were removed from slides, cleaned again with Micro Organic Soap, dried on a hot plate at 70°C, and mounted in epoxy resin. Mounted samples were then ground and polished on a manual grinding/polishing machine (M-Prep 5) by passing samples through a grinding series of 180, 320, 600 and 800 grit and then polishing with a 1 μm diamond suspension and finally a 0.04 μm colloidal silica suspension. Samples were cleaned with Micro Organic soap and checked under a metallurgical microscope after each step of the grinding/polishing process, and were re-polished if necessary until the surface of each sample was completely even and free of scratches. No etching of shells was observed during grinding or polishing.

Vickers microhardness tests were conducted using a microindentation hardness tester (Clark Instrument MHT-1, SUN-TEC, Novi, MI, USA) on polished shells at 0.245 N load and 5 s dwelling time. Indents were made within the bulk, foliated layer of the shell, which was easily differentiated from the prismatic and chalky regions of the shell at low magnification. Seven to eight indentations were made per sample and each indent was placed at least 45 μm away from other indents and the sample's edges. Vickers hardness numbers (VHN) were calculated as:

$$\boldsymbol{VHN = 1.854 \times (F \div d^2)} \qquad \textbf{(2)}$$

where F is the applied load and d is the mean length of the two diagonals produced by indentation. VHN were averaged for each shell sample. Following microhardness testing, each indent was photographed at 80x magnification on a metallurgical microscope (Jenco MET-233, Portland, OR, USA) equipped with a camera (Leica EC3, Buffalo Grove, IL, USA). Photographs were used to quantify the longest crack produced by each indent, which was measured using image analysis software (Leica LAS EZ, Ver. 3.0) as the radius of a circle radiating from the center of the indent enclosing all visible cracks (Figure S1). Hardness and crack radius measurements were used to calculate fracture toughness (K_c) for each sample as described elsewhere (Anstis et al., 1981; Baldassarri et al., 2008):

$$K_C = 0.0154 \times \left(\frac{E}{H}\right)^{1/2} \times \left(\frac{P}{C}\right)^{1.5} \quad (3)$$

where 0.0154 is a calibration constant, E is an elastic modulus (empirically determined for *C. gigas* as 73 GPa: Lee et al., 2008), H is hardness in GPa, P is applied load in N and C is crack radius in μm.

Statistical analysis for micromechanical properties was conducted using SPSS (Ver. 19, IBM, Armonk, NY, USA). Outliers were calculated in SPSS as values greater than 1.5 times the interquartile range below or above the first or third quartile respectively, and were removed from the dataset (at most two per treatment group). Data were analyzed using one-way analysis of variance followed by post-hoc testing. Normality and equal variance was tested using a Kolmogorov–Smirnov test with Lilliefor's correction and a Levene test, respectively. Fracture toughness data met both assumptions and a Tukey HSD post-hoc test was used. As hardness data was normally distributed but did not meet the equal variance assumption, a Welch ANOVA followed by Games-Howell post-hoc testing was applied.

Fatty acid and glycogen analyses

Fatty acid and glycogen analyses were carried out on oysters from three pCO_2 treatments (400, 800, and 2800 μatm; n = 8 per treatment). Whole body tissue (minus the dissected gill) was lyophilized overnight and tissues were homogenized with a pestle for use in fatty acid extractions (2.5 mg per extraction) and glycogen extractions (19.3-84.7 mg). Fatty acid extractions were performed following the protocol described in Galloway et al. (2012) except two chloroform removals were carried out. Fatty acid methyl esters were identified by running the samples on a HP 6958 gas chromatograph with an auto-sampler and flame-ionization detector using an Agilent DB-23 column (30 m, 0.25 mm diameter, 0.15 μm film) (Supelco, Bellefonte, PA, USA). Peaks were identified based on comparison of retention times with known standards. Individual amounts of fatty acids were normalized within each replicate by dividing the peak area by the sum of all fatty acid peak areas for that sample. Normalized fatty acid data were log-transformed and non-metric multidimensional scaling (NMDS) based on a Bray-Curtis

dissimilarity matrix was used to compare fatty acid profiles among treatments. NMDS was performed in R with the vegan package (R Core Team, 2013; Oksanen et al., 2013).

Glycogen was extracted using trichloroacetic acid (TCA). Three mL of 15% TCA was added to each homogenized tissue sample and samples were vortexed and stored at 4°C for 1 hour. Samples were then centrifuged at 3,000xg for 10 minutes and 4 mL of absolute ethanol was added to 500 μl of the resulting supernatant. After an overnight incubation at 4°C, samples were centrifuged 30 minutes at 4,000xg, supernatant was removed, and the resulting glycogen pellet was dissolved in 200 μl Nanopure water. Glycogen concentration was determined using Sigma's Glycogen Assay Kit following the manufacturer's protocol (MAK016, Sigma-Aldrich, St. Louis, MO). Each sample was diluted 1:30 in Hydrolysis Buffer and run in triplicate. A few samples that were still too concentrated were run again diluted 1:60. Absorbances were read on a Spectra Max M2 (Molecular Devices, Sunnyvale, CA) using Softmax Pro v.5 software (Molecular Devices). The coefficient of variation was <20% for all samples. Absorbance measurements were blank corrected and concentrations were corrected for dilution factor and original mass of tissue used for the extraction. Differences among groups were explored using a one-way ANOVA in R (R Core Development Team, 2013) with pCO_2 treatment as a fixed factor.

Heat shock

Oysters from each of the pCO_2 treatments of 400, 800, 1000, and 2800 μatm were subjected to acute heat shock. Three temperature shocks were implemented consisting of two sublethal temperatures (42° and 43°C) and one lethal temperature (44°C). The lethal heat shock temperature was previously determined for this group of oysters and is defined as the temperature at which 100% mortality occurs within one week after a one hour exposure (Clegg et al., 2009). The heat shock exposure occurred in 800 mL of seawater equilibrated to the correct temperature in a circulating water bath. Since oysters considerably decrease the temperature of the bath, we added a pre-heating step of 10 minutes in one beaker after which the oysters were transferred into another beaker for the full hour. After heat shock, oysters were returned to the flow through system at pH = 8.03 and 13°C. Mortality was the only parameter assessed for the temperature treatment.

Differences in mortality across treatments were assessed using the Cox proportional hazards regression model (Therneau 2013) in R (R Core Development Team, 2013) with pCO_2 and temperature as variables.

Liquid chromatography and tandem mass spectrometry (LC-MS/MS)

Protein extraction and desalting were performed on gill tissue from four mechanically stressed and four control oysters held in the present day and the highest treatment level, 400 and 2800 μatm, respectively (n = 16 oysters total) as described in Timmins-Schiffman et al. (2013b). Each of the 16 protein samples was injected into the LC-MS/MS three times, with injections occurring in a randomized order. LC-MS/MS and data acquisition were carried out as previously described (Timmins-Schiffman et al., 2013b).

Protein informatics analysis

Peptide tandem mass spectra were correlated to *in silico*-generated tandem mass spectra resulting from the Pacific oyster proteome (Fang et al. 2012) using SEQUEST (Eng et al., 1994). Using PeptideProphet from the trans-proteomic pipeline (TPP), peptides were assigned a relative score for best match to the database (Eng et al., 2008; Eng et al., 1994). Only peptides with a PeptideProphet probability score of at least 0.9 were considered for further analysis. Additionally, a protein was considered for analysis only if it had at least 8 spectral counts across all 48 injections (1 spectral count = 1 peptide matched to that protein). Within a biological replicate, a protein was considered to have a non-zero expression value if it had at least 2 unique peptide matches.

NSAF (normalized spectral abundance factor), a metric based on spectral counting (Florens et al., 2006), was used to quantify protein expression. Total spectral counts (SpC) for each oyster were averaged across the three technical replicates. NSAF was calculated by dividing average SpC for each protein by the protein length (L) and then dividing SpC/L by the sum of all SpC/L within a biological replicate (Florens et al., 2006). This workflow was executed in SQLShare (Howe et al., 2011) and workflow and input files are available (Timmins-Schiffman and Roberts 2014a).

Oyster proteins (Fang et al. 2012) were annotated by comparing sequences to the UniProt-KB/SwissProt database (http://uniprot.org) using the blastp algorithm (Altschul et al., 1997) with an e-value limit of 1E-10. Based on homology with the SwissProt database, oyster proteins were further annotated with Gene Ontology (GO) and GO parent categories (GO Slim).

Fold change in protein expression between treatment groups was found by dividing the average NSAF of four biological replicates in one treatment by the average NSAF of the other treatment. In order to statistically test for significant expression differences treatments were compared in a pairwise fashion (400 vs. 2800 μatm, 400 μatm vs. 400 + mechanical stress, and 2800 μatm vs. 2800 + mechanical stress) using the qvalue package in R (R Core Team, 2013; Dabney and Storey) with a q-value cut-off of 0.10. Use of a q-value instead of a p-value from a t-test allows for a multiple comparisons correction using the positive false discovery rate (Storey and Tibshirani, 2003; Storey, 2002). In an effort to determine the biological processes that were influenced by altered environmental conditions, proteins were considered differentially expressed if either there was 1) a 2-fold difference in expression between treatment groups or 2) a q-value < 0.10. The two caveats to these classifications were that only proteins expressed in more than one oyster were considered for fold-based analysis and only proteins expressed by all oysters within a treatment group were considered significant for the q-value cut-off. Proteins expressed in only one treatment within a comparison were included in the differentially expressed protein group. These differentially expressed proteins were visualized in iPath2 using Uniprot-KB/SwissProt annotations (Letunic et al., 2008; Yamada et al., 2011) for each treatment comparison. Enrichment analysis was performed on differentially expressed proteins using the Database for Annotation, Visualization, and Integrated Discovery (DAVID) v. 6.7 (Huang et al., 2009a, 2009b) (http://david.abcc.ncifcrf.gov/). The background protein list was made from the entire sequenced gill proteome. Biological processes were considered significantly enriched if p-value < 0.075. Overlaps in the responses to different stressors were explored using a Venn diagram of the proteins that were differentially expressed between treatments in eulerAPE v. 1.0 (http://www.eulerdiagrams.org/eulerAPE/).

Results

Seawater chemistry analysis

The pCO_2 levels for the four different treatments remained consistent throughout the one month experiment (Table III.1). Average pH (± s.d.) for treatments as measured by the DuraFET probe were 8.02 ± 0.02, 7.73 ± 0.04, 7.63 ± 0.10, and 7.29 ± 0.10 for the 400, 800, 1000, and 2800 μatm treatments, respectively. Spectrophotometric pH corroborated the DuraFET measurements (spectrophotometric pH data not shown). The pCO_2 in containers with oysters was approximately 40 μatm higher than the source water pCO_2, except for the 2800 μatm treatment where it was approximately 75 μatm lower than the source water. Total alkalinity was 9% higher in the chambers (data not shown) compared to the source water for 400 μatm, 10% higher at 800 μatm, 13% higher at 1000 μatm, and 3% lower at 2800 μatm. Calcite was undersaturated ($\Omega_c < 1.0$) only at the highest pCO_2 level and aragonite was undersaturated at the two highest pCO_2 levels (1000 μatm and 2800 μatm).

Oyster growth

Relative growth rate (RGR) for shell mass of oysters exposed to increased pCO_2, as measured by buoyant weight, was not significantly different among treatments ($p > 0.05$) (Table III.2). Shell mass changed with time across all treatments ($F = 6.1190$, $p = 0.014$), indicating shell growth.

Micromechanical properties

Micromechanical properties were tested within the outer 3 mm of the growing edge (posterior) of left shell valves for oysters in the treatments of 400, 1000, and 2800 μatm. Both Vickers microhardness and fracture toughness differed significantly among pCO_2 treatments (microhardness: Welch ANOVA, $p = 0.014$; fracture toughness: one-way ANOVA, $p = 0.003$) (Figure III.1). The microhardness of shells grown at 1000 μatm was significantly lower than that of shells grown at 400 μatm (Games-Howell: $p < 0.05$). Shells grown at 2800 μatm showed a trend toward lower microhardness as compared to the 400 μatm control group, but this comparison was not statistically significant (Games-

Howell: $p = 0.119$). In contrast, fracture toughness was significantly lower in shells grown at 2800 μatm as compared to both the 400 and 1000 μatm treatments, but the 400 and 1000 μatm treatments did not differ (Tukey HSD: $p < 0.05$). Representative cracks formed by micromechanical testing are shown in Figure III.S1.

Fatty acids and Glycogen

Fatty acid profiles did not differ among three treatments (400, 800, and 2800 μatm) ($p > 0.05$; Figure III.2). The nonmetric multidimensional scaling (NMDS) approach shows the relative position of each oyster according to its entire fatty acid profile (i.e. oysters that are plotted close together have similar fatty acid profiles). Total fatty acid content (per milligram tissue) did not vary among treatments ($p > 0.05$; data not shown). Twenty-one fatty acid peaks were identified in the 24 samples, which is within the range of 16-35 fatty acids found in other studies of bivalves (Both et al., 2011; Milke et al., 2004; Pettersen et al., 2010; Soudant et al., 1999). Some of the more important fatty acids identified were 16:0; 18:0; 18:1n-9; 18:1n-7; 18:2n-6; α-linolenic acid (18:3n-3); arachidonic acid (20:4n-6); eicosapentaenoic acid (20:5n-3); two docosapentaenoic acids (22:5n-6 and 22:5n-3); and docosahexaenoic acid (22:6n-3). Raw and normalized fatty acid data are available in Table III.S1.

Glycogen content did not differ among treatments (400, 800, and 2800 μatm) ($p > 0.05$, Figure III.S2). For whole body tissue, glycogen measurements ranged from 2466-102127 μg/mg of tissue with a mean (± 95% confidence interval) glycogen content of 10927 ± 8312 μg/mg of tissue.

Heat shock response

Although pCO_2 did not affect risk of oyster mortality in response to heat shock ($p > 0.05$) (Figure III.3), increased temperature did increase mortality risk ($z = 2.073$, $p = 0.0382$). One hundred percent mortality ($n = 8$ oysters per temperature per treatment) occurred across all three treatments by day 5 post-heat shock at the lethal temperature (44°C). No mortality occurred by day 6 post-heat shock in the 42°C group (data not shown).

Proteomics

After filtering, 700 733 peptides were considered for analysis corresponding to 1 616 proteins (Table III.S2, Table III.S3, Table III.3). Eighty-nine percent (1 449) of proteins were annotated using the UniProt-KB/SwissProt database and 77% (1 250) of those were further categorized with Gene Ontology information (Table III.S4). Raw files and Protein Prophet search files have been deposited to the ProteomeXchange with identifier PXD000835.

Pairwise comparisons were made based on gill protein expression between 1) oysters held at 400 μatm versus oysters held at 2800 μatm, 2) oysters held at 400 μatm versus oysters held at 400 μatm subjected to subsequent mechanical stress, and 3) oysters held at 2800 μatm versus oysters held at 2800 μatm subjected to subsequent mechanical stress. The proteomic response of oyster gill tissues under high pCO_2 conditions compared to 400 μatm was characterized by increased expression of 148 proteins and decreased expression of 136 proteins (Figure III.4A, Figure III.S3). Proteins identified as differentially expressed include those involved in carbohydrate metabolism (i.e. α-L-fucosidase, probable β-D-xylosidase 5, succinyl-CoA ligase, and UDP-glucose 4-epimerase), cell growth (i.e. thymidine phosphorylase and tyrosine-protein kinase Yes), transcription and translation (i.e. calcium-regulated heat stable protein 1, prohibitin-2, and translational activator BCN1), response to reactive oxygen species (i.e. glutathione S-transferase Ω-1), and signaling (i.e. dual specificity mitogen-activated protein kinase kinase 1, calcium-dependent protein kinase C). Gene enrichment analysis revealed enriched proteins are associated with transcription (i.e. transcription elongation regulator 1, 5'-3' exoribonuclease 2), cell junction organization and cell adhesion (i.e. myosin heavy chain 95F, protocadherin Fat 4), and cell proliferation and tissue development (i.e. integrin β-PS, growth arrest-specific protein 8) (Table III.S5).

Two hundred forty-five proteins were differentially expressed upon mechanical stimulation at 400 μatm. One hundred seven were elevated under mechanical stress and 138 proteins were expressed at a lower level (Figure III.4B, Figure III.S3). The proteins that were differentially expressed included those involved in apoptosis (i.e. programmed cell death protein 5, CDGSH iron-sulfur domain-containing protein 2), carbohydrate

metabolism (i.e. α-L-fucosidase, lysosomal α-mannosidase, phosphoacetylglucosamine mutase), and transcription and translation (i.e. histone deacetylase complex subunit SAP18, eukaryotic translation initiation factor 3 subunit A). Significantly enriched biological processes in the response to mechanical stress included RNA metabolism (i.e. histone deacetylase complex subunit SAP18, U1 small nuclear ribonucleoprotein A), transcription (i.e. nucleosome assembly protein 1-like 1), and gamete generation (i.e. tyrosine-protein kinase Btk29A).

One hundred forty-nine proteins were elevated and 137 proteins were expressed at decreased levels when oysters held at 2800 μatm were subjected to mechanical stress (Figure III.4C, Figure III.S3). Differentially expressed proteins included those involved in response to reactive oxygen species (i.e. glutathione S-transferase μ 3 and dual oxidase 2), apoptosis (i.e. caspase-7 and engulfment cell motility protein 2), cell adhesion (i.e. protocadherin Fat 4, contactin), and signaling (i.e. E3 ubiquitin-protein ligase MIB2, prohormone-4). Polysaccharide metabolism and synthesis processes were affected by mechanical stress at elevated pCO_2 as evidenced by their enrichment in this treatment, resulting from the differential expression of proteins including glycogen debranching enzyme, glycogenin-1, UDP-glucose 6-dehydrogenase, putative glycogen [starch] synthase, lysosomal α-glucosidase, and β-hexosaminidase subunit β (Table III.S3). Transcription was also significantly enriched in this stress response (i.e. transcription elongation regulator 1 and basic leucine zipper and W2 domain-containing protein 1).

The magnitude of the proteomic responses in the three different between-treatment comparisons was similar (245-286 differentially expressed proteins), though many proteins were treatment specific (Figure III.5). In addition, for those proteins identified as differentially expressed in more than one comparison, the directional responses of the proteins to each treatment often diverged. For example, proteins in carbohydrate metabolism and nucleotide metabolism were affected differently across treatments (Figure III.S4). These contrasting proteomic profile variations were the most dramatic in a comparison between the responses to ocean acidification alone and to mechanical stimulation at high pCO_2. All 75 differentially expressed proteins shared between these two responses had opposite relative levels in response to stress, i.e. if a protein was found at an increased level in response to ocean acidification then it was

found at decreased levels in response to ocean acidification and mechanical stimulation (Table III.S3, Figures III.S2 and III.S3). Many differentially expressed proteins that were common across stress responses were consistent in having either increased or decreased levels in response to stress: 96% of the proteins (n = 79) in the responses to ocean acidification and to mechanical stress at low pCO_2 had the same directional change and 76% of the proteins (n = 25) in the responses to mechanical stress at both pCO_2.

Forty-eight proteins were differentially expressed in response to all treatments and these represent the general proteomic stress response. These proteins are associated with a wide range of biological processes, including carbohydrate metabolism (malectin and α-L-fucosidase), cell adhesion (neurexin-4 and cadherin-23), cytoskeleton processes (talin-1, dynein heavy chain 3, and coactosin), mRNA processing (small nuclear ribonucleoproteins and serine/arginine-rich splicing factor 6), the immune response (allograft inflammatory factor 1), polypeptide and protein degradation (aspartyl aminopeptidase, ubiquitin carboxyl-terminal hydrolase FAF-X, and insulin-degrading enzyme), the stress response (Hsp90 co-chaperone Cdc37, universal stress proteins MSMEG_3950 and A-like), and transcription and translation (nucleolar protein 56, 60S ribosomal proteins L21 and L38, and nucleosome assembly protein 1-like 1).

Discussion

Ocean acidification is an on-going and global scale phenomenon that has been shown to negatively impact most taxonomic groups. A large number of studies have characterized these negative impacts across species and life stages (e.g. Kroeker et al., 2013; Kroeker et al., 2010). With the goal of achieving a better understanding of the effects of ocean acidification and responses to additional acute stressors across multiple physiological processes, we employed an integrative approach, combining analyses of shell micromechanical properties, fatty acids, glycogen concentration, and proteomics. Our findings illustrate the value of using complementary approaches to explore interactions and trade-offs among different fundamental processes during environmental stress.

Relative shell growth was not impacted by exposure to elevated pCO_2 (800, 1000 and 2800 μatm) for one month. The lack of significant difference in growth among treatments is somewhat surprising, especially considering that calcite, the main component of adult oyster shells, was undersaturated in the 2800 μatm treatment. Over longer exposures to ocean acidification, other bivalve species have demonstrated decreased shell growth as compared to individuals held at ambient pCO_2. After six weeks, mussel (*Mytilus edulis*) shell length growth was negatively impacted by elevated pCO_2 of 2400 and 4000 μatm (Melzner et al., 2011). Juvenile oysters, *Crassostrea virginica*, also had relatively lower shell mass after 45 days at 1 665 μatm (Talmage and Gobler, 2011) and after a 20 week exposure at 3 523 μatm (Beniash et al., 2010). Based on these data we might expect to see differences in shell growth if exposure was continued for a longer period of time. In addition to the duration of exposure, level of pCO_2 may also be an important factor in effects observed on shell growth. Elevated pCO_2 may in fact prompt an over-compensation in terms of shell deposition. For instance, hard shell clams, *Mercenaria mercenaria*, had higher shell mass at moderately elevated pCO_2 (about 800 μatm) after 16 and 21 weeks of exposure, but no significant difference in shell mass between the control treatment and highly elevated pCO_2 (about 1500 μatm) was observed (Dickinson et al., 2013). At least some of the variability in the effects of elevated pCO_2 on shell growth is likely due to intra- and interspecies differences in population history of exposure to low pH events.

Given that shell growth persisted in all elevated pCO_2 treatments, we were able to perform mechanical testing on new shell that was deposited. Shell microhardness and fracture toughness were both affected by exposure to elevated pCO_2. Microhardness, a measure of a material's resistance to deformation, was reduced at elevated pCO_2 (1000 μatm) as compared to the control (400 μatm), whereas fracture toughness, a measure of the propensity for cracks to propagate within a material, was reduced only at 2800 μatm. Both measurements are affected by the arrangement and dimensions of the microstructures that comprise the shell and the extent and distribution of elastic elements within the shell (i.e. the shell organic matrix) (Lee et al., 2008). Hence, exposure to elevated pCO_2 may lead to dose-dependent differences in the structure and/or

composition of newly formed shell. Such changes could result either from alterations in the physiology of shell deposition or an inability to prevent dissolution and erosion of individual microstructures under varying seawater hydrochemistry. In the current study, changes to micromechanical properties were detected at both $\Omega_{calcite}$ (Ω_c) = 0.5 (2800 μatm) and at Ω_c = 1.3 (1000 μatm). Alterations in shell growth and structure would be expected at $\Omega_c < 1$, however, there is increasing evidence that shell modifications also occur at $\Omega_c > 1$. Even when seawater is saturated with respect to calcite, bivalves experience both shell dissolution (Dickinson et al., 2013; Lannig et al., 2010) and changes to shell microstructure (Beniash et al., 2010; Dickinson et al., 2013; Welladsen et al., 2010). These results indicate that as Ω decreases the driving force towards biomineralization is reduced. Source population evolutionary history may also affect sensitivity to changes in Ω. Since calcification is an energetically intensive process (Paine, 1971; Palmer, 1992; Rosenberg & Hughes, 1991), one explanation for significant effects on $CaCO_3$ structures at $\Omega > 1$ is that resources for energy metabolism are being reallocated to other, non-calcification physiological processes in order to maintain homeostasis.

In order to gain insight into changes in energy metabolism that could be a result of elevated pCO_2, we examined fatty acid profiles and glycogen content. Relative proportions of fatty acids and glycogen content in whole body tissue were similar after one month of exposure to 800 μatm or 2800 μatm pCO_2, suggesting that extended stress of ocean acidification did not alter fundamental metabolites. Oysters and other bivalves are highly dependent on fatty acids as a main energy source, especially poly-unsaturated fatty acids (Milke et al., 2004; Pettersen et al., 2010; Soudant et al., 1999; Trider and Castell, 1980). Changes in physiological state, such as those induced by reproduction or poor nutrient supply, can alter the relative proportions of fatty acids in oyster tissue (Both et al., 2011; Soudant et al., 1999). Glycogen stores represent important sources of stored energy that are accumulated during the non-reproductive season and then mobilized for use as glucose during gametogenesis (Berthelin et al. 2000). It is possible that an environmental stress can trigger a change in bivalve physiology and result in changes in lipid or carbohydrate metabolism and/or storage. In the case of ocean acidification, *C.*

gigas is able to maintain homeostasis of both total and relative amounts of both of these energy-providing molecules by restructuring the proteome to metabolize or synthesize lipids and carbohydrates as needed. In contrast to our results, after 11 weeks of exposure to pCO_2 of 800 μatm, juvenile *C. virginica* had significantly less lipid and glycogen per gram body weight than control oysters (Dickinson et al., 2012). The extended stress of the 11 week exposure in Dickinson et al. (2012) may have overwhelmed *C. virginica*'s ability to maintain lipid and carbohydrate homeostasis, suggesting that oyster energy metabolism may fail under consistent ocean acidification stress. There are some instances where ocean acidification did not influence lipid levels in invertebrates. For example, in larval sea urchins, despite the fact that individuals at elevated pCO_2 were smaller than control larvae, they maintained the same lipid and protein levels (Matson et al., 2012).

Consistent with the hypothesis that elevated pCO_2 impacts underlying physiology, we predicted that lower pH would depress the temperature threshold for mortality after heat exposure. The lack of influence on acute heat shock response across the four pCO_2 treatments could be evidence that pCO_2 has little effect on the oyster's macro-physiological response. We are not aware of other studies that have investigated ocean acidification and acute heat stress, but there are studies that have explored moderately elevated temperatures and ocean acidification over an extended period. In *C. virginica*, elevated pCO_2 did not impact the oyster's response to elevated temperature (Ivanina et al., 2013). In fact, Ivanina et al. (2013) demonstrated that exposure to elevated pCO_2 limited high temperature-associated mortality in *C. virginica*. It appears that extended exposure to elevated pCO_2 did not mitigate oyster mortality in response to acute heat shock as it can do with long-term exposure to a moderately elevated temperature.

Proteomic response to ocean acidification

To achieve a comprehensive assessment of the underlying physiological impact of ocean acidification on oysters, we characterized the proteomic response. Ocean acidification significantly affected the underlying molecular physiology of *C. gigas* after

one month of exposure. Among the main processes affected were lipid and carbohydrate metabolism, cell adhesion, cytoskeleton processes, detoxification and the antioxidant response, the cellular stress response, DNA repair, transcription, and translation. The details of some of these proteomic changes in response to elevated pCO_2 are outlined below.

Carbohydrate metabolism

One clear trend identified in gill protein expression patterns in oysters exposed to elevated pCO_2 was the differential expression of proteins associated with carbohydrate metabolism. Changes in these pathways imply alterations in energetic resource use upon exposure to elevated pCO_2. Protein expression changed for a range of enzymes involved in producing glucose, perhaps revealing a shift in glucose production pathways during ocean acidification stress. Proteins in the galactose metabolism pathway (UDP-glucose 4-epimerase, UDP-N-acetylhexosamine pyrophosphorylase, and N-acetylgalactosamine kinase), which can lead to increased glucose production, were expressed higher in oysters from the high pCO_2 treatment. Those involved in gluconeogenesis (serine-pyruvate aminotransferase) and conversion of other carbohydrates to glucose (glycogen debranching enzyme and pyruvate kinase muscle enzyme) were expressed at higher levels in oysters from the low pCO_2 treatment. One explanation for these changes is that during exposure to ocean acidification oysters need more glucose production in order to maintain homeostasis. Interestingly, the oysters did not mobilize glycogen stores to meet this demand as glycogen content did not differ among pCO_2 treatments. Glycogen stores may have been maintained because they are typically mobilized as an immediate response to a short-term stress and/or an energetic priority is placed on maintaining glycogen as an investment in fitness. In other taxa, the general stress response usually leads to increased carbohydrate metabolism and decreased carbohydrate storage, which is similar to observations from this study (Mizock, 1995; Parrou et al., 1997). Ocean acidification appears to impact energy resource demands in the oyster, which could be of consequence during periods of immune stress or reproduction, which also require many energetic resources.

Lipid metabolism

The expression of proteins involved in lipid metabolism, another important energy source, and lipid transport were significantly affected by exposure to ocean acidification. Proteins implicated in fatty acid metabolism (enoyl-CoA hydratase), fatty acid transport (fatty acid-binding protein, heart) and lipid synthesis (ATP-citrate synthase) were expressed at higher levels after exposure to elevated pCO_2. A protein involved in desaturation and elongation of fatty acids (NADH-cytochrome b5 reductase 1), likely for incorporation into cellular membranes, was expressed lower in the ocean acidification-exposed oysters. Highly unsaturated fatty acids are more sensitive to oxidative damage, therefore a lower level of unsaturation may not only protect cellular membranes from reactive oxygen species (ROS) damage but may also protect molecules within the cell (reviewed in Pamplona et al., 2002). Lipid metabolism-associated genes/proteins were also expressed at higher levels in larval barnacles (Wong et al., 2011) and adult coral (Kaniewska et al., 2012) exposed to elevated pCO_2. Changes in lipid metabolism, similar to the observed changes in carbohydrate metabolism, represent a shift in how energetic resources are used during extended environmental stress.

Frequently during extended ocean acidification stress bivalves shift from metabolism of mostly carbohydrates and lipids to greater use of protein resources (Clark et al., 2013; Michaelidis et al., 2005). In this study, the observed proteomic changes were not yet reflected at the level of oyster fatty acid profiles, but the results suggest that with extended exposure both carbohydrate and lipid reserves would be altered by exposure to ocean acidification. For example, lipid and glycogen stores were reduced in *C. virginica* after eleven weeks at low pH (Dickinson et al., 2012). The effects of changes in metabolism may already be seen at the proteomic level in *C. gigas* with decreased expression of proteins instrumental to muscle growth (kyphoscoliosis peptidase) and muscle repair (dysferlin) as well as the immune response (lymphocyte cytosolic protein 2 and allograft inflammatory factor 1). Maintenance of a robust immune response and of

healthy muscle mass are both important for the long-term fitness of oysters and ocean acidification may be affecting these processes via the reallocation of resources.

Oxidative metabolism

Oxidative metabolism proteins were also affected by exposure to ocean acidification conditions, imposing further changes on energy supply and perhaps increasing oxidative stress**.** Increased expression of proteins cytochrome c oxidase and NADH dehydrogenase implies that oysters exposed to elevated pCO_2 experienced a heightened demand for energy (i.e. increased ATP production in mitochondria). Heightened metabolism can occur in response to an ongoing stress (Mizock 1995) and may be an important adaptive strategy to counteract the physiological effects of elevated environmental pCO_2 (Melzner et al., 2009). However, this response can be species specific: increased metabolic rate was observed in *M. mercenaria*'s response to elevated pCO_2 and temperature (Matoo et al., 2013), while *C. gigas*' metabolic rate was suppressed (Lannig et al., 2010). Expression of proteins and genes associated with metabolic processes are among the most common changes when invertebrates are exposed to elevated pCO_2. Genes associated with metabolism were expressed at lower levels in larval urchins (Todgham and Hofmann, 2009), adult corals (Kaniewska et al., 2012), larval oysters (Dineshram et al., 2012, 2013), and larval tube worms (Mukherjee et al., 2013). In the mantle tissue of *C. virginica*, proteins associated with energy metabolism (mitochondrial malate dehydrogenase, 40S ribosomal protein, and proteasome α type 3) were expressed at higher levels after exposure to low pH (Tomanek et al., 2011). Most of these other studies revealed down-regulation of metabolic pathways, while we found a shift between different pathways, perhaps indicating preferred methods of metabolism during stress. These slight differences in results may be due to life stage and tissue type or simply the increased sensitivity of using shotgun proteomics.

Cellular stress

Elevated expression of antioxidant response proteins (two isoforms of glutathione S-transferase Ω-1) and cytochrome P450 1A5, which produces ROS, provided further evidence of increased oxidative metabolism. The cellular need for an antioxidant response could arise from greater ROS generation during increased metabolism (Mohanty et al., 2000) or ocean acidification may directly lead to oxidative stress through elevated cellular CO_2 and H^+ (Dean, 2010; Tomanek et al., 2011). Perhaps as a result of increased oxidative stress, the apoptotic response was also elevated. Nucleoside diphosphate kinase homolog 5, a protein that prevents apoptosis, was expressed at lower levels at elevated pCO_2. Additionally, autophagy was increased through the relatively greater expression of CDGSH iron-sulfur domain-containing protein 2. Evidence of oxidative stress at the protein/gene level (Tomanek et al., 2011; Kaniewska et al., 2012; Clark et al., 2013) as well as apoptosis (Todgham and Hofmann 2009; Kaniewska et al. 2012) was also observed in other invertebrates exposed to elevated pCO_2. The findings in this and in previous studies support the universal occurrence of increased oxidative stress during invertebrate exposure to ocean acidification.

In the current study, a broad-scale increase in expression of chaperones and stress response proteins was observed (heat shock 70 kDa protein 4, HSP90 co-chaperone Cdc37, universal stress protein A-like protein, Hsc70-interacting protein, universal stress protein MSMEG_3950, and stress-induced-phosphoprotein 1), providing further evidence of increased cellular stress and damage during ocean acidification exposure. These results contrast with other studies, which generally report decreased expression of cell stress proteins and genes in response to ocean acidification (Kaniewska et al., 2012; Todgham and Hofmann, 2009; Wong et al., 2011), however increased expression of hsp70 was reported in *C. gigas* (Clark et al., 2013). Some of these discrepancies among studies may be due to differences in life stage, tissue type, amount of food available, or equilibrium among transcription, translation, and post-translational modifications. It is clear that elevated pCO_2 impacts the cellular stress response, but likely in a manner that addresses the changing physiological needs of the organism.

DNA repair, transcription, and translation

There were widespread changes in proteins involved in DNA repair, transcription, and translation in oysters exposed to elevated pCO_2, illustrating a significant molecular response to the physiological effects of ocean acidification. At the nucleotide level, changes in protein expression included decreased nucleoside metabolism (purine nucleoside phosphorylase) and differential expression of proteins associated with nucleotide metabolism (nicotinamide riboside kinase 1 and adenylosuccinate lyase). Concurrently, DNA repair proteins were expressed at lower levels in high pCO_2-exposed oysters (poly [ADP-ribose] polymerase 3, RuvB-like 2, and X-ray repair cross-complementing protein 5), seven cell growth proteins were differentially expressed (three at increased levels: hemicentin-1, thymidine phosphorylase, and tyrosine protein kinase yes), and one DNA synthesis protein had elevated expression (prohibitin). One hypothesis for this observation is that the decrease in DNA repair proteins coupled with changes in nucleotide metabolism and DNA synthesis may indicate a shift towards cell growth and DNA synthesis over repairing DNA damaged by increased oxidative stress. Expression of proteins associated with transcription and translation would necessarily change in order to support the myriad other molecular responses to ocean acidification. The importance of these processes is reflected in the enrichment of proteins associated with transcription in the differentially expressed proteins in response to pCO_2, mechanical stimulation, and both stressors at once. In ocean acidification-exposed oysters, twenty-two proteins associated with transcription and mRNA processing were differentially expressed. In terms of protein synthesis and degradation, six proteins associated with amino acid metabolism were differentially expressed: two were expressed at lower levels at in 2800 µatm-exposed oysters (amidohydrolase ytcJ and betaine-homocysteine S-methyltransferase 1) and four had elevated expression (aminoacylase-1, dihydrolipoyl dehydrogenase, glutaryl-CoA dehydrogenase, and C-1-tetrahydrofolate synthase). Twenty-three proteins involved in protein synthesis and translation were differentially expressed and eleven proteins associated with protein degradation underwent significant changes in expression, including increased expression of two that prevent protein degradation (cystatin-B, ubiquitin caroxyl-terminal hydrolase FAF-X). In larval sea urchins, genes in associated with translation decreased expression in response to elevated pCO_2 (Todgham and Hofmann, 2009), while in larval barnacles and adult *C.*

virginica these proteins increased expression (Tomanek et al., 2011; Wong et al., 2011). Transcription and translation are the processes that support all other molecular and phenotypic changes. The large number of differentially expressed proteins involved in these processes illustrates their integral role in responding to environmental stress.

The effects of pCO_2 on the stress response

Elevated pCO_2 alone may be a stressor for many species, but it may also impair the ability to respond to other physical, chemical, or biological stressors. To investigate the ability of an organism to respond to stressors under ocean acidification conditions, we subjected oysters to mechanical stimulation. Qualitative differences between the proteomic responses to mechanical stimulation at 400 and 2800 μatm were reflected in the enrichment analysis, which identified differences between treatment groups at the process level. At 400 μatm, RNA metabolic process, transcription, and gamete generation were enriched in the response to mechanical stimulation. At 2800 μatm a different set of processes were enriched: polysaccharide biosynthesis, polysaccharide metabolic process, and transcription.

At the metabolic pathway level, there were different proteomic responses to mechanical stimulation between the two pCO_2 treatments. At low pCO_2 (400 μatm) seven proteins involved in carbohydrate metabolism were expressed at higher levels upon mechanical stimulation and seven were expressed at lower levels. In contrast, at 2800 μatm nine proteins associated with carbohydrate metabolism had increased expression and only four decreased expression after mechanical stimulation. Specifically, in the mechanically stimulated 2800 μatm-exposed oysters, there was increased expression of proteins that convert stored glycogen into glucose (glycogen debranching enzyme, lysosomal α-glucosidase, and glycogenin-1) as well as proteins involved in gluconeogenesis (glucose-6-phosphate isomerase and serine-pyruvate aminotransferase). Rapid mobilization of glycogen stores to make glucose is a common physiological response to stress. In food-stressed rainbow trout an additional handling stress caused a rapid decrease in liver glycogen and increase in plasma glucose (Vijayan & Moon, 1992). The same exogenous stress in oysters held at low pCO_2 prompted a decrease in

expression of proteins associated with carbohydrate metabolism and gluconeogenesis (neutral α-glucosidase AB, glucose-5-phosphate isomerase, and α-N-acetylgalactosaminidase) as well as increased expression of a protein in the glycogen synthesis pathway (putative glycogen [starch] synthase), implying a relatively decreased need for readily available carbohydrate resources. At both pCO_2, fewer lipid metabolism proteins were differentially expressed (four differentially expressed proteins at 400 μatm and three at 2800 μatm) compared to carbohydrate metabolism. Mechanical stimulation is a transient stress and carbohydrates represent a more readily available resource compared to lipids for a short-term response. The different changes observed in response to mechanical stimulation illustrate that an additional stress at high pCO_2 necessitated greater resource use and a need to access energy reserves. Given the resources needed to sustain a response to an environmental stress, this increase in energetic demand could be detrimental.

In contrast to the proteomic response to mechanical stimulation at 400 μatm, oysters from the elevated pCO_2 treatment had decreased expression of many proteins associated with oxidative metabolism and had a much larger antioxidant response. Four mitochondrial NADH dehydrogenases were expressed at lower levels after mechanical stimulation in the high pCO_2 oysters, while at low pCO_2 three were expressed at higher levels and one was decreased. Expression levels of cytochrome b-c1 complex, cytochrome c, and cytochrome c oxidase subunit 5B were elevated in the 2800 μatm after mechanical stress (and were not affected at low pCO_2). These expression changes suggest that at high pCO_2 mechanical stress caused a decrease in electron supply from NADH to the electron transport chain (ETC) but an increase in the transfer of electrons to the terminal oxidase, while at low pCO_2 more electrons entered the ETC from NADH. In marine invertebrates ROS production occurs during forward electron transport (reviewed in Abele et al., 2007) and a decrease in electron supply may be a physiological compensation against further ROS production. Greater oxidative stress at high versus low pCO_2 was also evidenced by the increased expression of five antioxidant response proteins upon mechanical stimulation at elevated pCO_2 (glutathione S-transferase (GST) A, GST 3, GST μ 3, thioredoxin domain-containing protein 17, and dual oxidase 2) compared to just one protein at low pCO_2 (GST Ω-1). These changes are further

evidence that ocean acidification alters the cellular balance between energy resource supply and oxidative stress, especially upon exposure to an additional exogenous stressor.

Ocean acidification appears to significantly impact apoptotic and cellular stress responses of oysters exposed to mechanical stress (Figure III.S4). Mechanical stimulation elicited a larger response in apoptosis pathways at 400 μatm with differential expression of five proteins (programmed cell death protein 5, CDGSH iron-sulfur domain-containing protein 2, histidine triad nucleotide-binding protein 1, EF-hand domain-containing protein D2, and programmed cell death protein 6). At 2800 μatm only two proteins involved in apoptosis were differentially expressed: caspase-7 decreased expression and engulfment cell motility protein 2 increased expression. Five cell stress response proteins increased expression upon mechanical stimulation in 400 μatm-exposed oysters (protein lethal(2)essential for life, hsp90 co-chaperone Cdc37, Hsc70-interacting protein, and universal stress proteins A-like and MSMEG_3950), while four increased in expression in the 2800 μatm-exposed (Hsp90 co-chaperone Cdc37, MAP kinase-activated protein kinase 2, heat shock 70 kDa protein 12B, and universal stress protein Sll1388). These data suggest that mechanical stress is associated with apoptosis, which would be consistent with cell damage. However, apoptosis and the cellular stress response follow slightly different trajectories in response to mechanical stimulation at different pCO_2 perhaps reflecting different resource availability in responding to the cellular damage inflicted by the additional stress. Changes to the normal apoptotic and stress responses could be detrimental to oysters, highlighting the importance of considering other environmental conditions when examining biological impacts of ocean acidification.

Stress from mechanical stimulation impacted expression of proteins involved in many of the processes that were influenced by elevated pCO_2, further illustrating the potential synergistic impacts of these two stressors on oyster physiology. Together these protein expression patterns indicate the complex nature of how multiple stressors influence physiology and how exposure to additional stressors (i.e. increased temperature or disease exposure) in combination with ocean acidification could have significant implications for survival and potential for adaptation.

Conclusion

Ocean acidification is frequently portrayed as being detrimental to marine calcifiers, but its effects on invertebrates range well beyond changes to the calcification process. In this study, a wide variety of processes and responses were assessed in the Pacific oyster's response to elevated pCO_2 to better understand the physiological trade-offs that occur during this particular stress response. Shell growth was not affected by ocean acidification after one month, but elevated pCO_2 did affect the integrity of the deposited shell material. Relative amounts of fatty acids and glycogen content, which are necessary for continued survival and execution of other energy-consuming processes, were also unaltered at elevated pCO_2. Mortality in response to acute heat shock remained unaffected as well. The proteomic profile of *C. gigas* gill tissue was significantly altered by ocean acidification, elucidating the molecular physiological costs of elevated environmental pCO_2. These changes in proteomic profile suggest that oysters experience shifts in their energy budget as they allocate resources to combat extended exposure to ocean acidification. From a proteomics perspective, ocean acidification also affected *C. gigas*'s response to an additional stress event. Shell integrity and response to a second stress become important in a dynamic environment, and in this way ocean acidification may decrease *C. gigas* fitness under chronic exposure.

Tables

Table III.1. Water chemistry summary data. Mean and ± standard deviation are provided for the 29 day experiment. Salinity is an average of nineteen measurements and A_T was measured four times. pH and temperature values are from the continuous monitoring by the DuraFET probe. pH, temperature, salinity, and A_T were directly measured and all other parameters were calculated using CO_2calc (Robbins et al., 2010).

Treatment (ppm)	pH	Temperature (°C)	Salinity	A_T (µmol/kg)	Source Water pCO_2 (µatm)	Oyster Container pCO_2 (µatm)	Ω (calcite)	Ω (aragonite)	CO_3^{2-} (µmol/kg)
400	8.02±0.02	12.97±0.41	29.9±0.2	2085.4±15.9	427±33	464±54	2.7±0.1	1.7±0.1	109.9±5.8
800	7.73±0.04	12.92±0.41	29.9±0.2	2086.4±12.1	810±61	936±17	1.6±0.1	1.0±0.1	65.3±4.3
1000	7.63±0.10	12.82±0.21	29.9±0.3	2084.9±15.3	991±10	1119±40	1.3±0.0	0.8±0.0	54.7±1.2
2800	7.29±0.10	12.87±0.51	29.9±0.2	2085.6±14.9	2848±873	2776±603	0.5±0.1	0.3±0.1	22.0±4.5

Table III.2. Average buoyant weight ± 95% confidence intervals at start and end of experiment.

	Mass at Start (grams)	Mass at 29 Days (grams)
400 µatm	7.1 ± 0.47	7.8 ± 0.64
800 µatm	7.0 ± 0.48	7.6 ± 0.74
1000 µatm	7.1 ± 0.43	7.4 ± 0.70
2800 µatm	7.6 ± 0.54	8.1 ± 0.89

Table III.3. Total number of proteins identified for each oyster across all three technical replicates with numbers of proteins for each individual technical replicate in parentheses. Number of proteins shared among all three technical replicates (with percentage of total) are in the third column.

Oyster (pCO_2 – biological replicate)	Total Proteins (Technical replicate #1, #2, #3)	Proteins Across All 3 Replicates (% of Total)
400-1	882 (869, 871, 873)	853 (96.7%)
400-2	878 (861, 863, 861)	841 (95.8%)
400-3	836 (819, 824, 819)	802 (95.9%)
400-4	867 (855, 856, 857)	839 (96.8%)
400-MechS1	861 (850, 850, 846)	832 (96.6%)
400-MechS2	815 (803, 806, 801)	788 (96.7%)
400-MechS3	854 (840, 848, 841)	826 (96.7%)
400-MechS4	862 (842, 850, 848)	825 (95.9%)
2800-1	873 (854, 858, 856)	837 (95.9%)

2800-2	924 (910, 917, 910)	894 (96.8%)
2800-3	901 (888, 884, 893)	871 (96.7%)
2800-4	874 (861, 866, 865)	849 (97.1%)
2800-MechS1	889 (877, 878, 879)	858 (96.5%)
2800-MechS2	891 (886, 876, 880)	867 (97.3%)
2800-MechS3	867 (860, 859, 856)	844 (97.3%)
2800-MechS4	941 (923, 925, 929)	905 (96.2%)

Figures

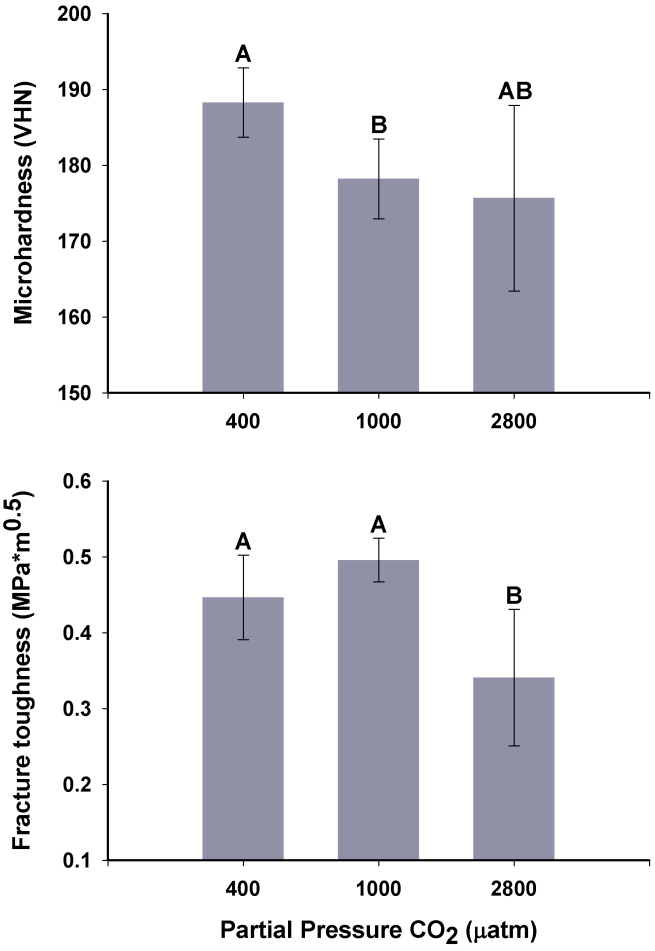

Figure III.1. Mean Vickers microhardness and fracture toughness of *C. gigas* shells (± 95% C.I.) from 400, 1000, and 2800 µatm, tested within the outer 3 mm of the shell's

growing edge. Groups marked with different letters are significantly different ($p < 0.05$; n = 5-7 shells per treatment).

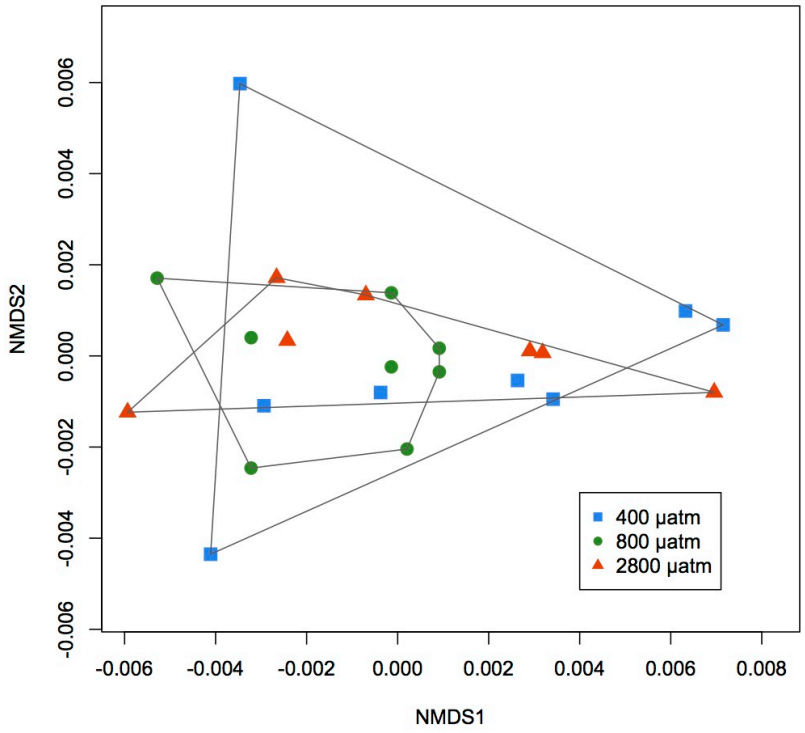

Figure III.2. Non-metric multidimensional scaling (NMDS) analysis of fatty acid profiles for oysters from 400, 800 and 2800 μatm. There are no differences in relative amounts of fatty acids among the three treatment groups.

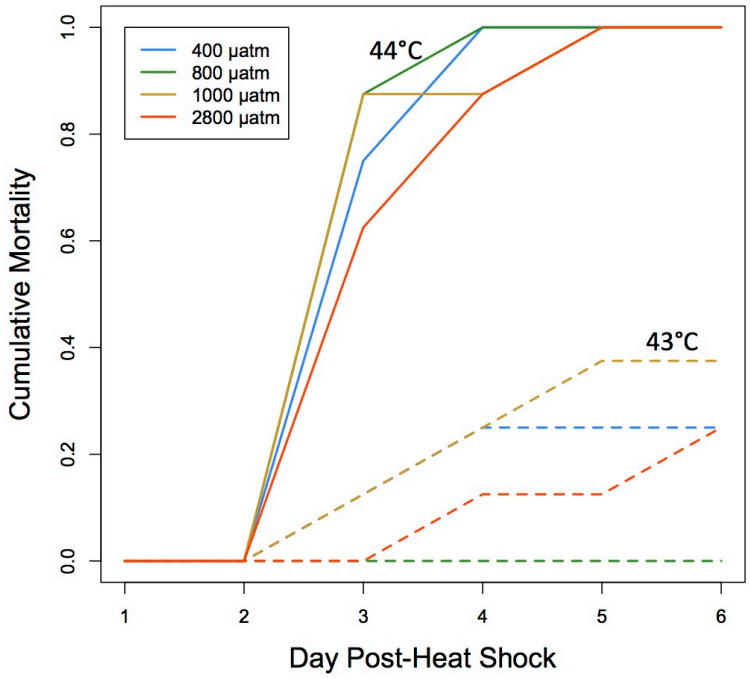

Figure III.3. Oyster mortality after 1 hour heat shock at 43°C (dashed lines) or 44°C (solid lines). Mortality from heat shock did not differ among groups of oysters exposed to different pCO_2 for 1 month - 400 μatm (blue), 800 μatm (green), 1000 μatm (yellow), 2800 μatm (orange).

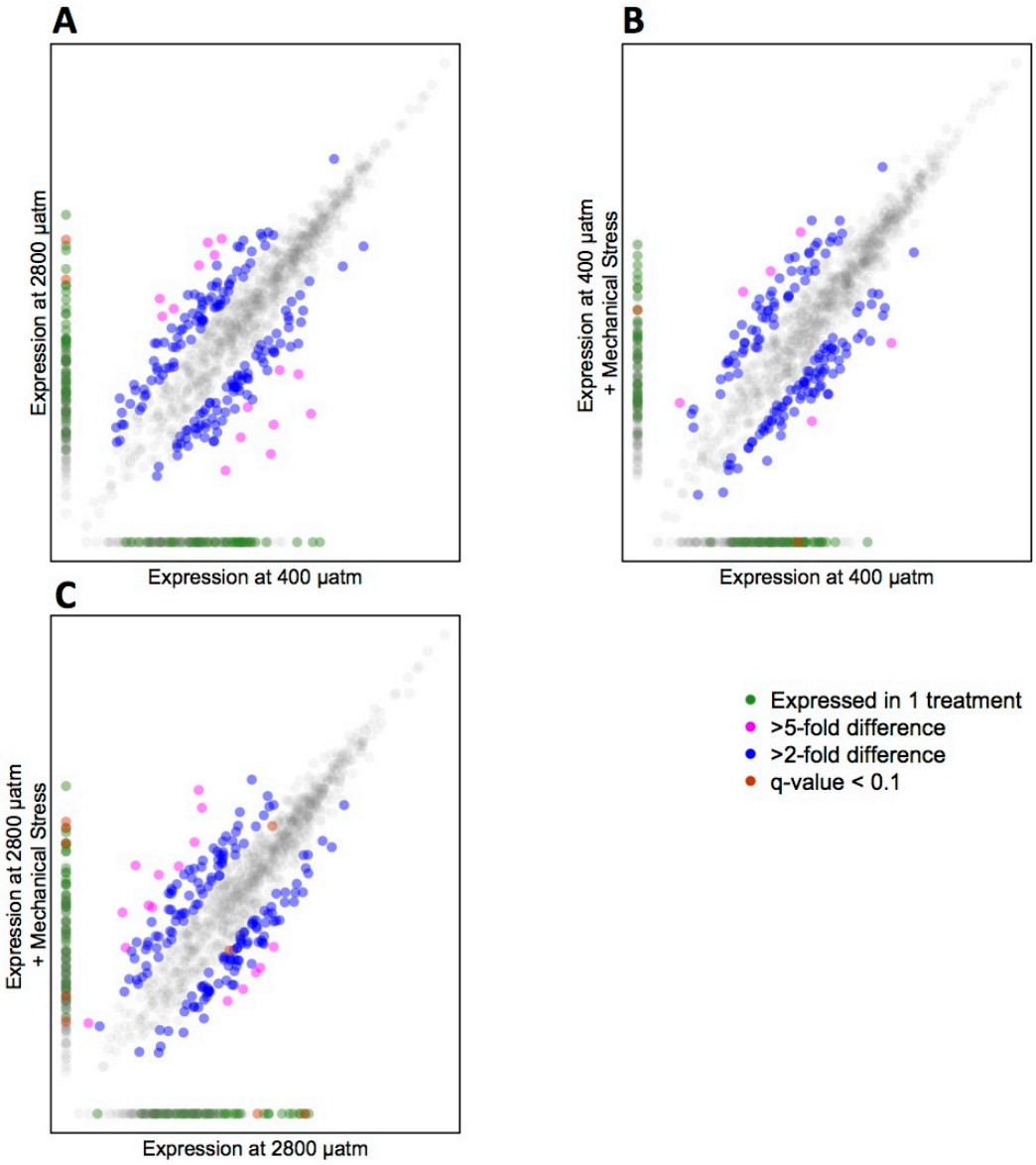

Figure III.4. Characterization of protein expression values (log([normalized spectral abundance factor]*10000)) for experiments designed to examine the influence of ocean acidification (A), mechanical stress at 400 μatm (B), and mechanical stress at 2800 μatm (C). Pink and green dots represent differentially expressed proteins as defined in the methods.

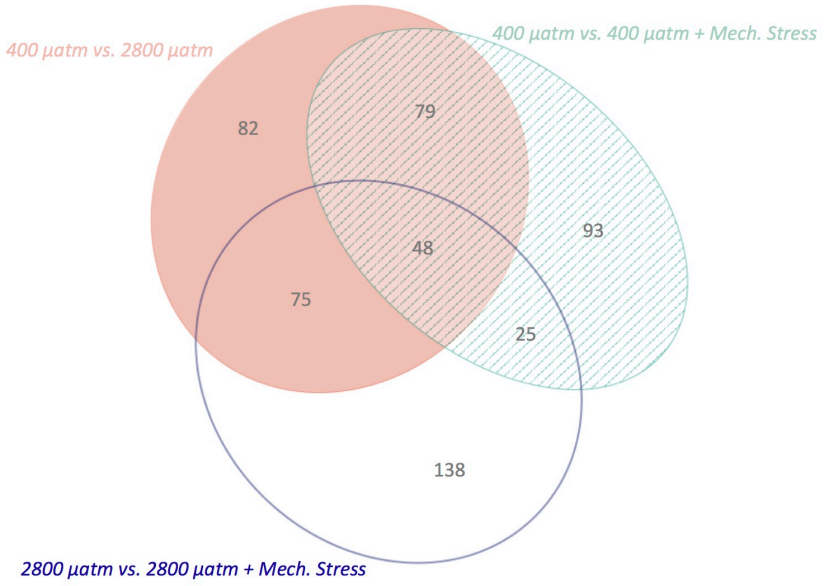

Figure III.5. Differentially expressed proteins among treatments. The proteins represented by the solid pink ellipse were those implicated in the response to ocean acidification alone, those in the open blue ellipse are different in response to mechanical stress in the 2800 μatm-exposed oysters, and those in the striped aqua ellipse changed in response to mechanical stress at 400 μatm. Numbers represent the number of proteins in each segment of the ellipses.

Supplementary Information

Supplementary information is available as a file set in (Timmins-Schiffman and Roberts 2014c).

The proteomics dataset has been deposited to the ProteomeXchange with identifier PXD000835.

Figure S1. Representative indents made during micromechanical testing for the (A) 400 μatm and (B) 2800 μatm treatment. The radius of a circle radiating from the center of the indent enclosing all visible cracks was used to calculate fracture toughness, a portion of which is shown for each treatment. Arrow denotes the longest crack found for each

indent. Radius length is shown on the image in μm. Mean crack radius was similar between the 400 and 1000 μatm treatments.

Figure S2. Glycogen content (μg glycogen per mg tissue) for oysters from the pCO2 treatments of 400, 800, and 2800 μatm. There is no difference in glycogen content among treatment groups.

Figure S3. Heat maps of differentially expressed proteins annotated with protein names. Protein expression values have been log-transformed. The dendrograms on the left of the heat maps represent the clustering of proteins according to expression profile.

Figure S4. Representation of key metabolic pathways that are significantly affected by ocean acidification (A), mechanical stress at low pCO_2 (B), and mechanical stress at high pCO_2 (C). Red lines are proteins/pathways that are differentially expressed at higher levels in the stress treatments and blue lines are those that are differentially expressed at lower levels. In the key, the different colored lines represent different metabolic pathways that are affected by oyster exposure to ocean acidification and/or mechanical stimulation. Figures are also available on FigShare with input files for iPath2 to allow for interactive exploration of the data (Timmins-Schiffman and Roberts 2014b).

Table S1. Raw and normalized (proportion) fatty acid data for 8 oysters each from 3 treatments: 400, 800, and 2800 μatm.

Table S2. ProteinProphet output for each technical replicate. Information for each protein includes percent coverage by sequenced peptides, total number unique peptides, total independent spectra (spectral count), and peptide sequences.

Table S3. Protein expression values (NSAF) for each oyster for the 1 616 proteins identified. Also included are average expression values across treatments (i.e. 2800 avg NSAF is the average expression across all four high pCO_2-exposed oysters); fold change for treatment/control oysters (i.e. Fold Diff OA is [2800 avg NSAF]/[400 avg NSAF]);

columns for each of the three treatment comparisons with an asterisk indicating if the protein is >5-fold up- or down-regulated; SwissProt annotation, e-value, and gene description; proteins responsible for enrichment and the treatment comparisons in which they are enriched; a column indicating in which stress treatment proteins are differentially expressed (q-value < 0.1). In the fold difference columns "up" signifies that the protein was only expressed in oysters from the 2800 μatm treatment (versus the 400 μatm , Fold Diff OA), mechanical stress at 400 μatm treatment (versus 400 μatm, Fold Diff 400 MechS), or in the mechanical stress at 2800 μatm (versus 2800 μatm, Fold Diff 2800 MechS); "down" represents proteins that were only expressed in the other treatment for each comparison.

Table S4. *C. gigas* proteins with associated SwissProt/UniProt-KB, Gene Ontology (GO), and GO Slim annotations.

Table S5. Enriched biological processes for proteins >2-fold differentially expressed in the stress responses to elevated pCO_2 of 2800 μatm ("OA"), mechanical stress after a one month exposure to 400 μatm ("Mech Stress 400 μatm"), and mechanical stress after a one month exposure to 2800 μtam ("Mech Stress 2800 μatm"). Table includes enriched GO term, number of proteins contributing to that GO term, p-value indicating degree of enrichment, the SwissProt accession numbers for those proteins, the fold enrichment for each GO term, and the false discovery rate (FDR).

Acknowledgements

We would like to thank Taylor Shellfish for the donation of all oysters used in this research, particularly Dr. Joth Davis, Jason Ragan, and Dustin Johnson. Sam Garson and Ronen Elad donated their time to oyster collection and maintenance, respectively. Dr. Carolyn Friedman provided essential advice for many parts of the experimental design as well as edits for the manuscript. Drs. Ken Sebens and Emily Carrington generously provided use of the ocean acidification system at Friday Harbor Labs. Matt George, Dr. Moose O'Donnell, and Michelle Herko were indefatigable in their help with running the experiment and technical troubleshooting. Oyster sampling was aided by Sam White, Mackenzie Gavery, and Caroline Storer. Thank you pub-a-thon participants and Dr. Lorenz Hauser for comments throughout the manuscript writing process. Dr. Priska von Haller, Jimmy Eng, and Tahmina "Eva" Jahan were indispensable in executing the proteomics portion of the experiment. J. Sean Yeung and Dr. Mike Brett provided

training, lab space, and help with analysis for the fatty acids. This work was supported in part by the SQLShare project at the University of Washington eScience Institute.

Works Cited

Abele, D., Philipp, E., Gonzalez, P. M., and Puntarulo, S. (2007). Marine invertebrate mitochondria and oxidative stress. *Frontiers in Bioscience*, 12, 933–946.

Altschul, S. F., Madden, T. L., Schäffer, A.A., Zhang, J., Zhang, Z., Miller, W., and Lipman, D. J. (1997). Gapped BLAST and PSI-BLAST: a new generation of protein database search programs. *Nucleic acids research*, 25(17), 3389–402.

Anstis, G. R., Chantikul, P., Lawn, B. R., and Marshall, D. B. (1981). A critical evaluation of indentation techniques for measuring fracture toughness: I, direct crack measurements. *Journal of the American Ceramic Society*, 46(9), 533–538.

Baldassarri, M., Margolis, H. C., and Beniash, E. (2008). Compositional Determinants of Mechanical Properties of Enamel. *Journal of Dental Research*, 87(7), 645–649. doi:10.1177/154405910808700711

Barton, A., Hales, B., Waldbusser, G. G., Langdon, C., and Feely, R.A. (2012). The Pacific oyster, Crassostrea gigas, shows negative correlation to naturally elevated carbon dioxide levels: Implications for near-term ocean acidification effects. *Limnology and Oceanography*, 57(3), 698–710. doi:10.4319/lo.2012.57.3.0698

Beniash, E., Ivanina, A., Lieb, N., Kurochkin, I., and Sokolova, I. (2010). Elevated level of carbon dioxide affects metabolism and shell formation in oysters Crassostrea virginica (Gmelin). *Marine Ecology Progress Series*, 419, 95–108. doi:10.3354/meps08841

Berthelin, C., Kellner, K., and Mathieu, M. (2000). Storage metabolism in the Pacific oyster (*Crassostrea gigas*) in relation to summer mortalities and reproductive cycle (West Coast of France). *Comparative Biochemistry and Physiology Part B*, 125, 359-369. doi:10.1016/S0305-0491(99)00187-X

Both, A., Parrish, C. C., Penney, R. W., and Thompson, R. J. (2011). Lipid composition of Mytilus edulis reared on organic waste from a Gadus morhua aquaculture facility. *Aquatic Living Resources*, 301, 295–301.

Caldeira, K. and Wickett, M.E. (2005). Ocean model predictions of chemistry changes from carbon dioxide emissions to the atmosphere and ocean. *Journal of Geophysical Research*, 110, C09S04. doi:10.1029/2004JC002671

Clark, M. S., Thorne, M.A.S., Amaral, A., Vieira, F., Batista, F. M., Reis, J., and Power, D. M. (2013). Identification of molecular and physiological responses to chronic

environmental challenge in an invasive species: the Pacific oyster, Crassostrea gigas. *Ecology and evolution*, 3(10), 3283–97. doi:10.1002/ece3.719

Clegg, J. S., Uhlinger, K. R., and Jackson, S. A. (2009). Induced thermotolerance and the heat shock protein – 70 family in the Pacific oyster Crassostrea gigas, 7(1998), 21–30.

Dean, J. B. (2010). Hypercapnia causes cellular oxidation and nitrosation in addition to acidosis : implications for CO_2 chemoreceptor function and dysfunction. *Journal of Applied Physiology*, 108, 1786–1795. doi:10.1152/japplphysiol.01337.2009.

Dabney, A. and Storey, J.D. and with assistance from Warnes, G.R. (). qvalue: Q-value estimation for false discovery rate control. R package version 1.34.0.

Dickinson, G. H., Ivanina, A. V, Matoo, O. B., Pörtner, H. O., Lannig, G., Bock, C., Bock, C., Beniash, E., and Sokolova, I. M. (2012). Interactive effects of salinity and elevated CO_2 levels on juvenile eastern oysters, Crassostrea virginica. *The Journal of experimental biology*, 215(1), 29–43. doi:10.1242/jeb.061481

Dickinson, G. H., Matoo, O. B., Tourek, R. T., Sokolova, I. M., and Beniash, E. (2013). Environmental salinity modulates the effects of elevated CO_2 levels on juvenile hard-shell clams, Mercenaria mercenaria. *The Journal of experimental biology*, 216(14), 2607–18. doi:10.1242/jeb.082909Dineshram, R., Thiyagarajan, V., Lane, A., Ziniu, Y., Xiao, S., & Leung, P. T. Y. (2013). Elevated CO2 alters larval proteome and its phosphorylation status in the commercial oyster, Crassostrea hongkongensis. *Marine Biology*, *160*(8), 2189–2205. doi:10.1007/s00227-013-2176-x

Dickson, A.G., Sabine, C.L., and Christian, J.R. (Eds.) (2007). Guide to best practices for ocean CO_2 measurements. PICES Special Publication 3, 191 pp.

Dineshram, R., Wong, K. K. W., Xiao, S., Yu, Z., Qian, P. Y., and Thiyagarajan, V. (2012). Analysis of Pacific oyster larval proteome and its response to high-CO_2. *Marine pollution bulletin*, 64(10), 2160–7. doi:10.1016/j.marpolbul.2012.07.043

Duarte, C. M., Hendriks, I. E., Moore, T. S., Olsen, Y. S., Steckbauer, A., Ramajo, L., Carstensen, J., Trotter, J.A., and McCulloch, M. (2013). Is Ocean Acidification an Open-Ocean Syndrome? Understanding Anthropogenic Impacts on Seawater pH. *Estuaries and Coasts*, 36(2), 221–236. doi:10.1007/s12237-013-9594-3

Eng, J. K., Fischer, B., Grossmann, J., and Maccoss, M. J. (2008). A fast SEQUEST cross correlation algorithm. *Journal of proteome research*, 7(10), 4598–602. doi:10.1021/pr800420s

Eng, J. K., Mccormack, A. L., and Yates, J. R. (1994). An Approach to correlate tandem mass spectral data of peptides with amino acid sequences in a protein database. *Journal of the American Society of Mass Spectrometry*, 5, 976–989.

Fang, X., Li, L., Luo, R., Xu, F., Wang, X., Zhu, Y., Yang, L., and Huang, Z. (2012). Genomic data from the Pacific oyster (Crassostrea gigas). GigaScience. http://dx.doi.org/10.5524/100030

Feely, R.A., Alin, S. R., Newton, J., Sabine, C. L., Warner, M., Devol, A., Krembs, C., and Maloy, C. (2010). The combined effects of ocean acidification, mixing, and respiration on pH and carbonate saturation in an urbanized estuary. *Estuarine, Coastal and Shelf Science*, 88(4), 442–449. doi:10.1016/j.ecss.2010.05.004

Feely, R.A., Sabine, C. L., Byrne, R. H., Millero, F. J., Dickson, A. G., Wanninkhof, R., Murata, A., Miler, L.A., and Greeley, D. (2012). Decadal changes in the aragonite and calcite saturation state of the Pacific Ocean. *Global Biogeochemical Cycles*, 26(3), GB3001. doi:10.1029/2011GB004157

Florens, L., Carozza, M. J., Swanson, S. K., Fournier, M., Coleman, M. K., Workman, J. L., & Washburn, M. P. (2006). Analyzing chromatin remodeling complexes using shotgun proteomics and normalized spectral abundance factors. *Methods*, 40(4), 303–11. doi:10.1016/j.ymeth.2006.07.028

Friedrich, T., Timmermann, A., Bates, N. R., Chikamoto, M. O., Church, M. J., Dore, J. E., Gledhill, D.K., González-Dávila, M., Heinemann, M., et al. (2012). Detecting regional anthropogenic trends in ocean acidification against natural variability, 2, 167–171. doi:10.1038/NCLIMATE1372

Galloway, A. W. E., Britton-Simmons, K. H., Duggins, D. O., Gabrielson, P. W., and Brett, M. T. (2012). Fatty Acid Signatures Differentiate Marine Macrophytes At Ordinal and Family Ranks1. *Journal of Phycology*, 48(4), 956–965. doi:10.1111/j.1529-8817.2012.01173.x

Gazeau, F., Gattuso, J.-P., Greaves, M., Elderfield, H., Peene, J., Heip, C. H. R., and Middelburg, J. J. (2011). Effect of carbonate chemistry alteration on the early embryonic development of the Pacific oyster (Crassostrea gigas). *PloS one*, 6(8), e23010. doi:10.1371/journal.pone.0023010

Gazeau, F., Quiblier, C., Jansen, J. M., Gattuso, J.-P., Middelburg, J. J., and Heip, C. H. R. (2007). Impact of elevated CO_2 on shellfish calcification. *Geophysical Research Letters*, 34(7), L07603. doi:10.1029/2006GL028554

Gruber, N., Hauri, C., Lachkar, Z., Loher, D., Frölicher, T. L., and Plattner, G.-K. (2012). Rapid progression of ocean acidification in the California Current System. *Science*, 337(6091), 220–3. doi:10.1126/science.1216773

Hoffmann, W. A., and Poorter, H. (2002). Avoiding Bias in Calculations of Relative Growth Rate. *Annals of Botany*, 90(1), 37–42. doi:10.1093/aob/mcf140

Howe, B., Cole, G., Souroush, E., Koutris, P., Key, A., Khoussainova, N., and Battle, L. (2011). Database-as-a-service for long-tail science. In *Proceedings of the 23rd international conference on Scientific and statistical database management (SSDBM'11), Judith Bayard Cushing, James French, and Shawn Bowers* (ed. Springer-Verlag, Berlin), pp. 480-489. Heidelberg: Springer-Verlag.

Huang, D. W., Sherman, B. T., and Lempicki, R.A. (2009a). Systematic and integrative analysis of large gene lists using DAVID bioinformatics resources. *Nature protocols*, 4(1), 44–57. doi:10.1038/nprot.2008.211

Huang, D. W., Sherman, B. T., and Lempicki, R.A. (2009b). Bioinformatics enrichment tools: paths toward the comprehensive functional analysis of large gene lists. *Nucleic acids research*, 37(1), 1–13. doi:10.1093/nar/gkn923

Ivanina, A. V, Dickinson, G. H., Matoo, O. B., Bagwe, R., Dickinson, A., Beniash, E., and Sokolova, I. M. (2013). Interactive effects of elevated temperature and CO_2 levels on energy metabolism and biomineralization of marine bivalves Crassostrea virginica and Mercenaria mercenaria. *Comparative biochemistry and physiology. Part A, Molecular & integrative physiology*, 166(1), 101–11. doi:10.1016/j.cbpa.2013.05.016

Kaniewska, P., Campbell, P. R., Kline, D. I., Rodriguez-Lanetty, M., Miller, D. J., Dove, S., and Hoegh-Guldberg, O. (2012). Major cellular and physiological impacts of ocean acidification on a reef building coral. *PloS one*, 7(4), e34659. doi:10.1371/journal.pone.0034659

Kelly, M. W., Padilla-Gamiño, J. L., and Hofmann, G. E. (2013). Natural variation and the capacity to adapt to ocean acidification in the keystone sea urchin Strongylocentrotus purpuratus. *Global change biology*, 19(8), 2536–46. doi:10.1111/gcb.12251

Kroeker, K. J., Kordas, R. L., Crim, R., Hendriks, I. E., Ramajo, L., Singh, G. S., Duarte, C.M., and Gattuso, J.-P. (2013). Impacts of ocean acidification on marine organisms: quantifying sensitivities and interaction with warming. *Global change biology*, 19(6), 1884–96. doi:10.1111/gcb.12179

Kroeker, K. J., Kordas, R. L., Crim, R. N., and Singh, G. G. (2010). Meta-analysis reveals negative yet variable effects of ocean acidification on marine organisms. *Ecology letters*, 13(11), 1419–34. doi:10.1111/j.1461-0248.2010.01518.x

Kurihara, H., Kato, S., and Ishimatsu, A. (2007). Effects of increased seawater pCO_2 on early development of the oyster Crassostrea gigas. *Aquatic Biology*, 1(1), 91–98. doi:10.3354/ab00009

Lacoste, A., Malham, S. K., Cueff, A., Jalabert, F., Gélébart, F., and Poulet, S.A. (2001). Evidence for a form of adrenergic response to stress in the mollusc Crassostrea gigas. *The Journal of experimental biology*, 204(7), 1247–55.

Lacoste, A., Malham, S. K., Cueff, A., and Poulet, S.A. (2001). Stress-induced catecholamine changes in the hemolymph of the oyster Crassostrea gigas. *General and comparative endocrinology*, 122(2), 181–8. doi:10.1006/gcen.2001.7629

Lannig, G., Eilers, S., Pörtner, H. O., Sokolova, I. M., and Bock, C. (2010). Impact of ocean acidification on energy metabolism of oyster, Crassostrea gigas--changes in metabolic pathways and thermal response. *Marine drugs*, 8(8), 2318–39. doi:10.3390/md8082318

Lee, S. W., Kim, G. H., and Choi, C. S. (2008). Characteristic crystal orientation of folia in oyster shell, Crassostrea gigas. *Materials Science and Engineering: C*, 28(2), 258–263. doi:10.1016/j.msec.2007.01.001

Letunic, I., Yamada, T., Kanehisa, M., and Bork, P. (2008). iPath: interactive exploration of biochemical pathways and networks. *Trends in biochemical sciences*, 33(3), 101–3. doi:10.1016/j.tibs.2008.01.001

Matoo, O. B., Ivanina, A. V, Ullstad, C., Beniash, E., and Sokolova, I. M. (2013). Interactive effects of elevated temperature and CO_2 levels on metabolism and oxidative stress in two common marine bivalves (Crassostrea virginica and Mercenaria mercenaria). *Comparative biochemistry and physiology. Part A, Molecular & integrative physiology*, 164(4), 545–53. doi:10.1016/j.cbpa.2012.12.025

Matson, P. G., Yu, P. C., Sewell, M.A, and Hofmann, G. E. (2012). Development under elevated pCO_2 conditions does not affect lipid utilization and protein content in early life-history stages of the purple sea urchin, Strongylocentrotus purpuratus. *The Biological bulletin*, 223(3), 312–27.

Melzner, F., Gutowska, M. A., Langenbuch, M., Dupont, S., Lucassen, M., Thorndyke, M. C., Bleich, M., and Pörtner, H.-O. (2009). Physiological basis for high CO_2 tolerance in marine ectothermic animals: pre-adaptation through lifestyle and ontogeny? *Biogeosciences*, 6(10), 2313–2331. doi:10.5194/bg-6-2313-2009

Melzner, F., Stange, P., Trübenbach, K., Thomsen, J., Casties, I., Panknin, U., Gorb, S.N. and Gutowska, M.A. (2011). Food supply and seawater pCO_2 impact calcification and internal shell dissolution in the blue mussel Mytilus edulis. *PloS one*, 6(9), e24223. doi:10.1371/journal.pone.0024223

Michaelidis, B., Ouzounis, C., Paleras, A., and Pörtner, H. O. (2005). Effects of long-term moderate hypercapnia on acid – base balance and growth rate in marine

mussels Mytilus galloprovincialis. *Marine Ecology Progress Series*, 293, 109–118.

Milke, L. M., Bricelj, V. M., and Parrish, C. C. (2004). Growth of postlarval sea scallops, Placopecten magellanicus, on microalgal diets, with emphasis on the nutritional role of lipids and fatty acids. *Aquaculture*, 234(1-4), 293–317. doi:10.1016/j.aquaculture.2003.11.006

Mizock, B. A. (1995). Alterations in Carbohydrate metabolism during stress: A review of the literature. *The American Journal of Medicine*, 98, 75–84.

Mohanty, P., Hamouda, W., Garg, R., Aljada, A., Ghanim, H., and Dandona, P. (2000). Glucose challenge stimulates reactive oxygen species (ROS) generation by leucocytes. *The Journal of Clinical Endocrinology and Metabolism*, 85(8), 2970–2973.

Mukherjee, J., Wong, K. K. W., Chandramouli, K. H., Qian, P.-Y., Leung, P. T. Y., Wu, R. S. S., & Thiyagarajan, V. (2013). Proteomic response of marine invertebrate larvae to ocean acidification and hypoxia during metamorphosis and calcification. *The Journal of experimental biology*, 216(Pt 24), 4580–9. doi:10.1242/jeb.094516

O'Donnell, M. J., George, M. N., and Carrington, E. (2013). Mussel byssus attachment weakened by ocean acidification. *Nature Climate Change*, 3(6), 587–590. doi:10.1038/nclimate1846

Oksanen, J., Guillaume Blanchet, F., Kindt, R., Legendre, P., Minchin, P.R., O'Hara, R.B., Simpson, G.L., Solymos P., Stevens, M.H.H., and Wagner, H. (2013). vegan: Community Ecology Package. R package version 2.0-8. http://CRAN.R-project.org/package=vegan.

Orr, J. C., Fabry, V. J., Aumont, O., Bopp, L., Doney, S. C., Feely, R.A., Gnandesikan, A., Gruber, N., Ishida, A., Joos, F. et al. (2005). Anthropogenic ocean acidification over the twenty-first century and its impact on calcifying organisms. *Nature*, 437(7059), 681–6. doi:10.1038/nature04095

Paine, R. T. (1971). Energy flow in a natural population of the herbivorous gastropod Tegula funebralis. *Limnology and Oceanography*, 16(1), 86–98.

Palmer, A. R. (1992). Calcification in marine molluscs: how costly is it? *Proceedings of the National Academy of Sciences of the United States of America*, 89(4), 1379–82.

Pamplona, R., Barja, G., and Portero-Otín, M. (2002). Membrane Fatty Acid Unsaturation, Protection against Oxidative Stress, and Maximum Life Span. *Annals of the New York Academy of Sciences*, 959, 475–490.

Parker, L. M., Ross, P. M., and O'Connor, W.A. (2010). Comparing the effect of elevated pCO_2 and temperature on the fertilization and early development of two species of oysters. *Marine Biology*, 157(11), 2435–2452. doi:10.1007/s00227-010-1508-3

Parrou, J. L., Teste, M., Franqois, J., Durand, G., and Cnrs, U. M. R. (1997). Effects of various types of stress on the metabolism of reserve carbohydrates in Saccharomyces cerevisiae : genetic evidence for a stress-induced recycling of glycogen and trehalose. *Microbiology*, 143, 1891–1900.

Pespeni, M. H., Sanford, E., Gaylord, B., Hill, T. M., Hosfelt, J. D., Jaris, H. K., LaVigne, M., Lenz, E.A., Russell, A.D., Young, M.D., et al. (2013). Evolutionary change during experimental ocean acidification. *Proceedings of the National Academy of Sciences of the United States of America*, 110(17), 6937–42. doi:10.1073/pnas.1220673110

Pettersen, A. K., Turchini, G. M., Jahangard, S., Ingram, B.A., and Sherman, C. D. H. (2010). Effects of different dietary microalgae on survival, growth, settlement and fatty acid composition of blue mussel (Mytilus galloprovincialis) larvae. *Aquaculture*, 309(1-4), 115–124. doi:10.1016/j.aquaculture.2010.09.024

R Core Team (2013). R: A language and environment for statistical computing. R Foundation for Statistical Computing, Vienna, Austria. URL http://www.R-project.org/.

Robbins, L.L., Hansen, M.E., Kleypas, J.A., and Meylan, S.C. (2010). CO_2calc - A user-friends seawater carbon calculator for Windows, Mac OS X, and iOS (iPhone): U.S. Geoglogical Survey Open-File Report 2010-1280. 17 pp.

Rosenberg, G. D. and Hughes, W. W. (1991). A metabolic model for the determination of shell composition in the bivalve mollusc, Mytilus edulis. *Lethaia*, 24(1), 83–96.

Soudant, P., Van Ryckeghem, K., Marty, Y., Moal, J., Samain, J. F., and Sorgeloos, P. (1999). Comparison of the lipid class and fatty acid composition between a reproductive cycle in nature and a standard hatchery conditioning of the Pacific Oyster Crassostrea gigas. *Comparative Biochemistry and Physiology Part B: Biochemistry and Molecular Biology*, 123(2), 209–222. doi:10.1016/S0305-0491(99)00063-2

Storey, J. D. (2002). A direct approach to false discovery rates. *Journal of the Royal Statistical Society: Series B (Statistical Methodology)*, 64(3), 479–498. doi:10.1111/1467-9868.00346

Storey, J. D. and Tibshirani, R. (2003). Statistical significance for genomewide studies. *Proceedings of the National Academy of Sciences of the United States of America*, 100(16), 9440–5. doi:10.1073/pnas.1530509100

Stumpp, M., Wren, J., Melzner, F., Thorndyke, M. C., and Dupont, S. T. (2011). CO_2 induced seawater acidification impacts sea urchin larval development I: elevated metabolic rates decrease scope for growth and induce developmental delay. *Comparative biochemistry and physiology. Part A, Molecular & integrative physiology*, 160(3), 331–40. doi:10.1016/j.cbpa.2011.06.022

Talmage, S. C., and Gobler, C. J. (2011). Effects of elevated temperature and carbon dioxide on the growth and survival of larvae and juveniles of three species of northwest Atlantic bivalves. *PloS one*, 6(10), e26941. doi:10.1371/journal.pone.0026941

Timmins-Schiffman, E., Nunn, B. L., Goodlett, D. R., and Roberts, S. B. (2013). Shotgun proteomics as a viable approach for biological discovery in the Pacific oyster. *Conservation Physiology*, 1(1), cot009–cot009. doi:10.1093/conphys/cot009

Timmins-Schiffman, Emma, O'Donnell, M. J., Friedman, C. S., and Roberts, S. B. (2012). Elevated pCO_2 causes developmental delay in early larval Pacific oysters, Crassostrea gigas. *Marine Biology*, 160(8), 1973–1982. doi:10.1007/s00227-012-2055-x

Timmins-Schiffman, E. and Roberts, S.B. (2014a). SQLShare workflow for proteomics analysis. figshare. http://dx.doi.org/10.6084/m9.figshare.894323

Timmins-Schiffman, E. and Roberts, S.B. (2014b). iPath2 supplemental information. figshare. http://dx.doi.org/10.6084/m9.figshare.8999008

Timmins-Schiffman, E., and Roberts, S. (2014c). Supplementary Information accompanying proteomics manuscript. figshare. http://dx.doi.org/10.6084/m9.figshare.958951

Todgham, A. E., and Hofmann, G. E. (2009). Transcriptomic response of sea urchin larvae Strongylocentrotus purpuratus to CO2-driven seawater acidification. *The Journal of experimental biology*, 212(16), 2579–94. doi:10.1242/jeb.032540

Tomanek, L., Zuzow, M. J., Ivanina, A. V, Beniash, E., and Sokolova, I. M. (2011). Proteomic response to elevated PCO_2 level in eastern oysters, Crassostrea virginica: evidence for oxidative stress. *The Journal of experimental biology*, 214(11), 1836–44. doi:10.1242/jeb.055475

Trider, D. J., and Castell, J. D. (1980). Effect of dietary lipids on growth, tissue composition and metabolism of the oyster (Crassostrea virginica). *The Journal of nutrition*, 110(7), 1303–9.

Vijayan, M. M., and Moon, T. W. (1992). Acute Handling Stress Alters Hepatic Glycogen Metabolism in Food-Deprived Rainbow Trout (Oncorhynchus mykiss). *Canadian Journal of Fisheries and Aquatic Sciences*, 49, 2260–2266.

Welladsen, H. M., Southgate, P. C., and Heimann, K. (2010). The effects of exposure to near-future levels of ocean acidification on shell characteristics of Pinctada fucata (Bivalvia : Pteriidae). *Molluscan Research*, 30(3), 125–130.

Wong, K. K. W., Lane, A. C., Leung, P. T. Y., and Thiyagarajan, V. (2011). Response of larval barnacle proteome to CO(2)-driven seawater acidification. *Comparative biochemistry and physiology. Part D, Genomics & proteomics*, 6(3), 310–21. doi:10.1016/j.cbd.2011.07.001

Yamada, T., Letunic, I., Okuda, S., Kanehisa, M., and Bork, P. (2011). iPath2.0: interactive pathway explorer. *Nucleic acids research*, 39(Web Server issue), W412–5. doi:10.1093/nar/gkr313

Synthesis and Conclusion

The overall impacts of ocean acidification on marine bivalves are negative, leading to inhibited larval development and significant changes to molecular and phenotypic physiological responses across life stages. However, many invertebrates also demonstrate extensive phenotypic plasticity in the face of ocean acidification, which may pave the way to adaptation to this environmental change. Growth, development, and shell deposition continue at elevated pCO_2 (usually at reduced rates), indicating a certain degree of tolerance in bivalves (Gaylord et al. 2011; Barros et al. 2013; Thomsen and Melzner 2010; Melzner et al. 2011; Dickinson et al. 2013). This phenomenon may be due to the ecological and evolutionary history of many of these organisms. Variability in responses to ocean acidification, which can signify tolerance in certain individuals, has been observed between species (Parker et al. 2010, 2012; Miller et al. 2009), habitats (Kelly et al. 2013), family groups (Yu et al. 2011), and offspring of broodstock exposed to different pCO_2 regimes (Parker et al. 2012). Most species studied in ocean acidification impact experiments are found in the nearshore environment, where they have been subjected to strong fluctuations in pH and other environmental parameters for generations. Therefore, many of these species possess either the plasticity or a rapid evolutionary capacity (i.e. Pespeni et al. 2013) to adapt to this type of environmental change.

The main physiological struggle for bivalves during ocean acidification stress may be one of limited energy resources. The extended stress of low pH places an energetic toll on bivalves, perhaps as increased energy is needed to maintain $CaCO_3$ saturation in the calcifying compartment or cellular gradients of H^+. The effects of this energetic toll are seen in larvae and juveniles/adults. In larvae, the negative effects of ocean acidification are frequently observed at the transition from reliance on maternally derived energy reserves to exogenous energy resources (Kurihara et al. 2007; Barton et al. 2012; Timmins-Schiffman et al. 2012). Larval sensitivity to elevated pCO_2 cannot be fully ameliorated by the addition of increased food, as demonstrated in Olympia oyster larvae. Increased food concentrations only slightly mitigated some growth parameters and had no effect on percent metamorphosis (Hettinger et al. 2013). The larvae were

likely not able to overcome the negative effects of ocean acidification due to the heightened sensitivity of larval calcification to changes in carbonate saturation state and the plethora of physiological changes that occur during the larval period.

In contrast to larvae, the negative effects of ocean acidification on adult bivalves can sometimes be mitigated by increased food supply. In *M. edulis*, mussels fed a low concentration of food had significantly decreased shell mass and somatic growth and increased shell corrosion at elevated pCO_2 compared to mussels on a high food concentration regime (Melzner et al. 2011). Similar results were also observed for mussels in the field (Thomsen et al. 2013). The scallop *Pecten maximus* had a high tolerance for low pH in an experiment where food supply was high (Sanders et al. 2013). This trend has also been documented in cup corals (Crook et al. 2013). These results imply that many of these species possess the physiological mechanisms and plasticity to maintain normal physiological homeostasis during ocean acidification stress. Exposure to low pH necessitates compensation across a variety of physiological processes, but this compensation is feasible with access to sufficient resources. However, these species mostly live in environments where consistent access to abundant food is rare. This situation may lead to selection for individuals that are more efficient in their use of the energy that they are able to opportunistically capture from their environment.

There is increasing evidence that invertebrate populations harbor genotypes/phenotypes that are resistant to the detrimental effects of ocean acidification (Yu et al. 2011; Pespeni et al. 2013; Parker et al. 2012). These more resistant species and individuals within species may be the ones that maintain ecosystem function in a changing climate. Broadcast spawners may be especially adapted to thrive in a rapidly changing environment since many broodstock contribute to each spawning event, thus increasing the chances that a well-adapted phenotype will arise. However, since many individuals will not thrive under ocean acidification conditions there is a risk of population bottlenecks that will reduce standing genetic diversity and make further adaptation untenable (e.g. Kelly et al. 2012).

Works Cited

Barros, P., Sobral, P., Range, P., Chícharo, L., & Matias, D. (2013). Effects of sea-water acidification on fertilization and larval development of the oyster Crassostrea gigas. *Journal of Experimental Marine Biology and Ecology*, *440*, 200–206. doi:10.1016/j.jembe.2012.12.014

Barton, A., Hales, B., Waldbusser, G. G., Langdon, C., & Feely, R.A. (2012). The Pacific oyster, Crassostrea gigas, shows negative correlation to naturally elevated carbon dioxide levels: Implications for near-term ocean acidification effects. *Limnology and Oceanography*, *57*(3), 698–710. doi:10.4319/lo.2012.57.3.0698

Crook, E. D., Cooper, H., Potts, D. C., Lambert, T., & Paytan, A. (2013). Food availability and pCO_2 impacts on planulation, juvenile survival, and calcification of the azooxanthellate scleractinian coral, *Balanophyllia elegans*. *Biogeosciences Discussions*, *10*(5), 7761–7783. doi:10.5194/bgd-10-7761-2013

Dickinson, G. H., Matoo, O. B., Tourek, R. T., Sokolova, I. M., & Beniash, E. (2013). Environmental salinity modulates the effects of elevated CO2 levels on juvenile hard-shell clams, Mercenaria mercenaria. *The Journal of experimental biology*, *216*(Pt 14), 2607–18. doi:10.1242/jeb.082909

Gaylord, B., Hill, T. M., Sanford, E., Lenz, E.A, Jacobs, L.A, Sato, K. N., Rusell, A.D., & Hettinger, A. (2011). Functional impacts of ocean acidification in an ecologically critical foundation species. *The Journal of experimental biology*, *214*(Pt 15), 2586–94. doi:10.1242/jeb.055939

Hettinger, A., Sanford, E., Hill, T.M., Hosfelt, J.D., Russell, A.D., and Gaylord, B. (2013) The influence of food supply on the response of Olympia oyster larvae to ocean acidification. *Biogeosciences*, *10*, 6629-6638.

Kelly, M. W., Padilla-Gamiño, J. L., & Hofmann, G. E. (2013). Natural variation and the capacity to adapt to ocean acidification in the keystone sea urchin Strongylocentrotus purpuratus. *Global change biology*, *19*(8), 2536–46. doi:10.1111/gcb.12251

Kelly, M. W., Sanford, E., & Grosberg, R. K. (2012). Limited potential for adaptation to climate change in a broadly distributed marine crustacean. *Proceedings. Biological sciences / The Royal Society*, *279*(1727), 349–56. doi:10.1098/rspb.2011.0542

Kurihara, H., Kato, S., & Ishimatsu, A. (2007). Effects of increased seawater pCO2 on early development of the oyster Crassostrea gigas. *Aquatic Biology*, *1*(1), 91–98. doi:10.3354/ab00009

Melzner, F., Stange, P., Trübenbach, K., Thomsen, J., Casties, I., Panknin, U., Gorb, S.N., & Gutowska, M.A. (2011). Food supply and seawater pCO2 impact

calcification and internal shell dissolution in the blue mussel Mytilus edulis. *PloS one*, *6*(9), e24223. doi:10.1371/journal.pone.0024223

Miller, A.W., Reynolds, A. C., Sobrino, C., & Riedel, G. F. (2009). Shellfish face uncertain future in high CO2 world: influence of acidification on oyster larvae calcification and growth in estuaries. *PloS one*, *4*(5), e5661. doi:10.1371/journal.pone.0005661

Parker, L. M., Ross, P. M., & O'Connor, W.A. (2010). Comparing the effect of elevated pCO2 and temperature on the fertilization and early development of two species of oysters. *Marine Biology*, *157*(11), 2435–2452. doi:10.1007/s00227-010-1508-3

Parker, L. M., Ross, P. M., O'Connor, W.A., Borysko, L., Raftos, D.A., & Pörtner, H.-O. (2012). Adult exposure influences offspring response to ocean acidification in oysters. *Global Change Biology*, *18*(1), 82–92. doi:10.1111/j.1365-2486.2011.02520.x

Pespeni, M. H., Sanford, E., Gaylord, B., Hill, T. M., Hosfelt, J. D., Jaris, H. K., LaVigne, M., Lenz, E.A., Russell, A.D., Young, M.K., & Palumbi, S. R. (2013). Evolutionary change during experimental ocean acidification. *Proceedings of the National Academy of Sciences of the United States of America*, *110*(17), 6937–42. doi:10.1073/pnas.1220673110

Sanders, M. B., Bean, T. P., Hutchinson, T. H., & Le Quesne, W. J. F. (2013). Juvenile king scallop, Pecten maximus, is potentially tolerant to low levels of ocean acidification when food is unrestricted. *PloS one*, *8*(9), e74118. doi:10.1371/journal.pone.0074118

Thomsen, J., Casties, I., Pansch, C., Körtzinger, A., & Melzner, F. (2013). Food availability outweighs ocean acidification effects in juvenile Mytilus edulis: laboratory and field experiments. *Global change biology*, *19*(4), 1017–27. doi:10.1111/gcb.12109

Thomsen, J., & Melzner, F. (2010). Moderate seawater acidification does not elicit long-term metabolic depression in the blue mussel Mytilus edulis. *Marine Biology*, *157*(12), 2667–2676. doi:10.1007/s00227-010-1527-0

Timmins-Schiffman, E., O'Donnell, M. J., Friedman, C. S., & Roberts, S. B. (2012). Elevated pCO2 causes developmental delay in early larval Pacific oysters, Crassostrea gigas. *Marine Biology*, *160*(8), 1973–1982. doi:10.1007/s00227-012-2055-x

Yu, P. C., Matson, P. G., Martz, T. R., & Hofmann, G. E. (2011). The ocean acidification seascape and its relationship to the performance of calcifying marine invertebrates: Laboratory experiments on the development of urchin larvae framed by

environmentally-relevant pCO2/pH. *Journal of Experimental Marine Biology and Ecology*, *400*(1-2), 288–295. doi:10.1016/j.jembe.2011.02.016

Appendix A: Exploration of enzymatic activity of Pacific oyster antioxidant proteins in response to ocean acidification

Work accomplished in collaboration with Charlotte Corporeau, Catherine Seguineau, Pierre Boudry, and Claudie Quéré at the Institut français de recherche pour l'exploitation de la mer in Plouzané, France

Introduction

Oxidative stress has been implicated as a consequence of environmental stress in aquatic organisms, but how it occurs in response to ocean acidification has yet to be fully characterized. Previous studies into the effects of ocean acidification on invertebrates have uncovered evidence for the up-regulation of the antioxidant response (Matoo et al. 2013; Tomanek et al. 2011; Kaniewska et al. 2012; Clark et al. 2013). Oxidative stress arises from the over-production of reactive oxygen species (ROS), which are known to damage cells and can lead to apoptosis. Levels of ROS are kept in check by antioxidant enzymes, such as glutathione S-transferase (GST), superoxide dimutase (SOD), catalase, and others. Oyster basal ROS production occurs in the mitochondria during routine oxidative metabolism (Donaghy et al. 2012) and marine invertebrates produce lower levels of ROS than vertebrates, but sedentary invertebrates are less able to regulate ROS levels (reviewed in Abele et al. 2007). During environmental stress, the amount of ROS produced and the antioxidant enzyme activity to neutralize ROS become unbalanced. ROS may be produced as a direct result of the stressor or indirectly from elevated cellular metabolism in response to stress (Mohanty et al. 2000).

Glutathione S-transferase and superoxide dismutase are important components of the antioxidant response across taxonomic groups. GST is known to have both antioxidant (Daniel 1993; Berhane et al. 1994; Nakamura et al. 2000; Leaver and George 1996; Sharma et al. 2004) and detoxification roles, however its exact function is not elucidated in most studies and its various isoforms likely accomplish both functions. SOD acts solely in an antioxidant role and is responsive in marine invertebrates to

pathogens (Gonzelez et al. 2005; Gagnaire et al. 2007), hydrocarbons (Boutet et al. 2004a), heavy metal (Jo et al. 2008; Wu et al. 2011), and herbicides (Malécot et al. 2013).

In this study, we investigated the activity of two antioxidant enzymes (GST and SOD) in the oyster, *Crassostrea gigas*, after exposure to elevated pCO_2 (1000 and 2800 µatm).

Methods

Carbonate Chemistry

This experiment was conducted at the Friday Harbor Labs Ocean Acidification Environmental Laboratory, Friday Harbor, Washington, USA where oysters were exposed to pCO_2 values of 400 μatm, 1000 μatm, or 2800 μatm. The system and control of water chemistry has been previously described in detail (O'Donnell et al., 2013; Timmins-Schiffman et al., 2013a). Briefly, incoming water was filtered (0.2 μm) and stripped of CO_2. As the water flowed into the different treatment tanks, CO_2-free air and CO_2 were added back to reach set points that were continuously monitored by a DuraFET III pH probe (Honeywell, Morristown, NJ, USA). From the treatment tanks, water flow into the eight replicate chambers for each of the three treatment levels was 57.5 mL/min. For this experiment, set points were calculated for 13°C and estimated total alkalinity (A_T) of 2100 μmol/kg for pCO_2 values of 400 μatm (pH 8.03), 1000 μatm (pH 7.67), and 2800 μatm (pH 7.24).

Oysters

Adult oysters (average shell length ± s.d. = 51± 5 mm, average width = 38 ± 6 mm) collected from Oyster Bay, Washington were maintained in 3.5 L chambers (n = 6 oysters per container) and acclimated for two weeks (T = 13°C, pH = 8). The oysters originated from the same spawning event in March 2011 from approximately 25 broodstock oysters. Oysters were fed 120,000 cells per mL per day of Shellfish Diet 1800 (Reed Mariculture, Campbell, CA, USA). Containers were cleaned every other day with freshwater to prevent fouling.

At the end of 29 days, oysters were shucked and gill tissue was dissected and immediately flash frozen in liquid nitrogen. Before protein extraction, tissues were ground to a powder in liquid nitrogen using a mortar and pestle.

Glutathione S-transferase: protein extraction and enzymatic assay

For the glutathione S-transferase (GST) assay, protein from oysters gill tissue was extracted using Triton® X-100 (Bio Rad, Hercules, CA) extraction buffer for 4 oysters from the 400 μatm treatment, 4 from the 1000 μatm, and 2 from 2800 μatm. Whole tissue samples (18.7-98.4 mg) were homogenized on ice using an Ultra turrax (Kinematica, Luzern, Switzerland) in 300 μl of Triton buffer (10 mM PBS, 1 mM EDTA, and 50 μl of Triton® X-100). An additional 100 μl of the Triton buffer was used to rinse remaining tissue homogenate off of the Ultraturrax. The Ultraturrax was rinsed in two separate baths of deionized water between samples. The homogenate was incubated for 40 minutes at room temperature and then spun at 3000xg for 1 hour at 4°C. The upper layer (excluding the pellet) was pipetted into a clean tube and then centrifuged again at 10,000xg for 45 minutes at 4°C. The final supernatant (excluding the upper lipid layer) was transferred to a clean tube and stored at -80°C until analysis.

GST enzyme activity was measured using the Glutathione S-Transferase Assay Kit (Sigma, St Louis, Missouri, USA) following the manufacturer's instructions for the 96-well plate. Twenty microliters of undiluted protein extraction was used for the assay. All samples were measured in triplicate. The assay was read on a Synergy HT spectrophotometer at 340 nm (BioTek, Winooski, VT, USA) with Gen5 v. 2.03 software (BioTek Instruments Inc.) with readings every 50 seconds over a 20 minute period.

Superoxide dismutase: protein extraction and enzymatic assay

Protein extractions were executed similarly to the GST assay for superoxide dismutase (SOD) activity except a house-made lysis buffer was used instead of Triton buffer. Total protein was extracted from gill tissue (23.3-96.8 mg) from 4 oysters from the 400 μatm treatment, 4 from 1000 μatm, and 6 from 2800 μatm. The lysis buffer is

described in Guévélou et al. (2013) and the extraction method was carried out exactly as described above for the Triton buffer.

The activity of SOD was measured using the 19160 SOD determination kit (Sigma) following the manufacturer's instructions. Samples were diluted 1:2 in the kit dilution buffer before use in the assay. A standard curve was prepared using superoxide dismutase (SOD bovine Sigma Reference S7446) diluted to 20, 8, 4, 2, 1, and 0.5 U/mL. All samples were run in triplicate. The assay was read on a Synergy HT spectrophotometer at 450 nm (BioTek) with Gen5 v. 2.03 software (BioTek Instruments Inc.) over a 20 minute period with readings every 1 min, 10 sec. A single time point corresponding to the linear portion of the curve for each sample (at 15 minutes, 10 seconds) was chosen to calculate SOD activity.

Protein Concentration

For protein concentration, protein samples were diluted 1:10. Protein concentration was determined using the Bio-Rad DC Protein Assay kit following manufacturer's instructions, with a standard curve from 0-1500 μg/ml of BSA. Each sample was run in triplicate and absorbance was read at 750 nm on a Synergy HT spectrophotometer (BioTek) using KC4 v. 3 software (BioTek Instruments Inc.). If the triplicates had a coefficient of variation greater than 20%, then the outlier was removed from the average of protein concentration.

Statistical Analysis

All statistical analyses were performed in R (R Development Team 2013). To calculate GST activity, the first 5 data points were excluded to ensure linearity of the kinetic curve. The change in absorbance (ΔA) was calculated with the following:

$$\Delta A = (A_f - A_i)/(T_f - T_i)$$

Where A = absorbance at 340 nm, T = time point, the subscript f = final and the subscript i = initial. GST specific activity is then calculated by the equation:

([ΔA]*0.2mL)/(5.3 mM-1*0.02mL)

where 0.2 mL = reaction volume, 5.3 mM-1 is the extinction coefficient for CDNB in a 96-well plate, and 0.02 mL is the enzyme volume. For each sample, GST activity was divided by sample concentration to achieve an activity expressed per mg of tissue (μmol/mg/min).

SOD activity is measured as an inhibition rate of the assay. The inhibition rate is:

$\{([A_{blank\ 1}]-[A_{sample}])/(A_{blank\ 1})\} * 100.$

Blanks 2 and 3 were also run, as per the manufacturer's protocol, but since their kinetic slopes = 0 they were excluded from the calculations because they did not represent a significant contribution to the background SOD activity. Replicates were excluded (1 each for 6 samples) if linearity of the reaction curve was not achieved by the time point 15 min, 10s. The linear relationship between % inhibition and ln[standard concentration] was plotted and the equation for the line of best fit was used to calculate U/ml of SOD (based on % inhibition) for all of the samples (Supplementary Figure AppA.1).

For GST and SOD activity, effect of treatment on enzyme activity was explored with a one-way ANOVA with treatment as a fixed factor and significant differences were further investigated using Tukey's HSD.

Results

Glutathione S-transferase

Mean GST activity (mean ± 95% confidence interval) was 0.0198 ± 0.0098 μmol/mg/min for oysters in the 400 μatm treatment, 0.0156 ± 0.0078 μmol/mg/min for oysters from 1000 μatm, and 0.0161 ± 0.093 μmol/mg/min for oysters from 2800 μatm

(Figure AppA.1). There was no significant difference in GST activity among treatment groups (F=0.4596, p=0.6493).

Superoxide dismutase

Mean SOD activity (mean ± 95% confidence interval) was 0.75 ± 0.3 U/mg for the 400 μatm oysters, 1.05 ± 0.7 U/mg for the 1000 μatm oysters, 2.60 ± 0.4 U/mg for the 2800 μatm oysters (Figure AppA.2). There was significant effect of treatment on SOD activity (F=40.799, p=8.153e-6). This difference was due to the elevated SOD activity in oysters exposed to 2800 μatm compared to the other two treatments ($p < 0.05$), which were not different from each other.

Discussion

Moderately elevated pCO_2 (1000 μatm) does not lead to oxidative stress in *C. gigas*, but highly elevated pCO_2 (2800 μatm) instigates an antioxidant response. Superoxide dismutase activity was significantly elevated in oysters exposed to the highest pCO_2, a clear signal of oxidative stress during ocean acidification. A similar pattern was not seen for glutathione S-transferase activity, possibly due to the multifunctional nature of GST. Even though our sample size for the 2800 μatm-exposed oysters was smaller for the GST assay versus the SOD assay (n = 2 and n = 6, respectively), there is not even a trend of increased GST activity at the highest pCO_2. Since SOD responds solely to oxidative stress its up-regulation has a clear interpretation; however, a global activity assay of the different isoforms of GST would encompass some that respond to oxidative stress and some that may respond only to contaminant exposure (and therefore may not change in response to low pH). Alternatively, SOD and GST may function on different time scales in the oxidative stress response, but this is unlikely given that GST remains up-regulated after exposures to contaminants lasting multiple weeks (Letendre et al. 2011; Boutet et al. 2004a, 2004b).

These enzyme activity results further support what other work at the gene and protein expression levels have suggested: that exposure to elevated pCO_2 triggers production of ROS leading to an up-regulation of the antioxidant response. Enzyme

activity is a definitive measure of this response where gene and protein expression are not because increased gene/protein expression does not mean that a protein is functionally activated. The exact mechanism of ROS increase remains unknown and future studies should investigate whether elevated pCO_2 and subsequent increased H^+ concentrations are direct causes of oxidative stress or if the stress indirectly stimulates ROS production through elevated oxidative metabolism. It is also of interest that the moderate pCO_2 of 1000 μatm does not cause even a slight elevation of antioxidant enzyme activity. This finding may illustrate a tolerance of *C. gigas* to moderately elevated pCO_2, which is consistent with a species that inhabits the intertidal zone where there are frequent fluctuations in pH.

Increased oxidative stress followed by greater levels of antioxidant genes/proteins/enzymes is a common response of intertidal invertebrates to decreased pH. An up-regulated antioxidant enzyme response has been linked to greater periods of tidal emersion (Letendre et al. 2009), suggesting that ROS production increases either during emersion or during oxidative burst with re-immersion and that bivalves have well established antioxidant pathways to respond to this physiological change. During tidal emersion, many intertidal organisms experience decreased body fluid pH due to build up of CO_2 from respiration during valve closure (Jokumsen and Gyhn 1982; Duncan et al. 1994). Similarly, decreased environmental pH causes a concomitant decrease in bivalve hemolymph pH (e.g. Thomsen et al. 2013). Although the exact mechanism behind the production of ROS during exposure to elevated pCO_2 is unknown (e.g. Tomanek et al. 2011), a growing body of literature has linked the antioxidant response (and thereby ROS production) with decreased environmental pH (Todgham and Hofmann 2009; Tomanek et al. 2011; Matozzo et al. 2013). The decrease in hemolymph pH likely impacts mitochondrial activity - where ROS are produced in *C. gigas* (Donaghy et al. 2013) - either directly or indirectly through stimulating metabolism. Bivalves are able to efficiently respond to the oxidative stress resulting from ocean acidification due to an evolutionary history of exposure to environmental extremes in the intertidal.

Figures

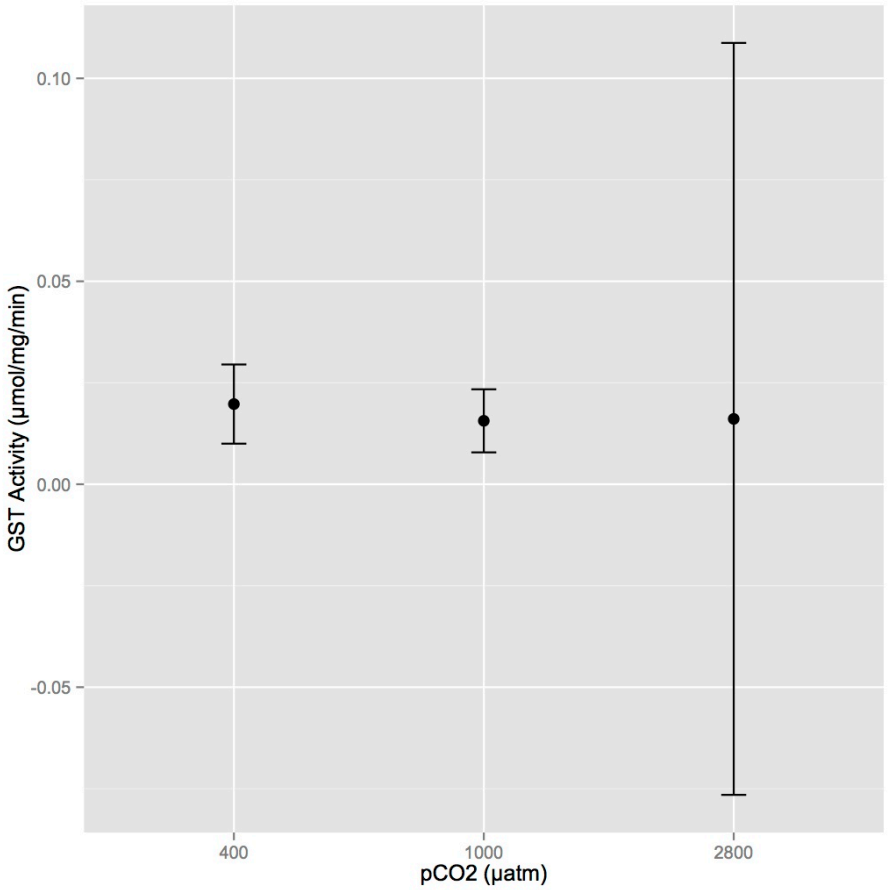

Figure AppA.1. Mean GST activity per treatment with 95% confidence intervals. There is no statistical difference among the treatments.

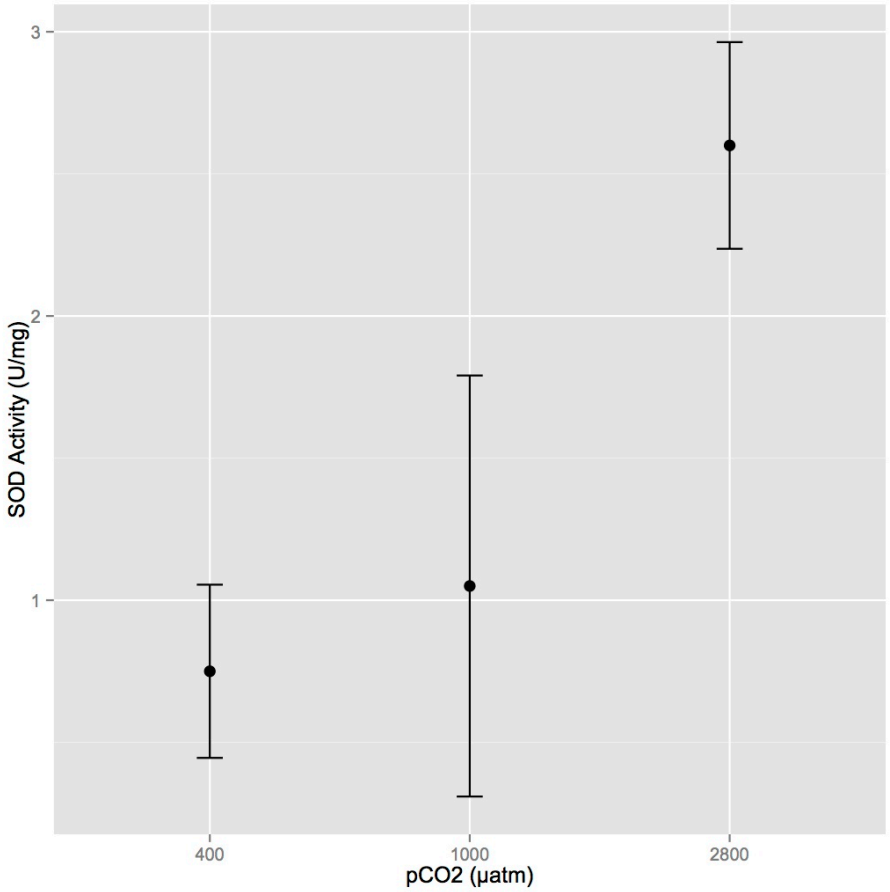

Figure AppA.2. Mean units of SOD per mg of tissue with 95% confidence intervals for each treatment. SOD activities in 2800 μatm-exposed oysters are statistically different from those at 400 and 1000 μatm.

Supplementary Information

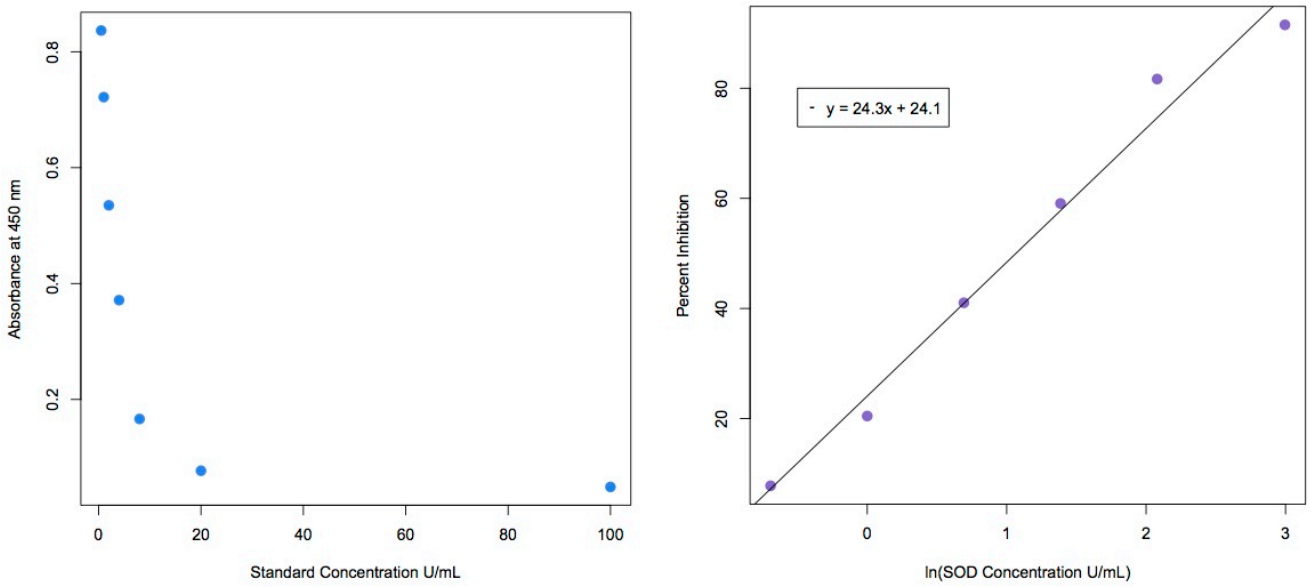

Supplementary Figure AppA.S1. Standard curve for the SOD standards (blue points) and percent inhibition vs. the natural log of the SOD concentration (purple points) with line of best fit used to calculate percent inhibition for samples of unknown concentrations (black line).

Works Cited

Abele, D., Philipp, E., Gonzalez, P. M., & Puntarulo, S. (2007). Marine invertebrate mitochondria and oxidative stress. *Frontiers in Bioscience*, *12*, 933–946.

Berhane, K., Widersten, M., Engström, A., Kozarich, J. W., & Mannervik, B. (1994). Detoxication of base propenals and other alpha, beta-unsaturated aldehyde products of radical reactions and lipid peroxidation by human glutathione transferases. *Proceedings of the National Academy of Sciences of the United States of America*, *91*(4), 1480–4.

Boutet, I., Tanguy, A.., & Moraga, D. (2004). Characterisation and expression of four mRNA sequences encoding glutathione S-transferases pi, mu, omega and sigma classes in the Pacific oyster Crassostrea gigas exposed to hydrocarbons and pesticides. *Marine Biology*, *146*(1), 53–64. doi:10.1007/s00227-004-1423-6

Boutet, Isabelle, Tanguy, A., & Moraga, D. (2004). Response of the Pacific oyster Crassostrea gigas to hydrocarbon contamination under experimental conditions. *Gene*, *329*, 147–57. doi:10.1016/j.gene.2003.12.027

Clark, M. S., Thorne, M. A.S., Amaral, A., Vieira, F., Batista, F. M., Reis, J., & Power, D. M. (2013). Identification of molecular and physiological responses to chronic

environmental challenge in an invasive species: the Pacific oyster, Crassostrea gigas. *Ecology and evolution*, *3*(10), 3283–97. doi:10.1002/ece3.719

Daniel, V. (1993). Glutathione S-Transferases: Gene Structure and Regulation of Expression. *Critical Reviews in Biochemistry and Molecular Biology*, *28*(3), 173–207.

Donaghy, L., Kraffe, E., Le Goïc, N., Lambert, C., Volety, A. K., & Soudant, P. (2012). Reactive oxygen species in unstimulated hemocytes of the pacific oyster Crassostrea gigas: a mitochondrial involvement. *PloS one*, *7*(10), e46594. doi:10.1371/journal.pone.0046594

Duncan, P., Spicer, J.I., Taylor, A.C., and Davies, P.S. (1994). Acid-base disturbances accompanying emersion in the scallop *Pecten maximus* (L.). *Journal of Experimental Marine Biology and Ecology*, *182*, 15-25.

Gagnaire, B., Gay, M., Huvet, A., Daniel, J.-Y., Saulnier, D., & Renault, T. (2007). Combination of a pesticide exposure and a bacterial challenge: in vivo effects on immune response of Pacific oyster, Crassostrea gigas (Thunberg). *Aquatic toxicology (Amsterdam, Netherlands)*, *84*(1), 92–102. doi:10.1016/j.aquatox.2007.06.002

Gonzalez, M., Romestand, B., Fievet, J., Huvet, A., Lebart, M.-C., Gueguen, Y., & Bachère, E. (2005). Evidence in oyster of a plasma extracellular superoxide dismutase which binds LPS. *Biochemical and biophysical research communications*, *338*(2), 1089–97. doi:10.1016/j.bbrc.2005.10.075

Guévélou, E., Huvet, A., Galindo-Sánchez, C. E., Milan, M., Quillien, V., Daniel, J.-Y., Quéré, C., Boudry, P., & Corporeau, C. (2013). Sex-specific regulation of AMP-activated protein kinase (AMPK) in the Pacific oyster Crassostrea gigas. *Biology of reproduction*, *89*(4), 100. doi:10.1095/biolreprod.113.109728

Jo, P. G., Choi, Y. K., & Choi, C. Y. (2008). Cloning and mRNA expression of antioxidant enzymes in the Pacific oyster, Crassostrea gigas in response to cadmium exposure. *Comparative biochemistry and physiology. Toxicology & pharmacology : CBP*, *147*(4), 460–9. doi:10.1016/j.cbpc.2008.02.001

Jokumsen, A. and Fyhn, H.J. (1982). The influence of aerial exposure upon respiratory and osmostic properties of ahemolymph from two intertidal mussles, *Mytilus edulis* L. and *Modiolus modiolus* L. *Journal of Experimental Marine Biology and Ecology*, *61*, 189-203.

Kaniewska, P., Campbell, P. R., Kline, D. I., Rodriguez-Lanetty, M., Miller, D. J., Dove, S., & Hoegh-Guldberg, O. (2012). Major cellular and physiological impacts of ocean acidification on a reef building coral. *PloS one*, *7*(4), e34659. doi:10.1371/journal.pone.0034659

Leaver, M. J., & George, S. G. (1996). Three repeated glutathione S-transferase genes from a marine fish, the plaice (Pleuronectes platessa). *Marine Environmental Research*, *42*(1-4), 19–23. doi:10.1016/0141-1136(95)00080-1

Letendre, J., Dupont-Rouzeyrol, M., Hanquet, A.-C., Durand, F., Budzinski, H., Chan, P., Vaudry, D., & Rocher, B. (2011). Impact of toxicant exposure on the proteomic response to intertidal condition in Mytilus edulis. *Comparative biochemistry and physiology. Part D, Genomics & proteomics*, *6*(4), 357–69. doi:10.1016/j.cbd.2011.08.002

Letendre, J., Chouquet, B., Manduzio, H., Marin, M., Bultell, F., Leboulenger, F., and Durand, F. (2009). Tidal height influences the levels of enzymatic antioxidant defences in *Mytilus edulis*. *Marine Environmental Research*, *67*, 69-74.

Malécot, M., Guével, B., Pineau, C., Holbech, B. F., Bormans, M., & Wiegand, C. (2013). Specific proteomic response of Unio pictorum mussel to a mixture of glyphosate and microcystin-LR. *Journal of proteome research*, *12*(11), 5281–92. doi:10.1021/pr4006316

Matoo, O. B., Ivanina, A. V, Ullstad, C., Beniash, E., & Sokolova, I. M. (2013). Interactive effects of elevated temperature and CO(2) levels on metabolism and oxidative stress in two common marine bivalves (Crassostrea virginica and Mercenaria mercenaria). *Comparative biochemistry and physiology. Part A, Molecular & integrative physiology*, *164*(4), 545–53. doi:10.1016/j.cbpa.2012.12.025

Matozzo, V., Chinellato, A., Munari, M., Finos, L., Bressan, M., and Marin, M.G. (2012). First evidence of immunomodulation in bivalves under seawater acidification and increased temperature. *PLoS ONE*, *7*(3): e33820. doi: 10.1371/journal.pone.0033820

Mohanty, P., Hamouda, W., Garg, R., Aljada, A., Ghanim, H., & Dandona, P. (2000). Glucose challenge stimulates reactive oxygen species (ROS) generation by leucocytes. *The Journal of Clinical Endocrinology and Metabolism*, *85*(8), 2970–2973.

Nakamura, Y., Ohigashi, H., Masuda, S., Murakami, A., Morimitsu, Y., Kawamoto, Y., Osawa, T., Imagawa, M. & Uchida, K. (2000). Redox Regulation of Glutathione S - Transferase Induction by Benzyl Isothiocyanate : Correlation of Enzyme Induction with the Formation of Reactive Oxygen Intermediates Advances in Brief Redox Regulation of Glutathione S -Transferase Induction by Benzyl Is. *Cancer Research*, *60*, 219–225.

Sharma, R., Yang, Y., Sharma, A., Awasthi, S., & Awasthi, Y. C. (2004). Antioxidant role of glutathione S-transferases: protection against oxidant toxicity and regulation of stress-mediated apoptosis. *Antioxidants & redox signaling*, *6*(2), 289–300.

Thomsen, J., Casties, I., Pansch, C., Körtzinger, A., & Melzner, F. (2013). Food availability outweighs ocean acidification effects in juvenile Mytilus edulis: laboratory and field experiments. *Global change biology*, *19*(4), 1017–27. doi:10.1111/gcb.12109

Todgham, A.E., and Hofmann, G.E. (2009). Transcriptomic response of sea urchin larvae *Strongylocentrotus purpuratus* to CO_2-driven seawater acidification. *The Journal of Experimental Biology*, *212*, 2579-2594.

Tomanek, L., Zuzow, M. J., Ivanina, A. V, Beniash, E., & Sokolova, I. M. (2011). Proteomic response to elevated PCO2 level in eastern oysters, Crassostrea virginica: evidence for oxidative stress. *The Journal of experimental biology*, *214*(Pt 11), 1836–44. doi:10.1242/jeb.055475

Wu, C., Zhang, W., Mai, K., Xu, W., & Zhong, X. (2011). Effects of dietary zinc on gene expression of antioxidant enzymes and heat shock proteins in hepatopancreas of abalone Haliotis discus hannai. *Comparative biochemistry and physiology. Toxicology & pharmacology : CBP*, *154*(1), 1–6. doi:10.1016/j.cbpc.2011.03.003

Appendix B: Histological Investigations into the Effects of pCO_2 and a second stressor in Pacific Oysters

Histology analysis done by Jessica Blanchette

Introduction

Intertidal species have evolved in a notoriously variable and stressful environment in which they frequently encounter conditions that are near the limit of their range of physiological function (Somero 2002). Climate change may push intertidal species beyond this range to the point of physiological damage, or these species may be uniquely adapted to withstand environmental change. Many processes that are part of the response to average fluctuations in the intertidal could be affected in the physiological response to future climate scenarios. Cuboidal metaplasia of digestive tubules, or digestive diverticula atrophy, is a common occurrence in bivalves (Owen 1966) and has also been documented in response to environmental stress. Cycles of metaplasia of the digestive diverticula can also fluctuate seasonally (Couch 1985; Weis et al. 1995). Increased cuboidal metaplasia has been associated with lesions in *Mytilus edulis* (Lowe and Moore 1979), *Crassostrea rhizophorae* die-offs (Nascimento et al. 1986), *Crassostrea virginica* exposure to environmental pollutants (Weis et al. 1995), and starvation in *C. virginica* (Winstead 1995).

This study investigates future ocean pH (ocean acidification) effects on digestive tubule cuboidal metaplasia in the Pacific oyster, *Crassostrea gigas*. Our hypothesis is that elevated pCO_2/decreased pH will increase the physiological stress experienced by the oysters and thus increase metaplasia.

Oysters were exposed to one of three pCO_2 levels - 400 µatm (control), 1000 µatm, or 2800 µatm - for one month. Subsequently, a subset of oysters from each pCO_2 treatment was subjected to mechanical stress to investigate the effects of ocean acidification on the oyster's stress response at the histological level.

Materials and Methods

Experimental set-up and oyster sampling were accomplished as described in Chapter III (see pages 69-71). Oysters from three of the pCO_2 treatments (400, 1000, and 2800 µatm) were analyzed for histological differences due to pCO_2 and mechanical stress. A transverse section was taken from each oyster to include tissues from digestive gland, gill, and mantle. Sample sizes were as follows: 9 oysters for 400 µatm, 8 for 400 µatm + mechanical stress, 8 for 1000 µatm, 8 for 1000 µatm + mechanical stress, 8 for 2800 µatm, and 5 for 2800 µatm + mechanical stress.

Each tissue cross-section was placed in a histology cassette and immediately transferred to Invertebrate Davidson's fixative (Shaw & Battle 1957). After 24 hours, cassettes were transferred to 70% ethanol for storage. Slides were prepared for routine paraffin histology by the Diagnostic Pathology Medicinal Group (Sacramento, CA) and were stained with haematoxylin and eosin. Digestive tubules were examined for signs of metaplasia. Tubules with open and round lumen (contrasted with a 3- or 4-point star-like shape) were considered to have undergone cuboidal metaplasia (Fig. AppB.1).

All analyses were performed in R (R Development Team 2013). ANOVA was performed with pCO_2 and mechanical stress as fixed factors.

Results

Elevated pCO_2 had no effect on proportion of digestive tubules undergoing metaplasia (Fig. AppB.2, $F = 0.0562$, $p = 0.9455$). Across pCO_2 treatments, mechanical stress resulted in fewer tubules with cuboidal metaplasia (Fig. AppB.2, $F = 4.7870$, $p = 0.0323$).

Discussion

One month exposure to elevated pCO_2 did not affect digestive tubule cuboidal metaplasia in *Crassostrea gigas*, however mechanical stimulation caused a decrease in the proportion of tubules undergoing metaplasia across all pCO_2 levels. Metaplasia is when digestive tubule cell type changes from columnar to cuboidal and is a natural occurrence in the daily feeding cycle of bivalves (Owen 1966), but can increase during

starvation (Winstead 1995). Some environmental stressors also instigate digestive tubule metaplasia, but this may be an indirect effect of decreased access to food. For example, lesions proximal to digestive tubules are associated with metaplasia (Lowe and Moore 1979), but the lesions may be inhibiting digestion. Additionally, exposure to high levels of pollutants causes metaplasia (Weis et al. 1995), but this could be a by-product of oyster shell closure during exposure to contaminated water (i.e. Doherty et al. 1987), which would prevent feeding. Elevated pCO_2 does not seem to affect access to food in *C. gigas*, as evidenced by lack of digestive tubule cuboidal metaplasia as well as by its lack of effect on fatty acid profiles (see Chapter 3).

Mechanical stress consistently caused a decrease in proportion of tubules undergoing metaplasia in all pCO_2 treatments. This finding is in contrast to previous hypotheses that metaplasia is a general stress response in bivalves (Couch 1985). The oysters that underwent mechanical stimulation may require more resources to counteract this exogenous stress and one response to this requirement may be to increase the number of digestive tubules in the digestion phase (Owen 1966). A similar effort to mobilize resources after exposure to mechanical stress was also seen at the proteomic level (see Chapter III Discussion). These results suggest that digestive tubule cuboidal metaplasia may not be a general stress response, but may in fact be a physiological response to change in access to food resources as a result of an environmental stressor. Further research into the signaling pathways and mechanisms that trigger cuboidal metaplasia would help to elucidate its causes.

Figures

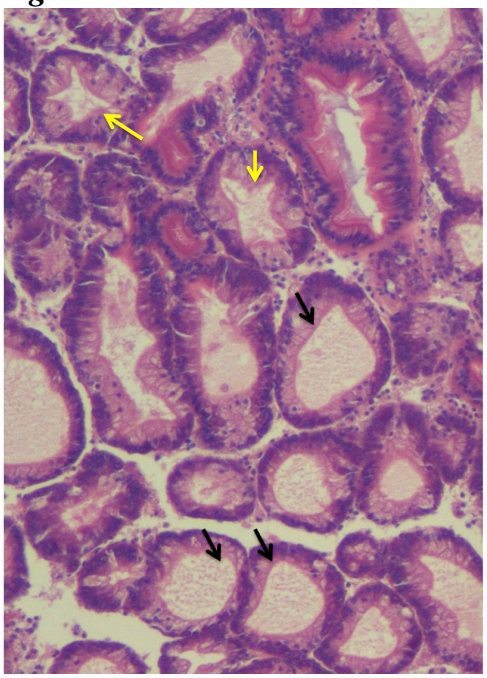

Figure Appendix B.1. Normal digestive tubules (yellow arrows) and tubules undergoing metaplasia (black arrows).

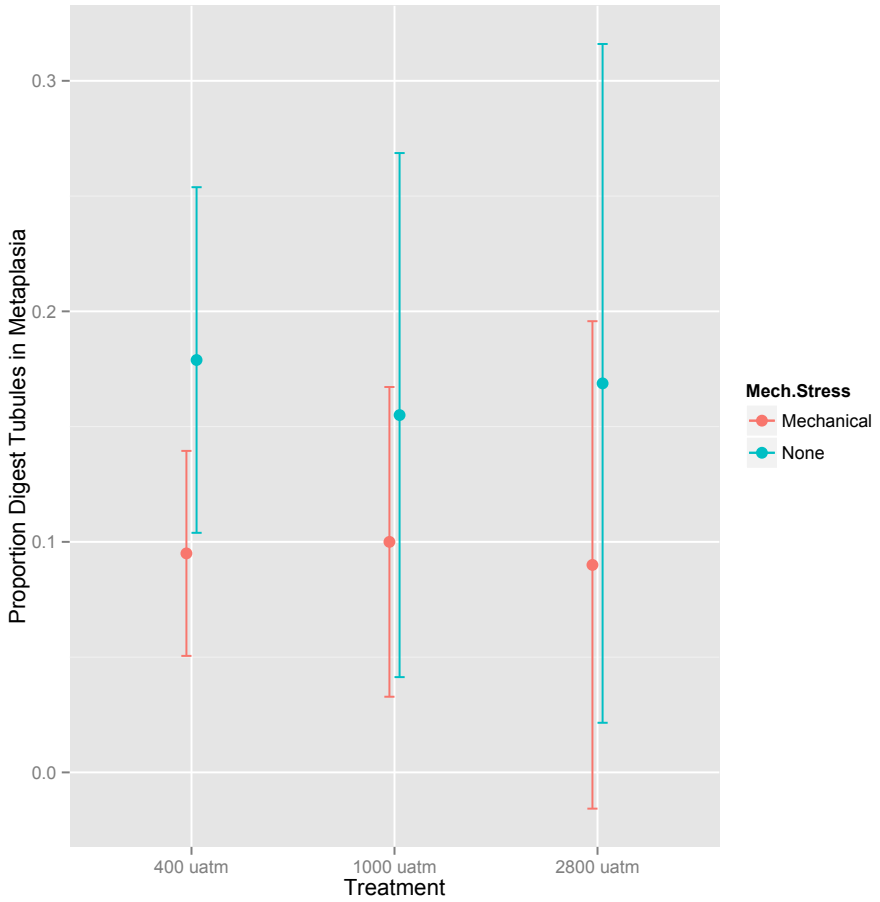

Figure Appendix B.2. Proportion of digestive tubules exhibiting cuboidal metaplasia. Means are plotted with 95% confidence intervals for mechanically stressed (red) and non-mechanically stressed (blue) oysters across the three pCO_2 treatments. Mechanical stress caused a significant decrease in metaplasia in all pCO_2 treatments.

Works Cited

Couch, J.A. (1985) Prospective study of infectious and noninfectious diseases in oysters and fishes in three Gulf of Mexico estuaries. *Diseases of Aquatic Organisms*, *1, 59-82*.

Doherty, F.G., Cherry, D.S., and Cairns, J. (1987) Valve closure responses of the Asiatic clam *Corbicula fluminea* exposed to cadmium and zinc. *Hydrobiologia*, *153*(2), 159-167.

Lowe, D.M. and Moore, M.N. (1979) The cytology and occurrence of granulocytomas in mussels. *Marine Pollution Bulletin*, *10*(5), 137-141.

Nascimento, I.A., Smith, D.H., Kern, F., and Pereira, S.A. (1986) Pathological findings in *Crassostrea rhizophorae* from Todos os Santos Bay, Bahia, Brazil. *Journal of Invertebrate Pathology*, *47*(3), 340-349.

Owen, G. (1966) Digestion. In *Physiology of Mollusca Volume II*. Wilbur, K.M. and Yonge, C.M. (eds). Academic Press: New York.

Shaw, B.L. and Battle, H.I. (1957) The gross and microscopic anatomy of the digestive tract of the oyster *Crassostrea virginica* (Gmelin). *Canadian Journal of Zoology*, *33*(3), 325-347.

Somero, G.N. (2002) Thermal physiology and vertical zonation of intertidal animals: Optima, limits, and costs of living. *Integrative and Comparative Biology*, *42*, 780-789.

Weis, P., Weis, J.S., Couch, J., Daniels, C., and Chen, T. (1995) Pathological and genotoxicological observations in oysters (*Crassostrea virginica*) living on chromated copper arsenate (CCA)-treated wood. *Marine Environmental Research*, *39* (1-4), 275-278.

Winstead, J.T. (1995) Digestive tubule atrophy in eastern oysters, *Crassostrea virginica* (Gmelin, 1791), exposed to salinity and starvation stress. *Journal of Shellfish Research*, *14*(1), 105-111.

Appendix C: List of Samples from 1 Week and 1 Month Elevated pCO_2 Exposures

Explanation:

Appendix C is a table of oyster tissues taken from an ocean acidification experiment done in January-February, 2012. Some of these samples were analyzed and results are presented in Chapters II and II and Appendices A and B. Samples with the prefix "Exp1" are from oysters that were exposed to elevated pCO_2 for 1 week (these results are not presented in this dissertation). A subset of oysters from each pCO_2 treatment were heat shocked at 38°C for 1 hour before sampling. There was a hiccup in the water chemistry for the 1-week experiment: for the 400 µatm treatment (the control) the DuraFET probe was not accurately calibrated and for the first 36 hours of the experiment the pH of this treatment was around 7 but was then switched to pH 8 for the remainder of the exposure. The following is taken from my lab notebook from January 7, 2012:

All probes were pretty accurate, except for 103A, which is the control treatment. The probe read a pH of about 8, but it was actually around 7. I verified this with a second spec pH. I calibrated the probe, drained the water and it quickly righted itself but the oysters were exposed to low pH water for about 36 hours.

Samples with the prefix "Exp2" are from the month-long experiment, the results of which are presented above.

Each row in the spreadsheet represents one oyster. For most oysters, two separate gill samples were taken and for Exp2 oysters the remaining body tissues ("whole body") were also preserved. Histology sections were taken for every oyster. Treatment indicates which pCO_2 the oyster was exposed to (400-2800 µatm) and which additional stress, if any (HS = heat shock, MS = mechanical stress). Cells highlighted in yellow indicate that a tissue sample was already used for an experiment. For many of these, there is still biological material available for further analysis (RNA, protein, glycogen, fatty acid, ground tissue). In the "Notes" column, the types of analyses done on each oyster are listed.

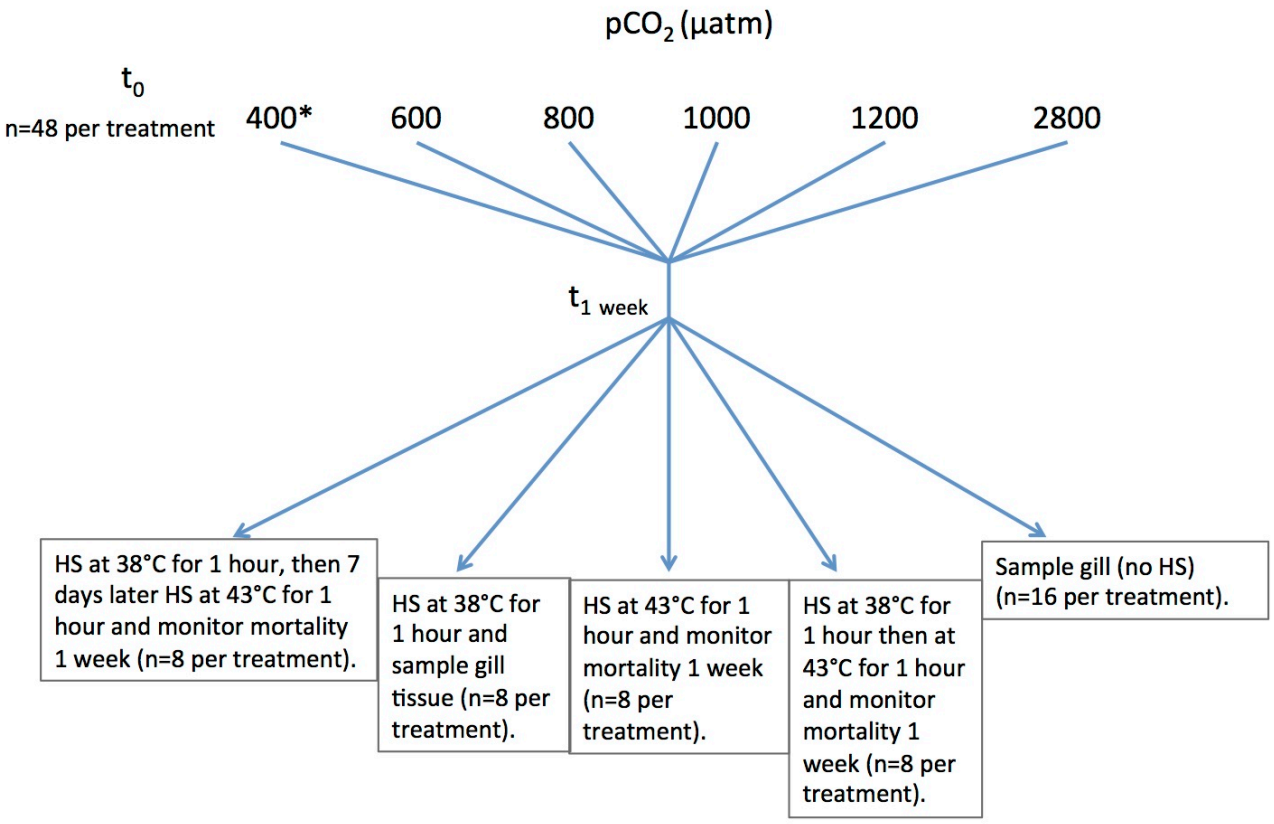

Figure Appendix C1. Sample use for experiment 1 (week-long exposure to ocean acidification). Sample allocation among heat shock treatments post ocean acidification incubation. None of these samples have been processed for analysis. For details, see attached Appendix C spreadsheet.

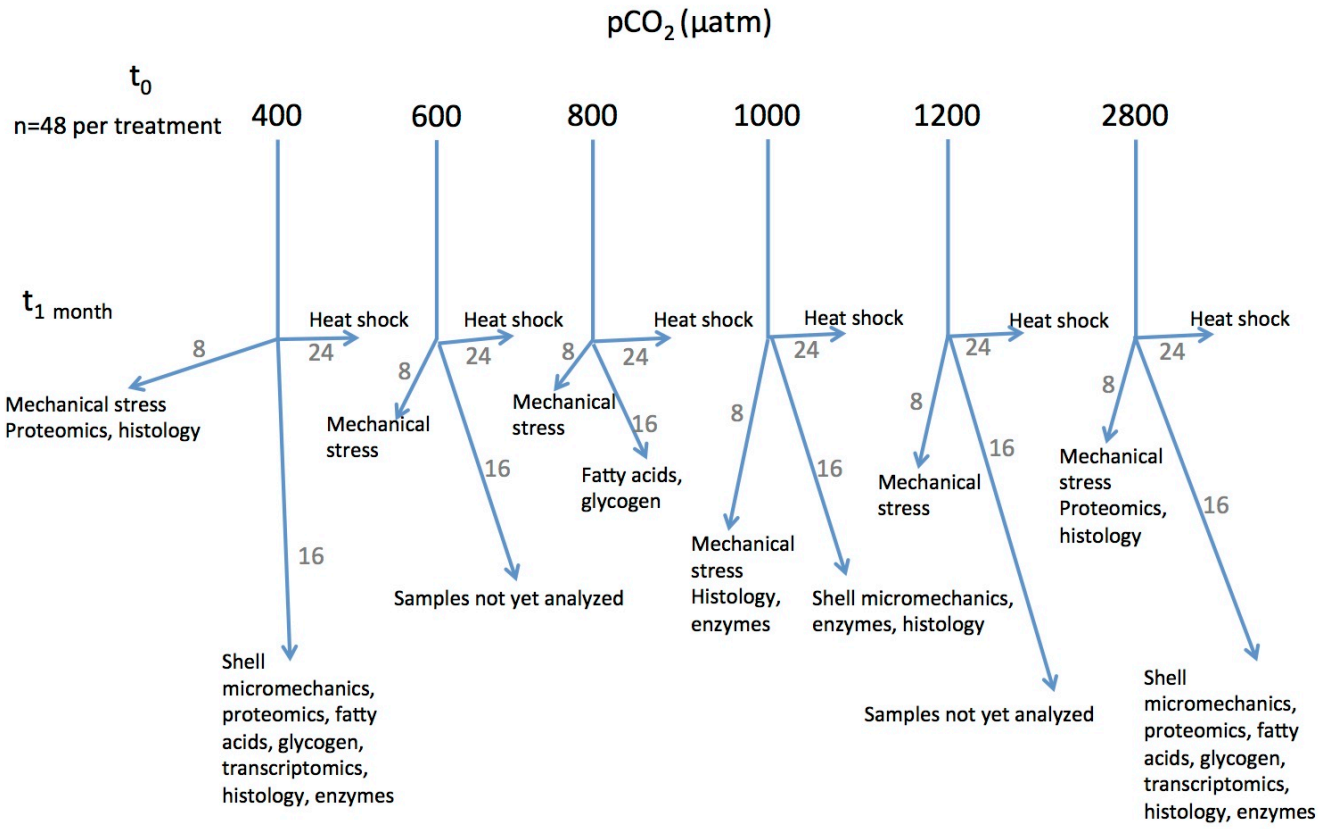

Figure Appendix C2. Sample use for experiment 2 (month-long exposure to ocean acidification). Gray numbers indicate sample size taken for different assays. The numbers of oysters used for each assay can be found in the supplemental spreadsheet for Appendix C. If no samples have been analyzed for a particular set of oysters, that is indicated.